Sayı / Number: 213

GEMİ ve DENİZ TEKNOLOJİSİ

GMO JOURNAL OF SHIP AND MARINE TECHNOLOGY

TMMOB GEMİ MÜHENDİSLERİ ODASI
The Turkish Chamber of Naval Architects and Marine Engineers

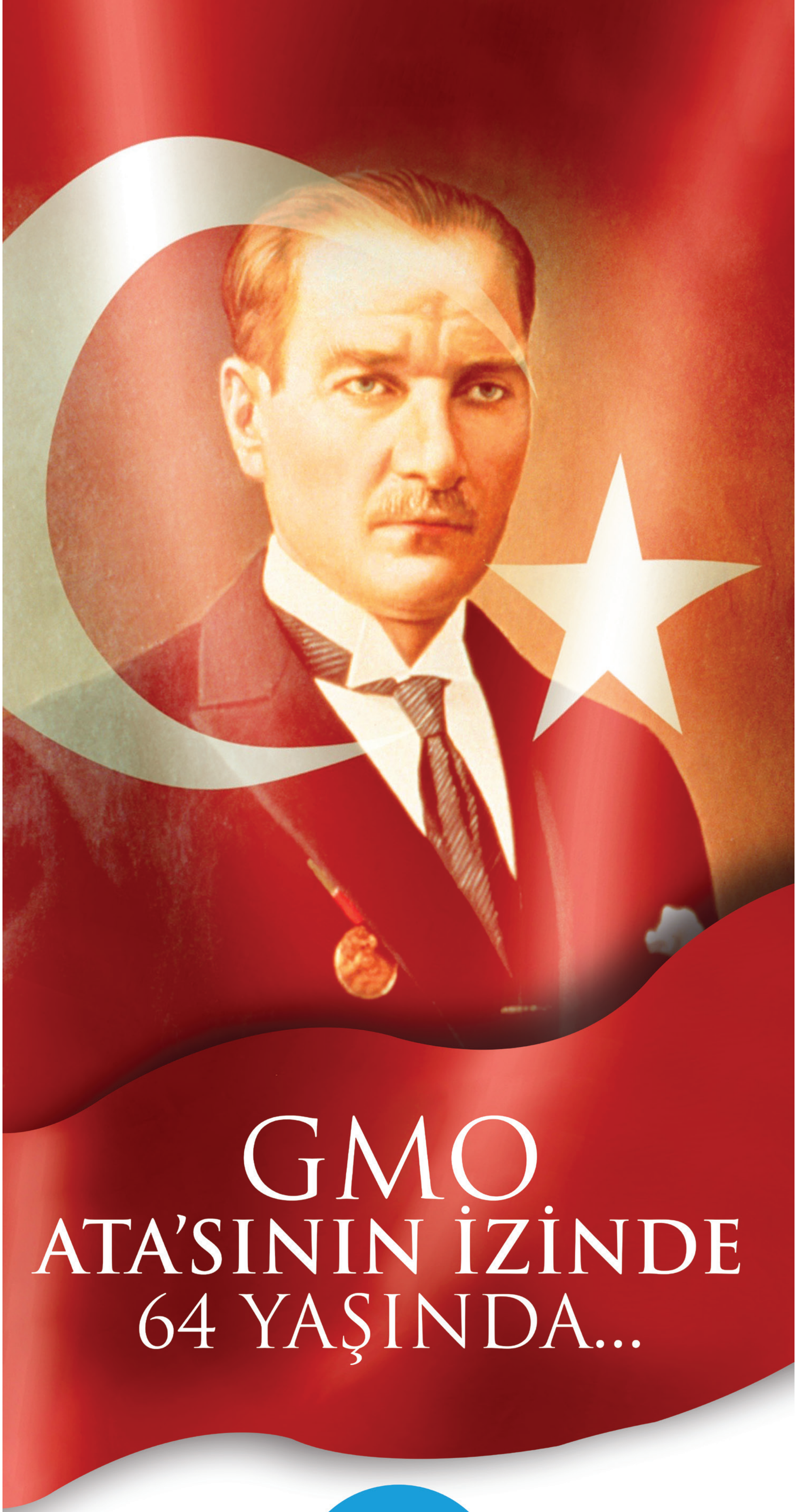

TMMOB
GEMİ MÜHENDİSLERİ ODASI

EDİTÖRDEN / EDITORIAL

Değerli Meslektaşlar ve Okurlar,

Dergimizin 213. sayısında sizlere; tekne direnç performansı, zararlı canlı türlerinin taşınımı ve çevre etkileri bakımından en etkin olaylar arasında olan tekne karina kirlenmesini işleyen dört ayrı makale sunulmaktadır. Makaleler daha önce aynı yazarların 3. Uluslararası Gemi İnşaatı ve Denizcilik Sempozyumu'nda (INT-NAM 2018) sunmuş olduğu bildirilerden geliştirilerek hazırlanmıştır. Dr. Atlar ve ekibinin hazırladığı yenilikçi çalışmada, fouling kontrol boyalarının geminin işletme performansı üzerine etkilerinin tahmini için tekne ve pervane koşullarını da içeren gerçekçi bir yöntem sunulmaktadır. Makalede deney kurgusu, performans tahmini ve gerçek tekne formunun HAD ile tanımlanabilmesi adına bu özel konuda yenilikler sunulmaktadır. "Gemi Boyalarında Yeni Ufuklar" adlı makalede Dr. Demirel, hidrodinamik yaklaşımlar kapsamında gemiler üzerindeki biyolojik yüzey kirlenmesi ve bu kirlenmenin önlenmesi konusunda uygulanan yeni yöntemleri işlemektedir. Biyobenzetim (biomimetic) yaklaşımı, bio-ilham (bio-inspired) antifouling boya stratejileri ve bio-ilham boyalarının dizaynında karşılaşılan zorluklar detaylı olarak tartışılmaktadır. Bunu takip eden makalede, Dr. Türkmen ve ekibi hidrodinamik sürtünme direncinin araştırılmasında kullanılacak deneysel bir yöntem geliştirilmiştir. Sayın Dindar tarafından hazırlanan "Zaman Çarteri Esnasında Meydana Gelen Karina Kirlenmesi: Geminin Düşük Performansından Doğan Sorumluluk" başlıklı deniz hukuku alanındaki makalede ise, karina kirlenmesi nedeniyle geminin performansındaki düşmeden dolayı doğacak sorumluluklar hukuksal bir bakış açısı ile analiz edilmiştir.

Saygılarımızla.

Prof. Dr. Ahmet Dursun ALKAN
Baş Editör

Distinguished Colleagues and Readers,

The issue 213 has been prepared to focus on hull fouling as one of the important issues on hull resistance, transportation of harmful non-indigenous species and environmental impacts. The selected articles were prepared by the same authors whose papers were submitted to the 3rd International Naval Architecture and Maritime Symposium (INT-NAM 2018). The innovative paper written by Dr. Atlar et al. fills the gap between laboratory measurements and predicting the performance of commercial marine vessels via a rational approach combining experimental and computational procedures, to predict the effects of modern-day fouling control systems on "in-service" ship performance. The article "New Horizons in Marine Coatings" by Dr. Demirel, reveals a research in coating/fouling hydrodynamics, biomimetic approach, bio-inspired antifouling strategies and the challenges in designing bio-inspired antifouling coatings. Following these papers, in the article presented by Dr. Turkmen and his team, an experimental method has been developed to investigate the hydrodynamic friction resistance. The fourth paper entitled "Hull Fouling During Time Charter Service: Liability for Deficient Performance of the Ship" by Mrs. Dindar discusses the limits of the responsibility for the ship's performance reduction due to hull fouling from a legal point of view.

Best regards,

Prof. Ahmet Dursun Alkan PhD
Editor-in-Chief

Sahibi / Publisher:
TMMOB GEMİ MÜHENDİSLERİ ODASI
UCTEA, The Turkish Chamber of Naval Architects & Marine Engineers

İmtiyaz Sahibi / Owner
Salih BOSTANCI

Baş Editör / Editor-in-Chief
Prof. Ahmet Dursun ALKAN PhD

Yardımcı Editör / Associate Editor
Assoc. Prof. Ömer Kemal KINACI PhD

Yayın Komisyonu / Editing Committee
Salih BOSTANCI
Dr. Onur USTA
Dr. Dursun Murat Sekban
Batuhan KARATAŞ
Tuğba TİKTAŞ
Burçin Gaye DİLEKMEN
Orçun BALBAŞ
Alper DİLCİ

Yönetim / Management
TMMOB GMO
Postane Mahallesi, Nil Sokak No: 39
34940 Tuzla, İstanbul, Turkiye
T : +90 216 447 40 30 - 31 -32
F : +90 216 447 40 33
E-Mail: gmo@gmo.org.tr,
GMOShipMar@gmo.org.tr
www.gmo.org.tr

Yayın Türü / Publication Type / Sayı / Number
Süreli Yayın (3 Aylık) / Periodical, 3 months
Sayı / Number : 213

Basıldığı Yer ve Tarih / Printed in / Date
Cenkler Matbaacılık Amb. San. Tic. Ltd. Şti.
İ. Karaoğlanoğlu Cad. Civan Sok. No: 7
Seyrantepe, 4 Levent, Istanbul, Turkiye
T: +90 212 283 02 77 – 264 18 21
F: +90 212 264 05 31
www.cenkler.com

ISSN 1300-1973
Baskı Tarihi / Date of print : September 2018
Baskı Sayısı / Number of prints : 500

İÇİNDEKİLER / CONTENTS

TMMOB

GEMİ MÜHENDİSLERİ ODASI

6. ÖĞRENCİ ÇALIŞTAYI

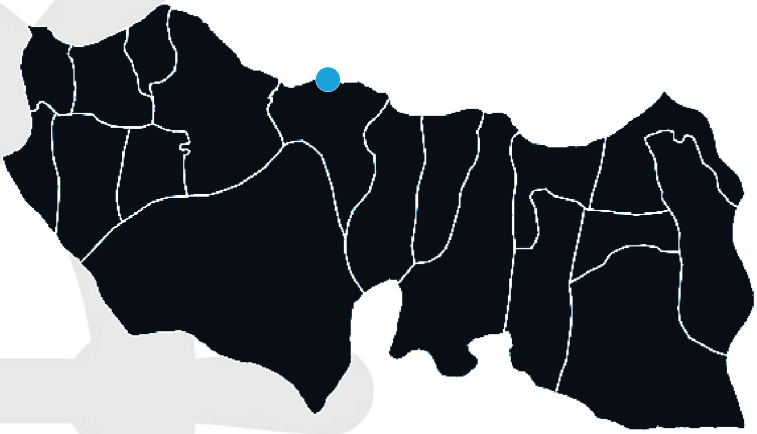

rotamız trabzon

13-14 EKİM 2018

PROF. DR. OSMAN TURAN
KÜLTÜR VE KONGRE MERKEZİ
TRABZON

Fouling Kontrol Boyalarının Servis Durumundaki Gemi Performansı Üzerine Etkilerinin Tahmini için Rasyonel bir Yöntem

M. Atlar[1], I.A. Yeginbayeva[2], S. Turkmen [3], Y.K. Demirel[4], A. Carchen[5], A. Marino[6], D. Williams[7]

mehmet.atlar@strath.ac.uk[1], irmay@chalmers.se[2], serkan.turkmen@ncl.ac.uk[3], yigit.demirel@strath.ac.uk[4]

[1] University of Strathclyde, UK

[2] Chalmers University of Technology, Sweden

[3]Newcastle University, UK

[4] University of Strathclyde, UK

[5]Newcastle University, UK

[6] University of Strathclyde, UK

[7] Akzo-Nobel, UK

Özet

Bu çalışma laboratuvar ölçümleri ve gemi performansı tahmini arasında ilişki kuran, son 20 yıldır gerçekleştirilen çalışmaları değerlendirmekte ve yine bu amaç için rasyonel bir yöntem sunmaktadır. Bu yöntem günümüzdeki modern fouling control sistemlerinin gemi üzerindeki performanslarının tahmini için kullanılan deneysel ve sayısal yöntemlerin bir kombinasyonudur. Burada "rasyonel" kelimesi tekne (ve pervane) koşullarını ve gemi boya sistemlerinin bu koşullar altında değerlendirilmesi anlamını taşımaktadır. Önerilen yaklaşım karmaşık gemi performansı problemi için tam bir çözüm sunmaktadır. Bu yöntem günümüz modern boya sistemlerinin genel özelliklerini, bahsi geçen deneysel ve modern sayısal yöntemlerin yardımıyla değerlendirdiği için "rasyonel" olarak tanımlanmaktadır. Önerilen yöntem genel kapsamlı olup herhangi bir gemi tipine ve gemi üzerinde bulunan boya sistemine uygulanabileceği gibi pasif direnç düşürücü sistemlerin değerlendirmesi icin de kullanılabilir. Bu yöntem gemi üzerindeki farklı yüzey koşullarını temsil eden düz levhalar kullanılarak elde edilen deneysel veriler ve bu verilerin gerçek gemi ölçeğine ekstrapolasyonunu içermektedir. Fakat gemi ölçeğinde daha gerçekçi ve direkt olarak performans tahmini için, kullanılan ekstrapolasyon prosedürü yerine Hesaplamalı Akışkanlar Dinamiği (HAD) yöntemi de kullanılabilmektedir. Bu yöntem özellikle yüzey kirliliği (fouling) dolayısıyla bozulan tekne yüzeyinin modellenmesinde kullanılmaktadır. Bu yöntemi kullanmak icin de deneysel veriler gereklidir. Önerilen yöntemin gerçekçiliği ve gücü "servis durumundaki" tekne yüzeylerinin etkilerini temsil etmesi ve son modern deneysel yöntem ve verilerin kullanılıyor olmasıdır. Bu yöntem araştırmacılara iki tahmin olasılığı sunmaktadır; pratik ve hızlı perfromans tahmini için ekstrapolasyon, ikincisi ise HAD metodu kullanılma olanağıdır. Bu yöntem sayesinde HAD methodu kullanma olasılığı, detaylı yüzey pürüzlülüklerinin fiziksel olarak modellenmesi zorluğu bariyerini de aşabilmektedir. Önerilen yöntemin doğrulanması için bahsi geçen gemi performansı gözlemi ve analizi sistemi kullanılarak tam-ölçekte gemi verilerinin toplanması gerekmektedir. Bu sistem gemi boyalarının yüzey kirliliği durumundaki etkilerinin değerlendirilmesi için özel olarak geliştirilmektedir.

Anahtar Kelimeler: Fouling kontrol sistemi, Antifouling boya, Gemi yüzey kirliliği (biofouling), Direnç azaltımı, gemi performansı, deney, HAD

A Rational Approach to Predicting the Effect of Fouling Control Systems on "In-Service" Ship Performance

M. Atlar[1], I.A. Yeginbayeva[2], S. Turkmen [3], Y.K. Demirel[4], A. Carchen[5], A. Marino[6], D. Williams[7]

mehmet.atlar@strath.ac.uk[1], irmay@chalmers.se[2], serkan.turkmen@ncl.ac.uk[3], yigit.demirel@strath.ac.uk[4]

[1] University of Strathclyde, UK

[2] Chalmers University of Technology, Sweden

[3]Newcastle University, UK

[4] University of Strathclyde, UK

[5]Newcastle University, UK

[6] University of Strathclyde, UK

[7] University of Strathclyde, UK

Abstract

This paper reviews two decades of bridging the gap between laboratory measurements and predicting the performance of commercial maritime vessels and presents a rational approach, which is based on the combination of an experimental and a computational procedure, to predict the effects of modern-day fouling control systems on "in-service" ship performance. Here the word "rational" reflects ship hull (and propeller) conditions as well as the approach to predicting the effect of the hull coating systems under such conditions. The proposed approach arguably provides a full solution to the complex ship performance problem. It is "rational" in terms of tackling the main features of modern-day hull coating systems with the aid of bespoke experimental testing facilities and state-of-the-art computational methods. The proposed approach is generic and can be applied to any ship type and hull coating system in the presence of biofouling and it may even be combined with passive drag reduction systems. This approach involves both the combination of experimental data from flat test panels treated with representative surface finishes and extrapolation of this data to full-scale. However, for more accurate and direct estimation of performance prediction at full-scale, the extrapolation procedure needs to be replaced with Computational Fluid Dynamics (CFD) methods, especially for deteriorated hull surfaces due to fouling; at present, such experimental data are still required. The rational nature and hence strength of the proposed approach is to represent the effect of the actual hull surfaces "in-service" by using state-of-the art experimental methods and data. This provides the option of an extrapolation procedure for practical performance estimations and also enables the use of CFD methods by avoiding the most difficult barrier of describing the actual hull surface numerically in CFD. Validation of the proposed approach requires full-scale data to be collected using a bespoke ship performance monitoring and analysis system which is dedicated to assessing the effect of coating systems in the presence of fouling. Such a system is under development as detailed in an accompanying presentation.

Keywords: Fouling control system, Antifouling coating, Biofouling, Drag reduction, Ship Performance, Experiments, CFD

1. Background

Fouling control systems for ship hulls have been under continual developments for better performance of ships, mainly for fuel economy, see e.g. (Almeida et al, 2007), (Chambers et al., 2006) These developments have been taking place under further scrutiny due to increasing environmental protection, see e.g. (Hellio and Yebra, 2009), (IMO, 2009) Hence many stakeholders of marine transportation are under the major spotlight how to predict the effect of these coating systems on a ship's performance in a rational way which is the main purpose of this paper.

Here the word "rational" reflects ship hull (and propeller) conditions as well as the approach to predicting the effect of the hull coating systems under such conditions. The proposed approach arguably provides a full solution to the complex ship performance problem. It is "rational" in terms of tackling the main features of modern-day hull coating systems with the aid of bespoke experimental testing facilities and state-of-the-art computational methods. Within this framework, the approach has its roots in the long-term research works which are led or involved by the present authors e.g. (Candries and Atlar, 2003), (Demirel et al., 2016), (Yeginbayeva et al., 2017), (Carchen et al., 2017), Turkmen et al (2018), Atlar et al (2013a) and hence it is worthy to review some of the past research works, which have contributed to the development of this approach, as summarised in Section 2 of the paper.

The accurate prediction of ship performance is still one of the most challenging problems for naval architects and has great interest to many stakeholders of the shipping transport. This is not only to improve the transport efficiency but also due to increasing scrutiny to reduce environmental impact. Because of these reasons, the ship hull fouling control systems have been continually developing and hull surfaces have become more and more complex to analyse.

Traditionally naval architects assume that the ship hull resistance is made of the skin-friction, which is viscous in origin and hence closely associated with the hull surface conditions (including fouling control systems), and that of the pressure component due to the 3D effects of the hull and waves. Until recently, the naval architects have had the comfort of approximating the hull-skin friction based on the Froude's equivalent flat approach combined with the empirical correlation allowance factors for different surface finish (including fouling control system) values based on their experience. However, due to the recent developments in hull coating industry, new experimental measurement facilities and techniques as well as the computational (CFD) methods, this approach is now under the spot light as discussed in the following.

The ship hull surfaces have been changing, primarily, due to the use of different coating systems, which can have a physical or fouling release based control mechanism, e.g. (Anderson et al., 2003) or chemical, bio-based fouling control defence mechanism, e.g. (Zhou, 2015). In addition, due to further scrutiny, these coating systems are recently being combined with novel drag reduction mechanisms, e.g. riblets being embossed on fouling release coating system or compliant coating system, (SEAFRONT, 2014). These developments have been bringing about the question of using the traditional skin friction data based on the flat plates of different sizes and their extrapolation to full-scale for ship hulls. At least, the correlation allowance factors to reflect the surface finishes with these new coating systems would require upgrading. Recent developments in the CFD field have lifted the barriers, at least for the scale effect. As such, there is no need to employ the Froude's flat plate approach and it is hence possible to directly calculate the viscous hull resistance in full-scale by taking into account the 3D effects, e.g. (Demirel, 2015). Although this is very powerful, the CFD methods in representing the realistic hull surface finish including different fouling control systems are still in their infancy and hence requiring practical approaches which can make use of some critical surface hydrodynamics data from model experiments in a laboratory environment. For this purpose, experimentally determined roughness function (or velocity loss function) of representative hull surfaces, which can even include the effect of biofouling, is the most practical data to be able to use of the power of CFD. However, the provision of this experimental data still requires relatively systematic tests by using bespoke testing facilities (e.g. friction pipes, channels, towing tanks, rotating discs/drums etc.) with special measuring equipment (e.g. LDA's, pressures gauges, load cells etc.) and even in a special environment to use actual or artificial seawater. Furthermore, the measured hydrodynamic data should be related to the surface roughness/texture characteristics and hence requiring the accurate measurements of the surfaces and roughness characteristics using special measurement devices (e.g. preferably non-contact optical or sophisticated mechanical devices)

In using the above-mentioned facilities, in comparison to the friction pipe or rotating disc methods, the use of the friction plane methods is more practical in terms of the required surface finish applications, surface roughness and force measurements due to the use of simpler flat surfaces with zero pressure gradients. However, the necessity of using large towing tanks with preferably large flat planes to be towed at high speeds to achieve high Reynolds numbers is one of the downside of these facilities resulting in higher costs. On the other hand, the analysis of the skin friction characteristics by measuring the pressure drop in a friction pipe or by measuring the tow force on a friction plane is an "indirect" method but it is still practical and cost economical as opposed to the "direct" method which requires the measurement of boundary layer profiles on the test surfaces by using e.g. expensive and complex Laser Doppler Anemometry (LDA) or water unfriendly hot-wire anemometry facilities. The use of LDA will require more accessible channels and costly set-up systems, which may not be readily available and requires much longer data collection time that further increases testing costs. Perhaps one compromised facility, that has been increasing in applications, is the fully turbulent flow channel (FTFC), e.g. (Politis et al., 2013), (Schultz and Flack, 2013). The FTFC can circulate the fully developed turbulent flow at its rectangular cross-section of measuring section, which can accommodate interchangeable flat panels with different finishes, as opposed to the circular cross-section of the friction pipe and the pressure drop over the test panels due to the skin friction can be measured. The FTFC facilities, apart from being practical in terms of much quicker measuring time and size compared to the larger towing tanks and other channel facilities, they have the advantage of circulating seawater which is an invaluable feature for testing coating surfaces in the presence of biofouling.

It is a well-known fact that the main purpose of using fouling control system on ship hulls is to control the development of biofouling in the most cost economical way. However, as soon as a newly coated hull is subjected to seawater, light biofilm immediately starts to build up as the conditioner and to attract other fouling types. Depending upon the fouling control system type and many other complex factors which include the vessel's operating waters and operational profile, the biofilm types, coverage and grades vary. In fact, these have been the subject for many researchers and still heavily occupies the marine biofouling and technology community since most of the hull fouling control systems still suffers from the biofilm one way to other, e.g. (Callow and Callow, 2002), (Durr and Thomason, 2010). It is, therefore, more realistic to include, at least, the effect of light biofilm in the performance prediction of any coating type. Under the circumstances, perhaps the most practical and rational approach to include the biofilm effect is to grow them on representative test panels to measure their effects on skin friction using the above-mentioned test facilities. However, this will in turn require special facilities either to grow the biofilm on the test panels in natural sea environment (e.g. attached to ship hulls or other means), e.g. (Atlar et al., 2015) or using bespoke seawater circulating tanks (e.g. slime farms) to grow in laboratories, e.g. (Yeginbayeva, 2017)

In this section of the paper, so far, a general background information is presented which has motivated the authors to propose the prediction method presented. However, any prediction method will require validation and as far as the ship performance is concerned, such a validation task should involve performance measurements on board of a ship. Within this context, the interest to ship performance measurements can be as old as the history of ships occupying the naval architects with ever-growing pace. This is particularly true due to the recent scrutiny by IMO on the GHG emission control of ships as well as volatile fuel prices (IMO, 2009). As a result, there has been some companies in the market offering their services and equipment for ship performance monitoring and analysis. Some of these companies are using their hardware and software systems which can monitor, collect and analyse the performance on-board (on-line) using the collected data, e.g. (BMT SMART, 2017), (ENIRAM, 2017), while some of them are analysing the performance onshore based on the customers' data, whatever way the data is collected e.g. (CASPER, 2017), (Munk, 2006). Perhaps the most important point from the fouling control system performance point of view, how dedicated these systems are to monitor solely the effect of fouling build-up on the ship hull and propeller, and hence analysing the fouling control system performance with an acceptable uncertainty level. This will need robust hardware (i.e. torque gauge, speed log, weather pack etc.) supported by dedicated online data collection system with practical filtering ability and robust, deterministic analysis method to extract mainly the unwanted effect of the environment and others as attempted e.g. by (Carchen et al., 2017b). Within the framework of ship performance measurements, one should also mention about the new ISO 19030 for hull and propeller performance measurements (ISO, 2016). This voluntary standard has been recently established to enable ship owners and operators to compare hull and propeller solutions, including fouling control systems, and to select the most efficient option for their vessels and fleet. Therefore, its wide spread adoption is being taken up by major coating stakeholders and integrated in their commercial products for prediction technologies, e.g. Intertrac ® (Intertrac, 2017).

2. Review of Research Activities

This section presents a review of the past and current research works which have contributed to the development of the approach presented in this paper and conducted by the present authors or through their participation in these works.

The first major research work campaign contributing into the present study conducted in early 2000s to provide scientific evidence on the surface roughness, boundary layer and drag characteristics of newly applied two different types of hull coatings which were silicon-based "Fouling Release" (FR) and biocidal "Self-Polishing Co-polymer" type, e.g. (Candries, 2001), (Candries et al., 2003). This research work established the superior surface roughness/texture and hydrodynamic drag characteristics of the FR coatings over the SPC types by using some bespoke hydrodynamic testing facilities, e.g. the Emerson Cavitation Tunnel boundary (ECT) layer set-up as well as using the traditional towing tank and rotating drum facilities. The boundary layer set-up also necessitated the provision of the 2D-LDA facility and its use for the velocity profile measurements of large flat panels (1m long) covered with different coating systems and applications, e.g. "Spray vs Roller" applications. The most important contribution of this campaign was that the confirmation of the superior drag performance of the FR coatings with the provision of the systematic surface roughness, boundary layer and skin friction data by using the three different types of testing facilities. Amongst them, the boundary layer test set-up established in ECT and LDA facility was the dark horse of the research works and data produced in this campaign which involved coating applications in the laboratory for “cleanly or newly applied” ship performance conditions and hence did not represent the applications on “in-service” performance conditions.

Whereas ships operate at sea “in-service” conditions and the hull surfaces in these conditions cannot be represented by relatively smooth test surfaces where subject coatings are applied cleanly in laboratory conditions. Therefore the second follow-up research campaign, which was recently completed, involved an experimental investigation into the performance characteristics of modern FR, SPC and Control Depletion Polymer (CDP) coatings in “cleanly applied” as well as “in-service” conditions, e.g. (Yeginbayeva et al., 2016), (Yeginbayeva, 2017) In this second campaign the “in-service” condition is to reflect the representative hull roughness at least in terms of the average hull roughness height and representative modern day commercial coatings applied on the flat test panels which were tested in the presence of light biofilm (i.e. slime) and clean condition (i.e. freshly applied).

In complementing the above stated two major research campaigns, the third research campaign has started relatively later and has been still continuing to develop a bespoke ship performance monitoring and analysis system, see e.g. (Carchen et al., 2017a), (Carchen et al. 2017b). The main objective and hence difference of this campaign from other ship performance monitoring system developments is to investigate and hence develop a dedicated system to assess the effect of any fouling control system on the ship performance when it is cleanly applied as well as under the effect of fouling growth at acceptable uncertainty levels. This research campaign has its origin in an earlier research, (Hasselaar, 2011) which was conducted by using a modest hardware system installed on-board the old research vessel, R/V Bernicia, of Newcastle University. Although that initial research had only made a modest contribution to the above-stated objective of the current research, it had highlighted the complexity of the ship monitoring problem by using such level hardware on an old small vessel which is subject to continuous external disturbances and hence motion control problems. The follow-up current research, therefore, has been initiated to achieve this objective using state-of-the-art equipment on a modern research vessel as will be discussed below.

In addition to the above reported three doctoral research campaigns, which made use of physical tests conducted in model and full-scale, there were other complementary research campaigns which resulted in the developments of various major and modest level of testing apparatus and facilities and hence making important contributions into the development of the proposed prediction approach in this paper. These R&D activities are briefly involved: (a) introduction of the Newcastle University (UNEW) standard test panels; (b) surface measurements of the UNEW test panels using bespoke surface analysers; (c) further development of the Emerson Cavitation Tunnel (ECT) boundary layer test-set up; (d) design and commissioning of the UNEW Full Turbulent Flow Channel (FTFC) for pressure drop measurements; (e) design and commissioning of a laboratory based slime growth facility; (f) design and commissioning of the UNEW multi-purpose research vessel, The Princess Royal, with the bespoke strut arrangement for the collection of naturally grown slime at sea; (g) design and installation of a bespoke ship performance monitoring and analysis system.

(a) UNEW standard test panels

While the use of large and flat test panels is a preferred option to produce systematic roughness and hydrodynamic test data, when these panels will be tested in different facilities and under challenging environmental conditions (e.g. at sea) they have to be practical and hence compromised in terms of size and materials to be made of. By taking these restrictions into account, the size of the flat test panels, which are interchangeably used in the different test facilities of UNEW are limited to practical dimensions of 600 mm x 210 mm x 35 mm and made from acrylic for easy transport as shown in Figure 1 although the earlier versions were made from steel.

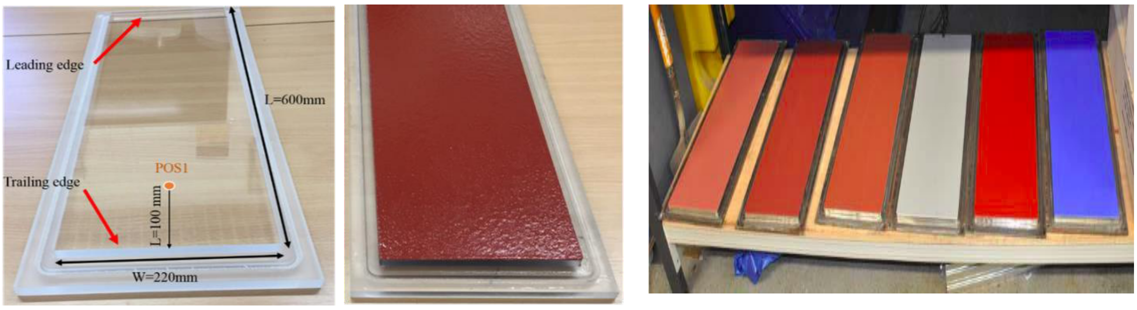

Fig. 1. UNEW Standard test panels

(b) Surface measurements of test panels

Accurate surface roughness measurements of the test panels with different finishes can be made by using different roughness measurement devices which can operate based on optical or mechanical principle. The manageable size of the UNEW test panels lend themselves to be surveyed by using the laser-based roughness profilometry device (see Figure 2) which provided the statistical roughness characteristics of these surfaces at focused areas with great accuracy. Furthermore, the measured data is independent of any potential surface contact problems that can be encountered with the mechanical contact based roughness devices especially with silicone based coatings.

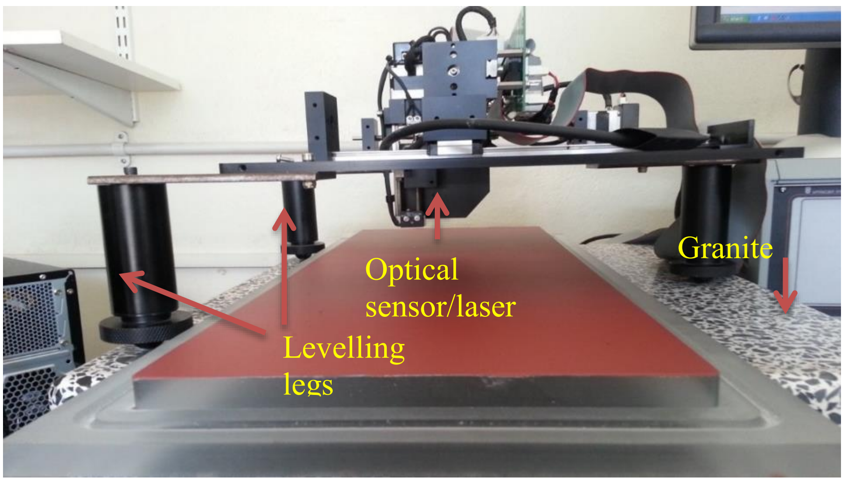

Fig. 2. Surface roughness profilometry device

(c) Further improvement of ECT boundary layer test set-up

While the Newcastle University has had the Emerson Cavitation Tunnel since 1949, this facility has never been used for coating research until the above mentioned 1st research campaign was started.

This facility, therefore, was equipped with the 1st boundary layer set-up in its testing section to accommodate 2.0 m long flat test panel, as shown in Figure 3, to measure the boundary layer development over the coated surfaces placed on the latter 1m part of the test panel.

Fig. 3. Initial boundary layer test set up in Emerson Cavitation Tunnel

While this set up served the purpose for the 1st research campaign, during the upgrading of the ECT in 2009, a specially designed insert section was commissioned to increase the tunnel inflow speed at the measuring section and a new boundary layer test set-up was combined with the insert, (Atlar, 2011). The new set-up was designed to accommodate the standard UNEW test panels at the latter part of the insert as opposed to the 1m long larger test plates used in the 1st research campaign which were not easy to handle and subject to vibrations. The improved test set-up would not only increase the tunnel inflow speed but also reduce vibration and efforts for the smaller size test panel installation. Furthermore, new measuring section of the ECT with enlarge and mono-block windows has provided much easier LDA access to the boundary layer set-up and hence more reliable and systematic boundary layer data collection with less effort. See Figure 4 for the current boundary layer set up at ECT.

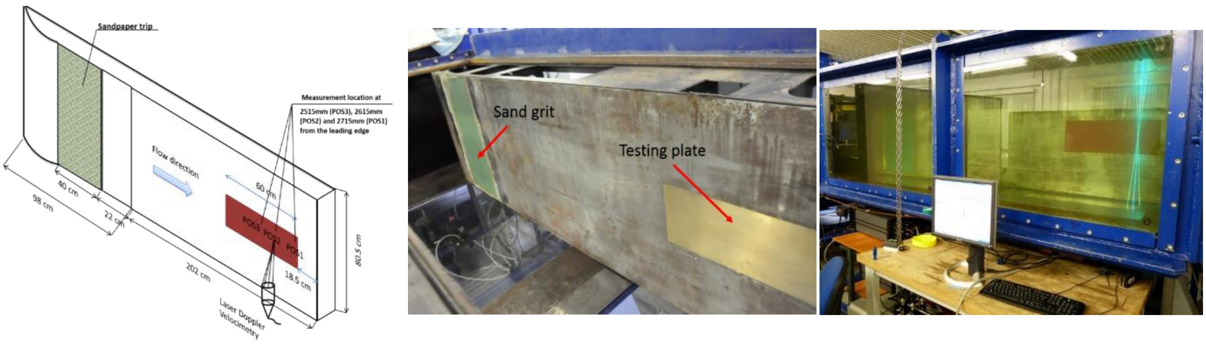

Fig. 4. Improved boundary layer test set up in Emerson Cavitation Tunnel

(d) Design and commissioning of Full Turbulent Flow Channel (FTFC)

As stated in the background section, hydrodynamic tests involving coating performance can benefit from bespoke facilities, e.g. FTFC, especially for tests in the presence of biofouling. Within this framework, classical flow cell facilities, which are used mainly by marine scientists, are designed to determine the shear force levels to release various type of marine biofouling (e.g. juvenile barnacles, slime etc.) grown on very small size test slides. The pressure drop across the surfaces of these test slides, which are located in the measuring section of the FTFCs, are measured by using differential pressure gauges at the measuring section.

An existing flow cell in the UNEW was converted to the FTFC for skin friction drag analysis by modifying its measuring section as such this section can accommodate two standard UNEW flat test panel at the top and bottom boundaries of the measuring section. By measuring the differential pressure along the test panels, which may be coated with different fouling control systems even in the presence of light biofilm, the skin friction characteristics of the test panels can be determined. Figure 5 shows the UNEW FTFC which was designed and commissioned as part of the recently completed FP7 SEAFRONT Project (SEAFRONT, 2014) Apart from developing a fully turbulent flow in its measuring section, a FTFC facility has the advantage of testing flat test panels with biofilms in sea water and with a very quick turn over time as opposed to longer testing times with more complex set-up of other testing facilities which have to use fresh water and costly to run, e.g. towing tanks, large circulation channels with LDA etc. The FTFC facilities, therefore, have been recently introduced in the hydrodynamic testing community, especially for coating research. FTFC facilities can be also used for ageing (or polishing) test of a SPC type coating system applied on these test panels. Such a multi-purpose system (i.e. to conduct ageing and pressure drop) has been designed and commissioned at the UNEW very recently to investigate the hydrodynamic performance of SPC type fouling control system “in-service” conditions, e.g. (Politis et al., 2013), (Yeginbayeva, 2017)

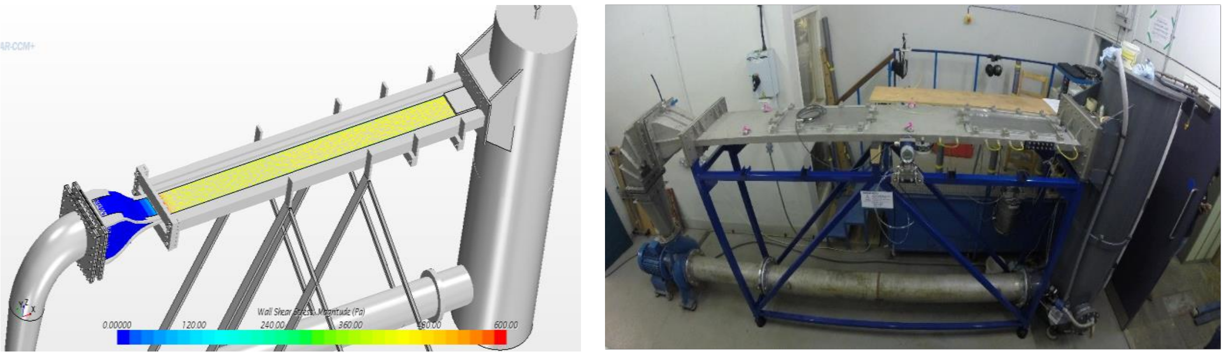

Fig. 5. UNEW Fully Turbulent Flow Channel: Testing section details (left); overall system view (right)

(e) Design and commissioning of a laboratory-based slime growth facility

As stated earlier, light biofilm or slime is an essential contribution to the “in-service” condition of a ship hull and hence should be part of the hydrodynamic modelling in performance assessment. As also discussed earlier, perhaps the most rational way of including the effect of biofilm in the performance assessment, is the experimental way by exposing the test panels coated with subject coatings to the slime growth. The exposure can be either naturally at sea, which will be discussed in the next section, or in specially designed tanks, which can be called as slime farm, at laboratories under controlled condition. Such a latter facility was designed and commissioned at the UNEW based on a jet flow based slime growth facility, which circulates the natural seawater at relatively slow speed to simulate the relatively dynamic action of the flow, as shown in Figure 6, (Yeginbayeva et al., 2016). This facility can accommodate four UNEW test panels and can develop slime much faster rate than grown at sea in a controlled manner.

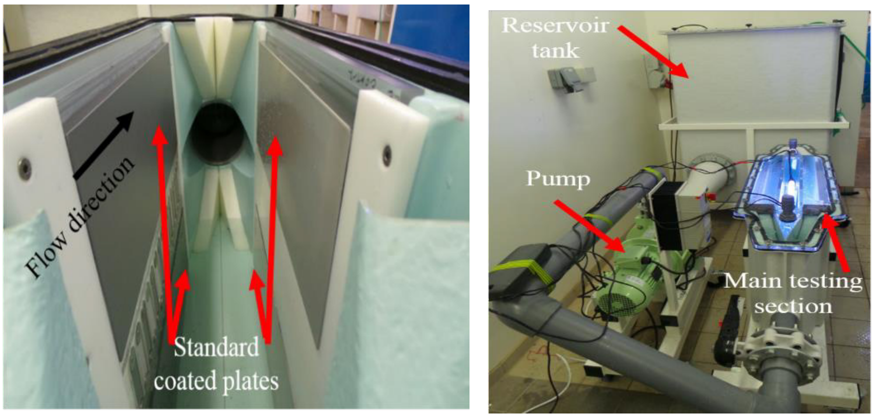

Fig. 6. UNEW laboratory-based slime growth facility

(f) Design and commissioning of multi-purpose research vessel with the bespoke strut arrangement for collection of naturally grown slime at sea

In 2009 UNEW was replaced their ageing old research vessel RV *"Bernicia"* with a new 18m, 43t displacement of modern catamaran RV *"The Princess Royal"* that can achieve 20 kn max speed while mostly operating at 15 knots of design speed. As shown in Figure 7 the vessel was named after the HRH The Princess Royal and designed by the lead Author and his research group, e.g. (Atlar et al. 2013b). The mission of the vessel is a multi-purpose encompassing number of marine science and technology R&D activities including marine fouling control research and ship performance monitoring. Hence, the Princess Royal was equipped with a specially designed strut arrangement, which is attached to the moon pool plug of the vessel and this arrangement can accommodate eight UNEW test panels, as shown in Figure 8, (Atlar et al., 2015). These panels are to be exposed to the seawater and hence grow natural slime on them under the full dynamic condition of the vessel in her motions as naturally expected. Such set up may not necessarily represent the "in-service" conditions as a large commercial vessel at world seas but still represent much closer simulations of naturally grown slime under the controlled "in-service" condition to model its effect.

(g) Design and installation of a bespoke ship performance monitoring and analysis system

As one of her most important missions and part of the ongoing research campaign on the ship performance monitoring, *The Princess Royal* has been equipped with a comprehensive bespoke performance monitoring hardware systems, as illustrated in Figure 8.

Fig. 7. UNEW RV- The Princess Royal (left) and its strut arrangement to carry fouling plates (right)

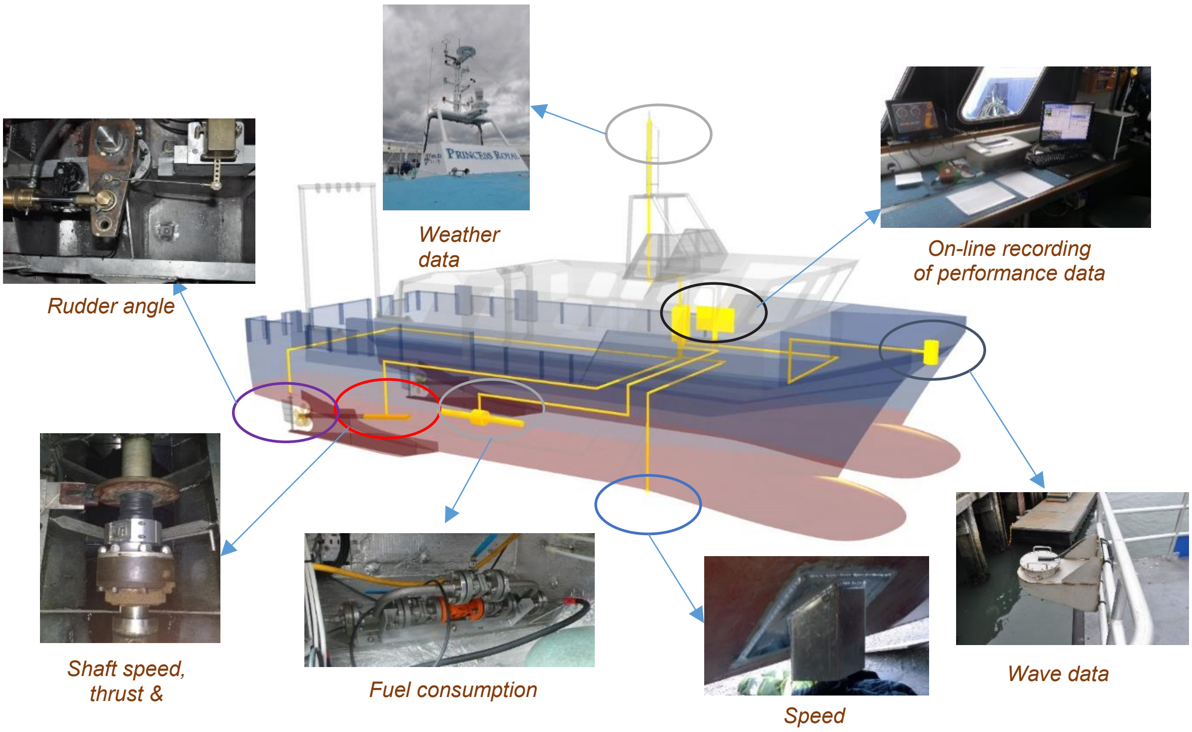

Fig. 8. UNEW Research Vessel performance monitoring hardware system

These hardware systems included tailor-made torque and thrust loading gauges on her both shafts as well as rotation speed gauges. In addition to the normal navigational data (e.g. speed over ground, heading course over ground etc.), the R/V exhibits a variety of speed logs to measure the vessel speed through the water and an accurate on-board weather station to measure the wind speed/direction. The wave height at forward vicinity of the vessel and vertical deck motions are measured through dedicated equipment located on board while the fuel consumptions of both engines are also measured by dedicated fuel meter systems. All these hardware systems are integrated and controlled by a specially developed software which collects and displays the collected data in time series or averaging on a dedicated display on the vessel navigation deck.

The above-reviewed activities, i.e. from *(a)* to *(g),* were mainly experimental and conducted by using the existing testing facilities of UNEW as well as recently developed new facilities. While these activities and facilities have provided great insight into the performance prediction of modern fouling control systems and collected invaluable data, the performance predictions in full-scale still require a sound extrapolation procedure or other prediction methods. Within this framework, (Granville, 1958 and 1987) proposed a similarity law scaling procedure to predict the effect of particular surface roughness on the frictional resistance of any arbitrary body covered with the same roughness, by extrapolation of data from flat plates with the particular roughness to full-scale lengths. This provides means of obtaining a plot of skin friction coefficient against the length based *Reynolds number* for different lengths of flat plates with the same roughness, in order to predict the full-scale resistance of ships having that roughness.

Based on his experimental work with different coating surfaces and grades of marine biofouling (Schultz, 2007) presented a simple and effective procedure in applying Granville's methodology to predict the effect of different ranges of coating roughness and biofouling on the resistance of a full-scale ship (*Oliver Hazard Perry class frigate or FF7*). In this procedure, the prediction of the effect of the roughness and fouling is restricted to the frictional resistance of a planar surface of arbitrary length which in fact represents both a test surface in model scale and an actual ship surface in full-scale with the same underwater length of the ship. In the algorithm of this procedure, the additional drag due to the coating roughness and fouling is predicted regarding roughness allowance, ΔC_F, to be included in the resistance coefficient of the ship. Within the assumptions of the Granville's extrapolation, Schultz's algorithm relies on the skin friction characteristics (mainly roughness functions) of the representative arbitrary length of flat surfaces with the same roughness. As long as the skin friction data is obtained from tests within model size test panel in a suitable hydrodynamic facility, this data can be extrapolated to full-scale flat plate, which represents the ship hull, by using the algorithm based on the wetted length of the full-scale ship and speed.

Practical application of Granville's extrapolation is based on the assumptions of flat plate and uniform distribution with the similar roughness function of the arbitrary size surfaces (i.e. model and full-scale). Apart from neglecting the 3D effects, the further assumption of the uniform and constant roughness function for one speed is another arguable assumption of Granville's approach even for a flat plate. This is due to the differences in local shear stress and hence expected change in the skin friction velocities along the flat plate. In order to improve these shortcomings, in his doctoral thesis, (Demirel, 2016) proposed a CFD based method, where the experimentally determined roughness functions, including the effects of biofouling, can be built in the wall functions of a commercial CFD code to predict the skin friction resistance of a ship hull in full-scale. Demirel demonstrated this effect on a representative full-scale ship by comparing the different approaches, which were all based on the Schultz's roughness function data (Schultz, 2007), namely by using: (1) Granville's extrapolation; (2) an unsteady RANS based CFD method but assuming that the hull still represented by flat plate; and (3) the same CFD method with the exact hull geometry.

While the above R&D activities mainly concentrated on the effect of coating roughness and fouling on ship hulls, the recent developments of hull coating systems, especially those of the FR types, have increased the applications of these coating systems on propellers to keep them free of biofouling. This has also triggered the investigations how to model the effect of the propeller surface roughness including the coatings and biofilm. Within this framework e.g. (Atlar et al., 2002) conducted numerical investigations on the open water performance analysis of propeller by using a boundary element theory based tool in which the effect of blade surface losses due to a different application of coating roughness was simulated in the appropriately selected drag coefficients of the propeller blade section. In this selection, the increase in sectional drag was represented by a semi-empirical formula which was related to different grades of measured paint application roughness based on various assumptions. In a later development, by taking advantage of the Granville's approach and its generic nature, which can be applied to any length of flat surface, Seo et al (2016) applied this approach to predict the blade surface losses for container ship propellers coated by foul release coatings, tested in EU-FP7 TARGETS Project, (TARGET, 2013) and different grades of biofoulings as proposed by (Schultz, 2007).

3. Main Objectives

Based up the background stated in *Section 1* and the review of the contributory research work in *Section 2* the main objective of this paper is to present a rational approach to predicting the effect of a modern-day fouling control system on "in-service" performance of ships as described in Section 4 and demonstrate its application *in Section 5*. Furthermore, the paper proposes a validation method for the proposed approach as described in *Section 6* and finally presents some concluding conclusions in *Section 7.*

4. Description of the Approach

As summarised in Section 2 the prediction approach, which is described in the following paragraphs from I to X, includes any of the following three procedures (1-3) that can be used depending on the level of accuracy required:

1) Granville's extrapolation with the flat plate assumption
2) CFD based method with the flat plate assumption
3) CFD method with the actual hull geometry

I. Each of the above methods is based on the hydrodynamic skin friction characteristics of the representative test surfaces which are flat panels. It is therefore essential to prepare these test surfaces which will be tested in a suitable hydrodynamic testing facility. Such practical test surfaces can be similar to e.g. UNEW standard test panel as described in Section 2 and shown in Figure 2.

II. Surface preparations of the test panels are critical, that should mimic the actual ship hull surface, in theory. Although this will not be possible in practice, a reasonable compromise can be made e.g. based on the experience and data of paint manufacturers or shipyards who regularly measure the hull roughness characteristics. If such data are available based on experience, this can be mimicked by using a suitable grade of sand grit to be applied on the standard test panels to represent the physical hull surface roughness excluding the paint. Next will be the application of the subject fouling control system using appropriate method (i.e. spraying or rollering etc.). Figure 9 shows the application of such surfaces and their roughness characteristics in Figure 11.

III. Surface preparation described in II excludes the effect biofilm which is an important contribution to the "in-service" condition. It is, therefore, necessary to expose the coated test panels to biofilm growth. As stated earlier this can be achieved either in a slime farm in the laboratory condition or naturally at sea which is preferable. Figure 10 shows the typical UNEW test panels having exposed to the slime growth on the strut arrangement of the UNEW research vessel.

	
Newly applied FR type with 'low' density of introduced sand grit	Newly applied FR type with 'high' density of introduced sand grit

Fig. 9. Flat test panels representing FR coatings with mimicked 'low' (left) and 'high' (right) density of hull roughness

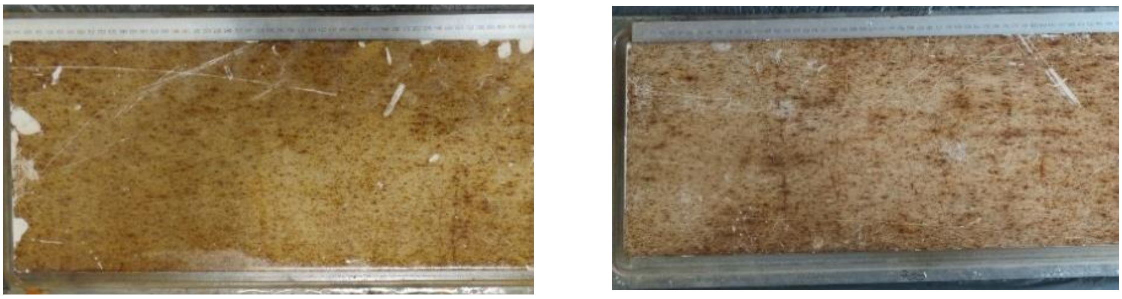

Fig. 10. Flat test panels with FR coatings (normal finish) exposed to natural slime growth for 6 months

IV. Having prepared and conditioned the test panels with representative "in-service" conditions, the next stage is to measure their surface roughness characteristics using, preferably, a laser-based optical profilometry device, e.g. as shown in Figure 2. Using such device enables to conduct detailed analysis with more detailed statistical roughness and texture parameters which in turn provides a better option for correlations with the skin friction data of the surfaces. For example, Figure 11 shows the sample test surface roughness characteristics with the FR coated surfaces applied using 'normal' and mimicked 'high density' hull roughness finishes.

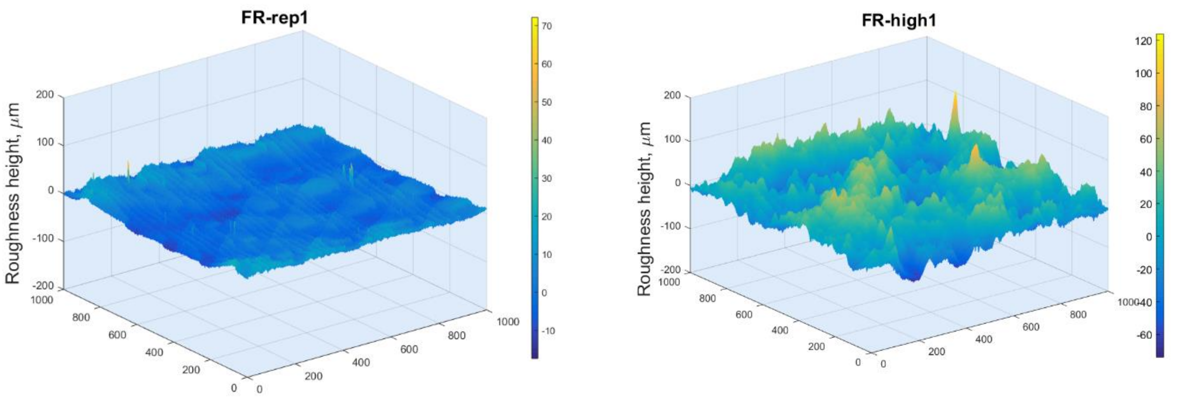

Fig. 11. Surface roughness images of FR test surfaces, normal finish (left); mimicked hull roughness (right)

The measurement of surface roughness with biofilm has its own challenges but can still be conducted by using the laser profilometry device when the test panel with the biofilm coverage is kept in the water.

V. Next stage of the procedure is to conduct basis hydrodynamic tests to determine the skin friction characteristics of the test panels. For this purpose, as reviewed in Section 2, various testing methods can be used. In this section, we refer to the well-established boundary layer measurement tests established in the Emerson Cavitation Tunnel using the 2D, LDV set up, as shown in Figure 4. These tests enable the measurements of boundary layer velocity profiles in 2 directions (in-flow and wall normal) at sufficient accuracy (e.g. 80 points vertically) at various longitudinal positions along the test panels as shown in Figure 12. It should be born in mind that the measured velocity profiles (and hence skin friction data) of the test panels are analysed and presented relative to the hydrodynamic characteristics of the hydraulically smooth reference surfaces (i.e. test panels), which are made usually made from clear acrylic and their hydrodynamic characteristics are also measured along the coated rough test panels.

VI. Whether Granville's extrapolation procedure or any of the above stated CFD methods will be used, there is a need to analyse the measured boundary layer velocity profiles in the previous step (V) using a suitable method and to represent this data in terms of "Roughness Function" of the representative surfaces.

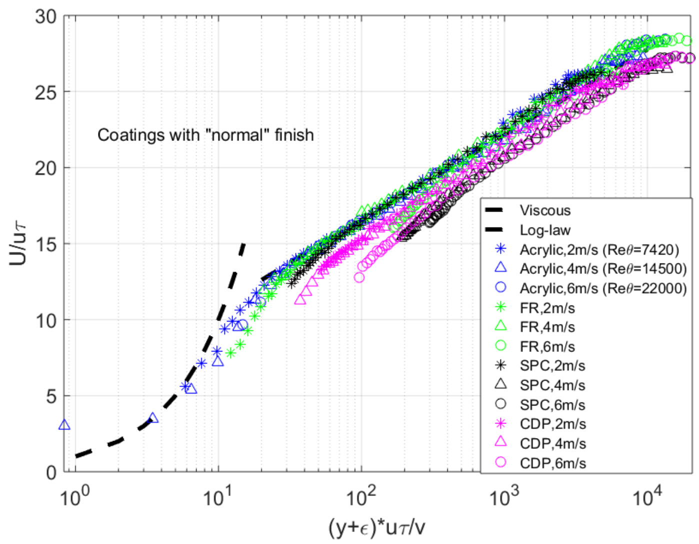

Fig. 12. Sample mean streamwise boundary layer velocity profiles of FR, SPC and CDP coatings with "normal finish". Inner scaling of velocity profiles normalised by skin friction velocity, u_τ and v/u_τ.

Here the roughness Function is further retardation (i.e. velocity loss) of the flow in the boundary layer due to the specific roughness of the test surfaces, which is caused by any of the mimicked hull roughness, coating, biofilm or combinations of these causes that manifest themselves as the additional skin friction drag. As given in Equation 1 and shown representatively in Figure 13, the determination of the Roughness Function ⍰U+ requires the presentation of the measured boundary layer velocity data as the non-dimensional boundary layer velocity U+ against the non-dimensional normal distance y+ from the test surface.

(1)

$$\Delta U^{+} = U^{+}_{smooth} - U^{+}_{rough}$$

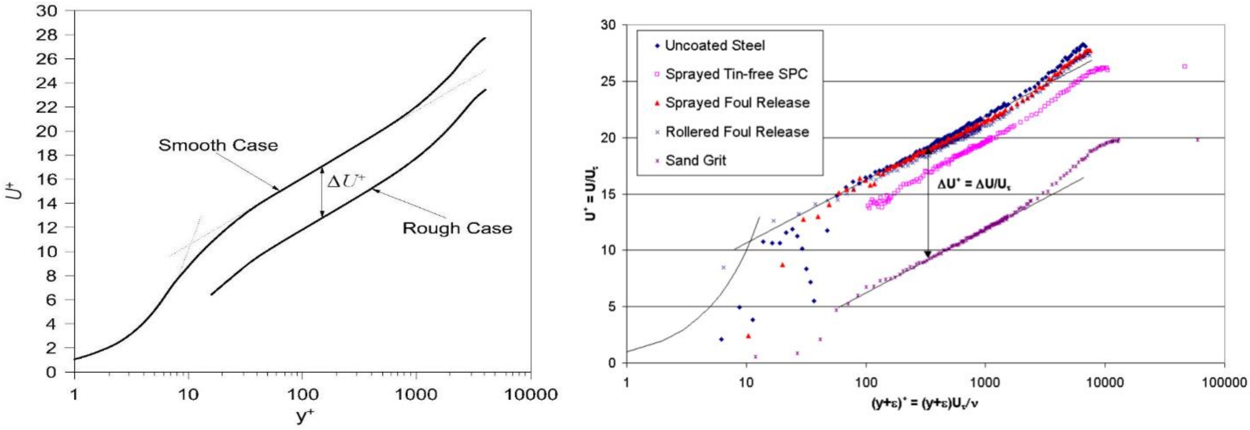

Fig. 13. Description (left) & sample determination of Roughness Function (right)

VII. Having determined the roughness function, which is non-dimensional and assumed to be the same for the full-scale hull at corresponding Reynolds number, if the Granville's extrapolation method will be preferred, all it remains to apply the Reynolds number based scaling by using the main input data which are: L_{PLATE}, the test surface length; L_{SHIP}, the ship wetted length; $C_{F,SMOOTH}$, the hydraulically smooth surface skin friction coefficient. By using Granville's extrapolation, as shown in Figure 14 schematically, Ship $C_{F,ROUGH}$, the skin friction coefficient of the ship in full-scale can be determined and hence the additional skin friction drag coefficient as in Equation 2:

$$\Delta C_F = \frac{C_{F,ROUGH} - C_{F,SMOOTH}}{C_{F,SMOOTH}} \tag{2}$$

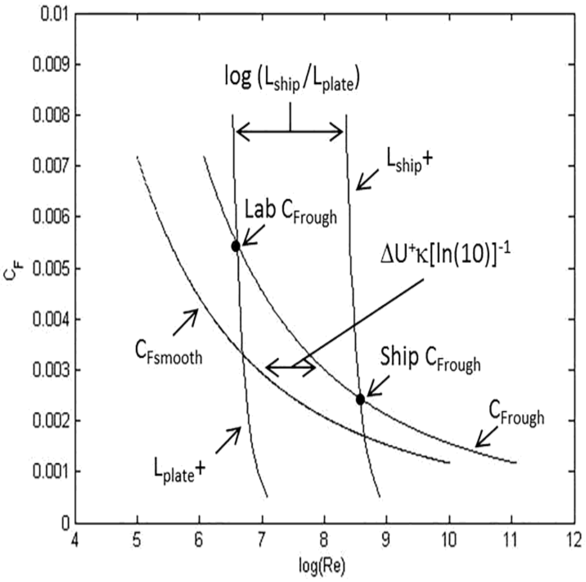

L_{plate} = Test panel length
L_{ship} = Ship length
$C_{F,\,smooth}$ = Smooth surface friction drag coeff.
C = Rough surface friction DC

$L^+ = Re\,.\left(\sqrt{\frac{C_F}{2}}\left(1 -\right.\right.$

Re = Reynolds number, length based
K = von Karman Constant
ΔU^+ = Roughness Function

$C_{F\,smooth}$, ΔU^+, L^+_{plate} → Input
$C_{F\,rough}$ for ship → To be estimated

Fig. 14. Schematic representation of Granville's algorithm

VIII. The estimation of the additional skin friction in the above step (VII) is based on the flat plate and uniform roughness function assumptions. As reviewed earlier, in Section 2, these shortcomings can be overcome by building the experimentally determined roughness function data of specific surfaces (i.e. in terms of $\Delta U^{+} = f(k^{+})$, where k^{+} is the Roughness Reynolds number) in the wall function or in the turbulence model of a CFD code, as originally proposed by (Patel, 1998). Demirel recently implemented this approach by using Schultz's experimental data for a representative coating surface and different grades of biofoulings, as shown in Table 1, (Demirel, 2015).

Table 1. A range of representative coatings and fouling conditions, Schultz (2007).

Description of condition	NSTM rating*	k_s (μm)	Rt_{50} (μm)
Hydraulically smooth surface	0	0	0
Typical as applied AF coating	0	30	150
Deteriorated coating or light slime	10-20	100	300
Heavy slime	30	300	600
Small calcareous fouling or weed	40-60	1000	1000
Medium calcareous fouling	70-80	3000	3000
Heavy calcareous fouling	90-100	10000	10000

*NSTM (2002)

This data was built in the wall functions of the commercial CFD software Star CCM+. The wall functions are mathematical expressions which relate the viscosity influenced regions between the surface (wall) and log-law of the boundary layer and hence makes the assumption that the near wall cells are positioned within the logarithmic region of the boundary layer. Their implementation in the code by no means is an easy matter by taking into account the different flow regimes (i.e. hydrodynamically smooth, transitional and fully rough) as function of k^{+} values. Figure 15 shows Demirel's proposed roughness function models, which are formulated as in Equation (3), to fit Schultz & Flack's experimentally determined roughness functions.

$$\Delta U^{+} = \begin{cases} 0 & \rightarrow \quad k^{+} < 3 \\ \frac{1}{\kappa}\ln\left(0.26k^{+}\right)^{\sin\left[\frac{\pi}{2}\frac{\log(k^{+}/3)}{\log(5)}\right]} & \rightarrow \quad 3 < k^{+} < 15 \\ \frac{1}{\kappa}\ln\left(0.26k^{+}\right) & \rightarrow \quad 15 < k^{+} \end{cases} \tag{3}$$

The above roughness function models were built based on the surface conditions given in Table 1. However, due to the fact that there is no universal roughness function for all roughness types, the roughness functions for any other particular surfaces need to be determined experimentally by using the experimental procedure described above and models need to be built-in the CFD software.

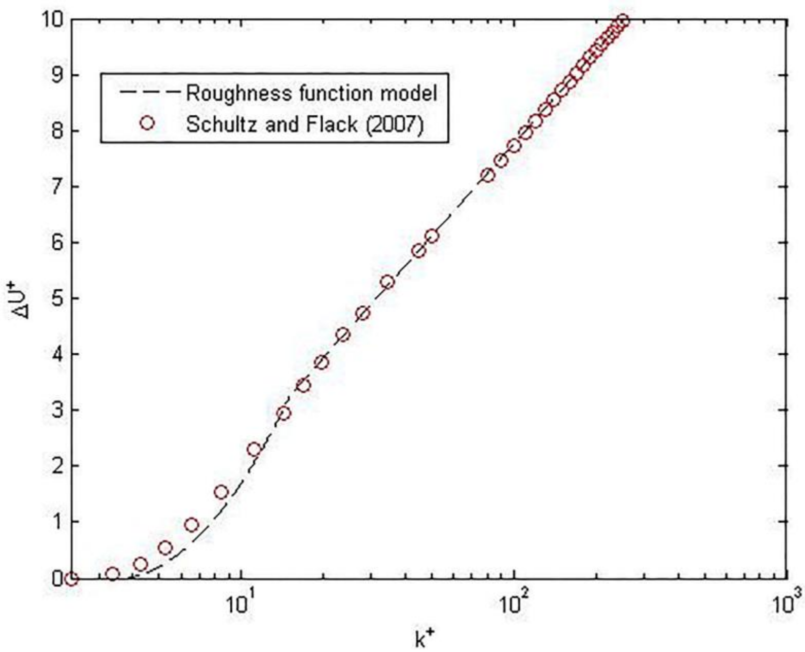

Fig. 15. The proposed CFD roughness function model for experimental Schultz & Flack (2007) roughness function data

IX. Having established the suitable wall-functions in the CFD code, next stage is the estimation of the hull resistance in full-scale which is a routine computation by applying suitable boundary conditions and meshing technique. At this stage, for practical reasons, the assumption of the hull form as a flat plate with no free surface may be preferred to reduce the computational time. Otherwise, the full 3D shape of the hull can be taken into account including the action of the propeller in the presence of the free surface to simulate the fully non-linear powering of the full-scale vessel by using unsteady RANS solver. Here, modeling of the propeller's action will require the experimental determination of the roughness functions and hence built-in CFD, for the representative propeller surfaces, similar to the hull surfaces (i.e. repeat of step I to VIII)

5. Application of the Approach

In this section, the above-described approach is applied to a benchmark container vessel, which is known to be *KRISO Container Ship (KCS)*, to demonstrate the effect of:

a. different types of coating systems (FR, SPC and CDP systems) by using Granville's extrapolation;
b. simulated hull roughness and FR coating system by using Granville's extrapolation;
c. biofilm (slime) with the combined effect of the simulated hull roughness and FR coating system by using Granville's extrapolation;
d. using different procedures to estimate the hull skin friction due to Granville's extrapolation, CFD-Flat plate and CFD-3D hull procedures.

Table 2 presents the main particulars of KRISO Container ship given by (Kim et al., 2011). The estimations are made for the powering characteristics of this vessel for the above-described cases of (a), (b) and (c) and results are presented in Table 3 for two different speeds which are 24 knots of original design speed and 19 knots of slow steaming speed.

Table 2. Main particulars of benchmark KRISO Container vessel, Kim et al. (2001)

Length between the perpendiculars (L_{BP})	230.0 m
Length of waterline (L_{WL})	232.5 m
Beam at waterline (B_{WL})	32.2 m
Depth (D)	19.0 m
Design draft (T)	10.8 m
Wetted surface area	9498 m^2
Displacement (□)	52030 m^3
Block coefficient (C_B)	0.6505
Design Speed	24 knots
Froude number (Fr)	0.26

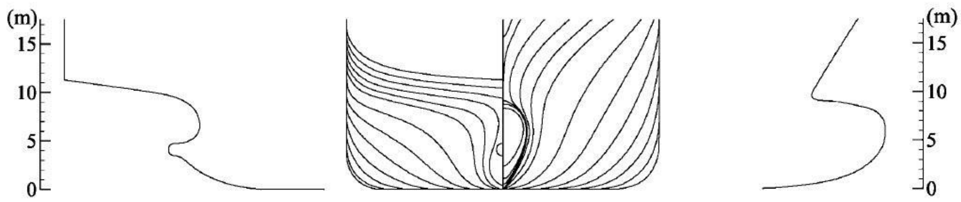

As shown in Table 3 the results in row (a) presents the percent increase in frictional drag coefficient, ΔC_F (%) and effective power ΔP_E (%) resulted for the FR, SPC and CPD coating types when these coating systems were applied using standard application procedures or "normal" finish to represent the relatively smooth application of coatings. Whereas the results in row (b) of Table 3 presents ΔC_F (%) and ΔP_E (%) due to the effect of "mimicked hull" roughness ranges at "low" and "high" density for the same coating types. In addition, Table 3, also presents ΔC_F (%) and ΔP_E (%) values for the FR coating system with "low" and "high" density hull roughness range including the effect of biofilm.

According to the results presented in Table 3, only a small frictional drag/power increase are predicted on the KCS hull from the application of typical FR, SPC and CDP type coatings with "normal" finish applications carried out under idealised laboratory conditions. However, with 'in-service' surface conditions described in b) and c) cases, the drag penalty becomes quite significant.

Table 3. Increase in frictional resistance coefficient, $\%\Delta C_F$ and effective power, $\%\Delta P_E$ for the KRISO Container Ship (KCS) at slow steaming speed of 19 knots and design speed of 24 knots for different hull surface conditions. Predictions are made by using Granville's extrapolation method

Ship type		KCS (L=232.5m)			
Ship speed		(19knots)		(24knots)	
Description of condition		$\%\Delta \boldsymbol{C_F}$	$\%\Delta \boldsymbol{P_E}$	$\%\Delta \boldsymbol{C_F}$	$\%\Delta \boldsymbol{P_E}$
a) Coatings with "normal" application	FR type	1.59	1.25	2.60	1.78
	SPC type	4.48	3.54	5.69	3.91
	CDP type	6.96	5.50	8.83	6.07
b) Coatings with mimicked hull roughness	FR, 'low' hull roughness	5.95	4.70	6.80	4.68
	FR, 'high' hull roughness	7.65	6.05	9.17	6.31
	SPC, 'low' hull roughness	14.43	11.41	14.88	10.23
	SPC, 'high' hull roughness	15.86	12.54	16.15	11.08
	CDP, 'low' hull roughness	17.16	13.56	17.50	12.03
	CDP, 'high' hull roughness	18.75	14.82	18.80	12.92
c) FR type coated panels with biofilms	FR, 'low' +biofilms	16.32	12.90	16.05	11.03
	FR, 'high' +biofilms	14.34	11.33	14.00	9.63

Figure 16 and 17 are added for graphical display of the tabulated results in Table 3 for easier comparison of the results at 19 knots and 24 knots for the slow steaming and design speeds, respectively. In the figures, FR, SPC and CDP coatings with "normal" surface finish or relatively smooth roughness conditions are represented by the solid blue bars, whilst the mimicked "hull" roughness applications, at "low" and "high", levels are represented by the dotted blue and patterned blue bars, respectively. The combined effect of FR type coatings with mimicked "low" and "high" levels are shown in dotted brown and patterned brown bars, respectively.

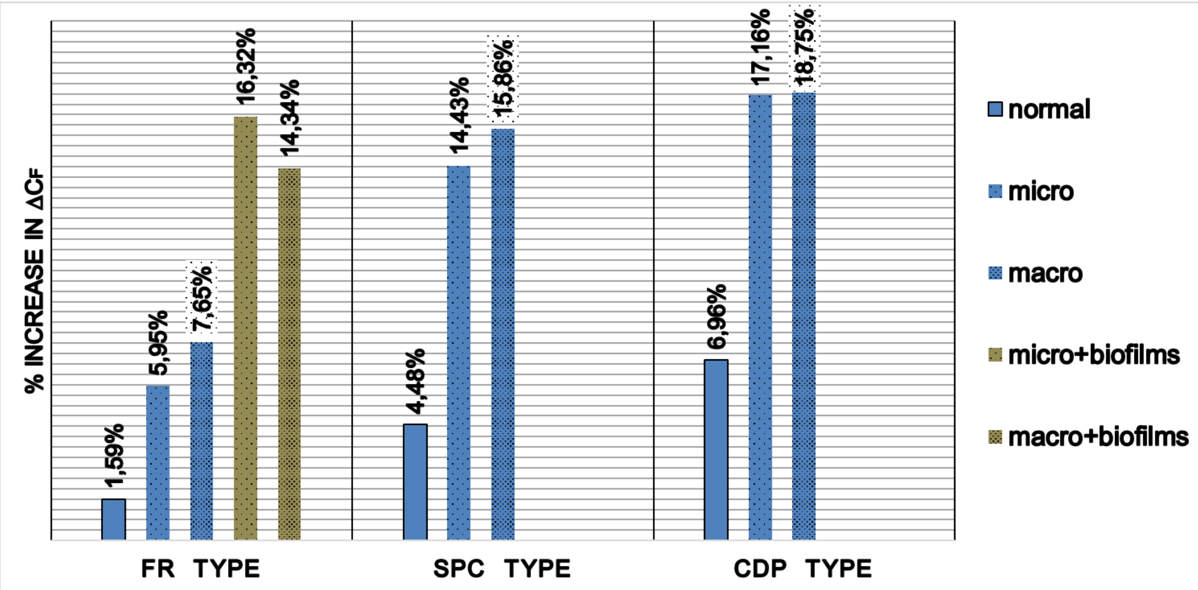

Fig.16. Estimation of percent increase in frictional resistance, $\%\Delta C_F$ for KRISO Container Ship for three different coatings types (FR, SPC and CDP) and hull surface conditions (condition a, b, c of Table 3) at 19 knots slow steaming speed. Estimation was based on Granville's extrapolation method.

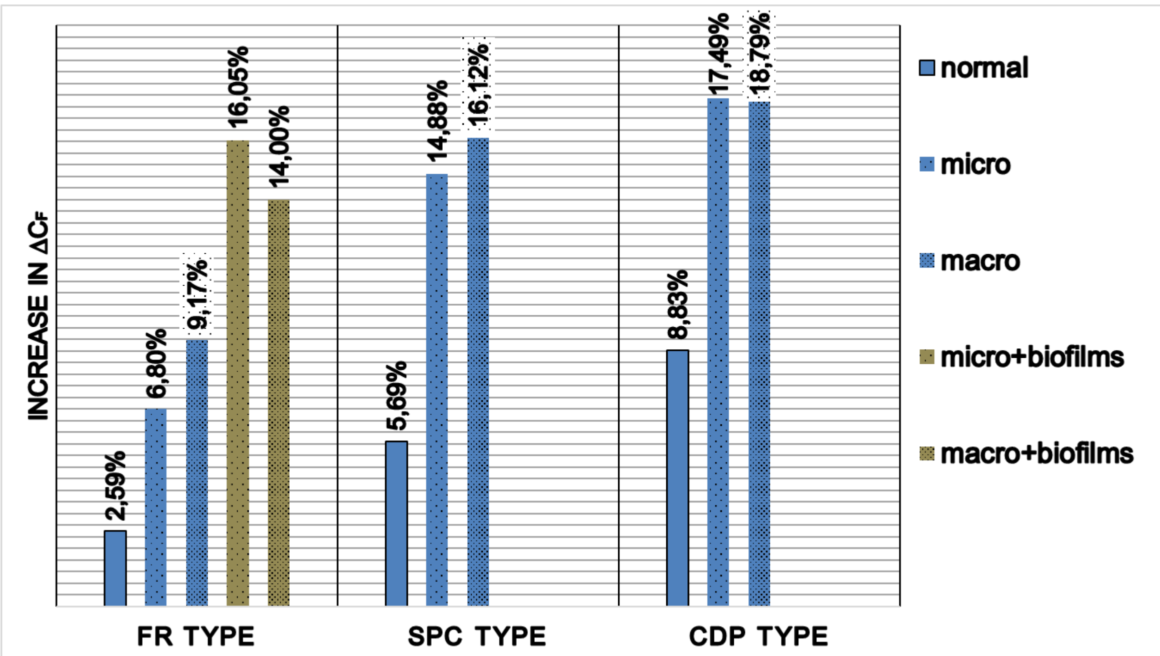

Fig. 17. Estimation of percent increase in frictional resistance, $\%\Delta C_F$ for KRISO Container Ship for three different coatings types (FR, SPC and CDP) and hull surface conditions (condition a, b, c of Table 3) at 24 knots design speed. Estimation was based on Granville's extrapolation method.

The results presented in Table 3 as well as in Figure 16 and 17 are based on the Granville's extrapolation method. In the following the results of the Granville method are compared with the CFD based procedures as applied on the KCS vessel for the same speeds (i.e. 24 knots and 19 knots). Since the Granville's extrapolation procedure makes use of the flat plate assumption, the same assumption was also made for the full-scale KCS vessel in one of the CFD based prediction methods used while in the other procedure the 3D geometry of the full-scale KCS hull is used. The results of these three methods are referred by using the following legends: "Granville" for the Granville extrapolation method; "CFD-Flat plate" for the CFD prediction for the flat plate case; and "CFD-KCS hull" for the CFD prediction for the actual 3D hull case, respectively.

Table 4 and 5 display the results of these three different procedures for the full-scale KCS hull at 24 knots and 19 knots, respectively and for different hull surface conditions, which are based on Schultz's different coating and fouling conditions as given in Table 1. The increase in the frictional resistance coefficient, ΔC_F (%) of the KCS due to seven different surface conditions with respect to those of a hydraulically smooth surface, was predicted by using the earlier mention three different methods and presented in Table 4 and Figure 18 for 24 knots design speed of the KCS and in Table 5 and Figure 19 for 19 knots slow steaming speed of the KCS, respectively.

Table 4. Comparison of the computed (%ΔCF) values using different methods at full scale at 24 knots

	(%ΔC_F)		
Description of condition	**CFD-KCS hull**	**CFD-Flat plate**	**Granville**
Hydraulically smooth surface	-	-	-
Typical as applied AF coating	10.9	10.7	9
Deteriorated coating or light slime	29.4	29.5	30
Heavy slime	49.2	49.7	51.8
Small calcareous fouling or weed	76.9	77.7	82.2
Medium calcareous fouling	112.1	113.6	118.3
Heavy calcareous fouling	163.2	164.3	171.0

Table 5. Comparison of the computed (%ΔCF) values using different methods at full scale at 19 knots

	(%ΔC_F)		
Description of condition	**CFD-KCS hull**	**CFD-Flat plate**	**Granville**
Hydraulically smooth surface	-	-	-
Typical as applied AF coating	7.4	7.1	6.3
Deteriorated coating or light slime	26.3	26.2	26.6
Heavy slime	45.6	45.9	47.8
Small calcareous fouling or weed	72.8	73.3	77.4
Medium calcareous fouling	107.1	108.2	118.3
Heavy calcareous fouling	157.1	158.2	163.9

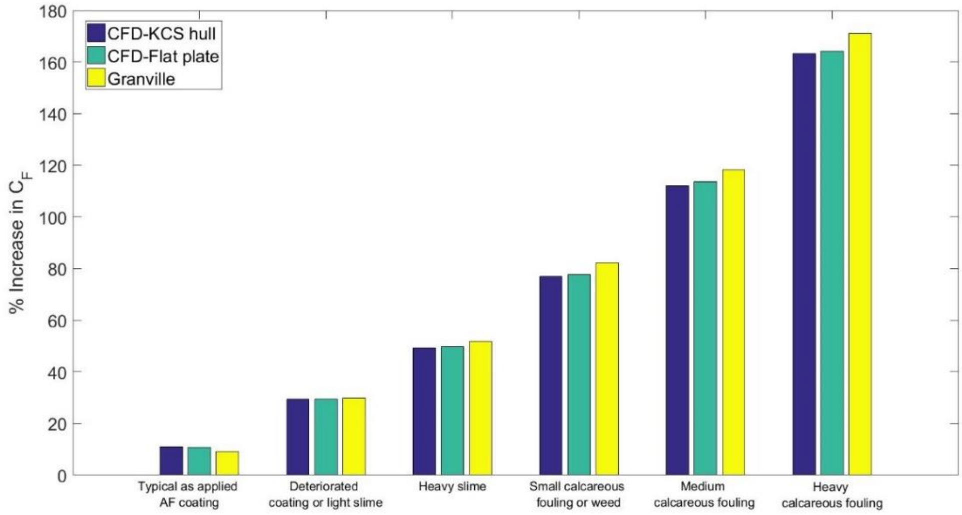

Fig. 18. Estimation of the percentage increase in the frictional resistance of the KCS due to different surface conditions at 24 knots (Re=2.89 x 109).

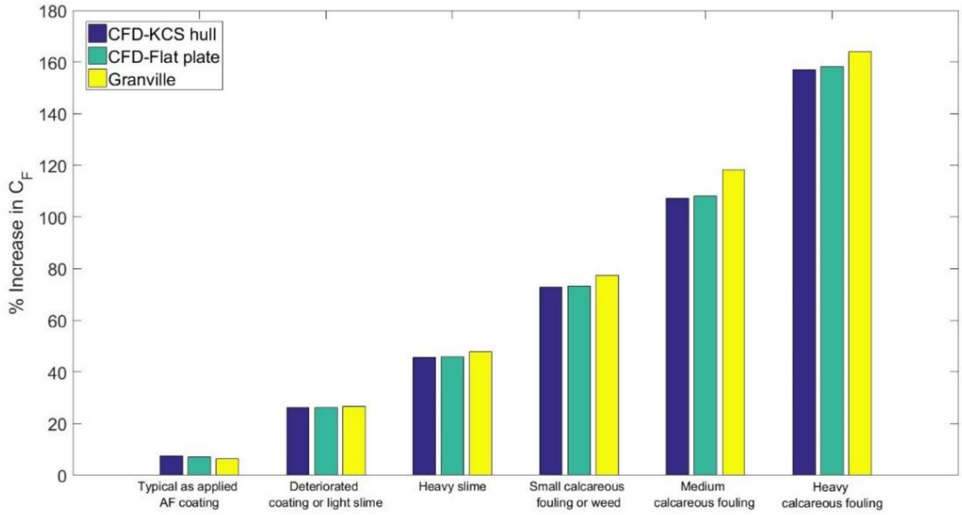

Fig.19. Estimation of the percentage increase in the frictional resistance of the KCS due to different surface conditions at 19 knots (Re=2.29 x 109).

As it can be seen in Table 5 & 6 as well as in Figure 18 & 19 the difference in the results due to the Granville and CFD procedures are negligibly small for the flat plate representation of the KCS hullform. However, this trend is changing when the 3D hull shape was taken into account as such the differences between the CFD-Flat plate, Granville and CFD-KCS (3D hull) predictions, become more noticeable as the hull surface conditions deteriorated.

Figure 20 demonstrates the percent increase in the total resistance coefficient, C_T (%) and hence in the effective power, P_E (%)of the KCS due to different surface conditions relative to the smooth condition at a design speed of 24 knots and at a slow steaming speed of 19 knots, respectively.

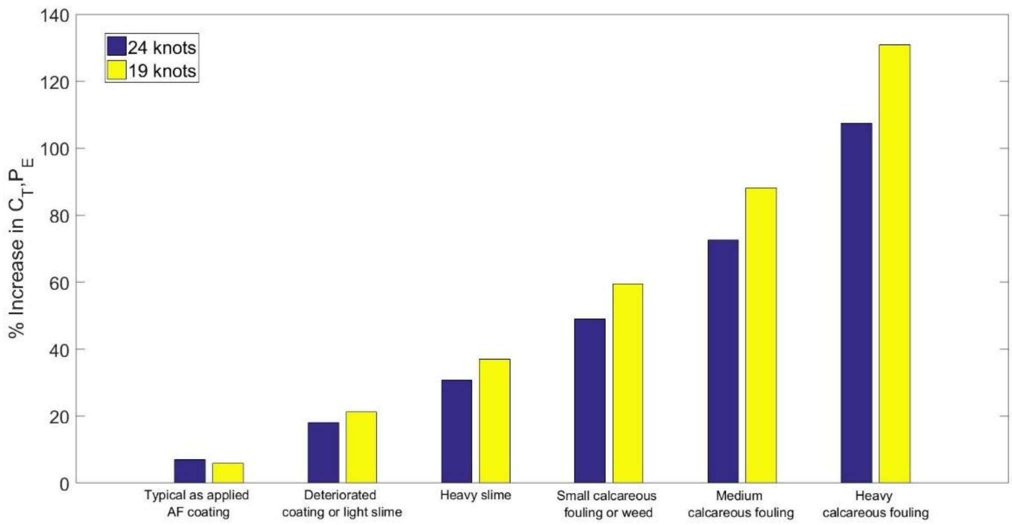

Fig. 20. Estimation of the percentage increase in the total resistance coefficient CT (%) and effective power, PE (%) of the KCS due to different surface conditions at two different speeds, 24 knots and 19 knots.

The results presented in Figure 20 indicate that the increase in the C_T and P_E of the KCS due to a typical newly applied fouling control system (with normal finish) were predicted to be 7.1% and 5.9% whereas those due to a deteriorated coating or with light slime may increase to 18.1% and 21.2% at ship speeds of 24 knots and 19 knots, respectively. The effect of heavy slime on the KCS hull was calculated to cause an increase in the C_T and P_E of 30.8% at 24 knots and 37% at 19 knots. The calcareous fouling would increase P_E by up to 107.5% at 24 knots and 130.9% at 19 knots. An interesting point to note is that the effect of a particular fouling condition on the effective power of the KCS is more dominant at lower speeds (i.e. at 19 knots slow steaming speed). This can be attributed to the fact that the contribution of the frictional resistance becomes more important than the residuary component of the total resistance at lower speeds. In other words, at higher speeds, the wave-making resistance component becomes dominant due to wave generation. Therefore, the effect of a given fouling condition on the total resistance of a ship is greater at low to moderate speeds than at higher speeds.

6. Validation of the Approach

A rational validation of the above-described approach in a real scenario, ideally, must be provided by the full-scale estimation of the changes in hull and propeller frictional drag caused by the application of different fouling control system or the growth of natural biofouling on the ship's wetted surfaces. Not being directly observable, this must be indirectly derived from other measurable quantities, the closest one being a speed-power relationship. The most important measurements to be carried out onboard a ship are therefore her speed through the water and the power needed to push her at that speed. Nonetheless, the complex environment and operational profile of a seagoing vessel contaminates the speed-power relationship by introducing other external resistance components. Factors of the like of winds, waves, ocean currents, vessel loading conditions affect the ship speed through water, her powering or both and these effects need to be accounted for in the estimation of the hull/propeller drag changes. Thus, other so-called "secondary" parameters need to be measured, for example, wind speed and direction or vessel draft.

Modern Ship Performance Monitoring Systems (SPMS) are mostly based on the earlier described set of measurements, their diversity stemming from the adopted data collection process, analysis method and scope of work. The SPMS installed on UNEW's *The Princess Royal* was conceived for the detection of changes in hull and propeller drag caused by alterations in their wetted surface roughness, whatever the cause, simultaneously targeting the smallest achievable uncertainty levels. The system, although developed on a small research vessel, can be applied to any vessel whose operator's intention would be to assess the effect of a fouling control system application or of biofouling build-up on the ship's wetted surface. The following sections aim at providing a concise description of the system in its main data treatment parts, namely *(i) Measurement, (ii) Filtering, (iii) Correction and (iv) Analysis.* Uncertainty of the system is then discussed.

(i) <u>Measurements</u>

As thoroughly shown by recent work, e.g. (Carchen et al., 2017), the primary feature of a competitively accurate SPMS stands in its measurement system. This should be completely automated and encompass a range of quality sensors. As shown in Figure 8, UNEW's RV *"The Princess Royal"* was therefore equipped with a new-generation Doppler Speed Log for the measurement of speed through water outside the ship's boundary layer and a pair of purpose-built instrumented shafts for the measurement of propeller power and thrust. These are complemented by complete navigational data, rudder angle potentiometers, an onboard weather station for the measurement of wind characteristics (speed, direction, temperature, and humidity), a wave radar (true wave height), two fuel flow meters (fuel consumption) and a water quality sensor. An in-house built Performance Monitoring software collects all the different signals and allows logging and displaying of relevant data to the crew.

(ii) <u>Filtering</u>

Raw measured data is always spurious for an immediate analysis, in that ship maneuvers (accelerations, course changes, etc.) and extreme conditions encountered (e.g. weather) alter the speed-power relationships and cannot be accurately corrected for. To exclude these and the random outliers from the dataset, situational, transient and statistical filters were implemented with the secondary aim of applying the least modifications to the raw data (Figure 21).

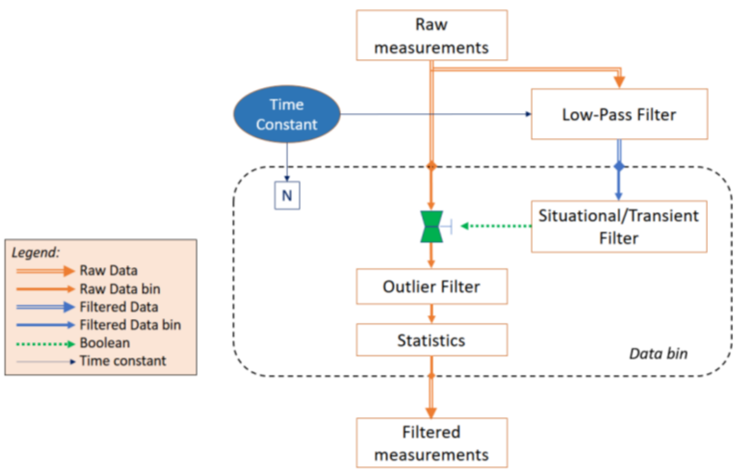

Fig. 21. Data flow through the filtering procedures

(iii) Correction

A deterministic approach to the data is one based on physical relationships between variables and it embraces the traditional naval architecture knowledge. Fundamentally, the total in-service ship resistance may be described as:

$$R_T = R_V + R_W + R_{add} \tag{4}$$

Where R_V is the viscous resistance, R_W is the wave making resistance and R_{add} the added resistance caused by factors intrinsic (e.g. loading condition) and extrinsic (e.g. wind, waves etc.) the ship. The purpose of the correction is the *a posteriori* determination and subtraction of R_{add} from the equation to allow a clearer observation of the change of R_V caused by a change of the coating system or biofouling growth. Because of its transparency and ease of obtaining different parameters to scrutinise, this approach was chosen to correct the data obtained in *(ii)* as shown schematically in Figure 22 and from full-scale measurements in Figure 23.

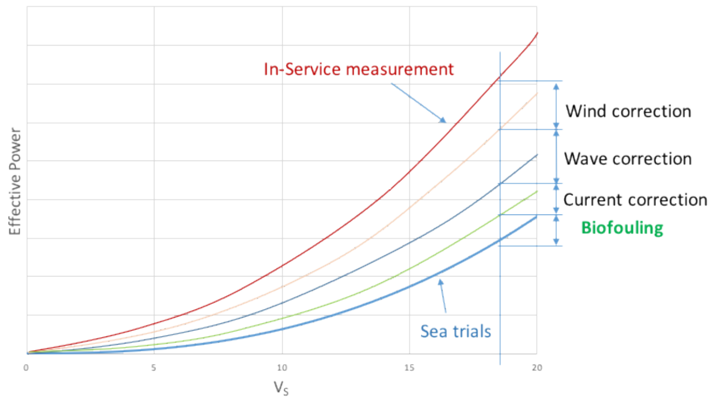

Fig. 22. Schematic representation of deterministic corrections for external disturbances

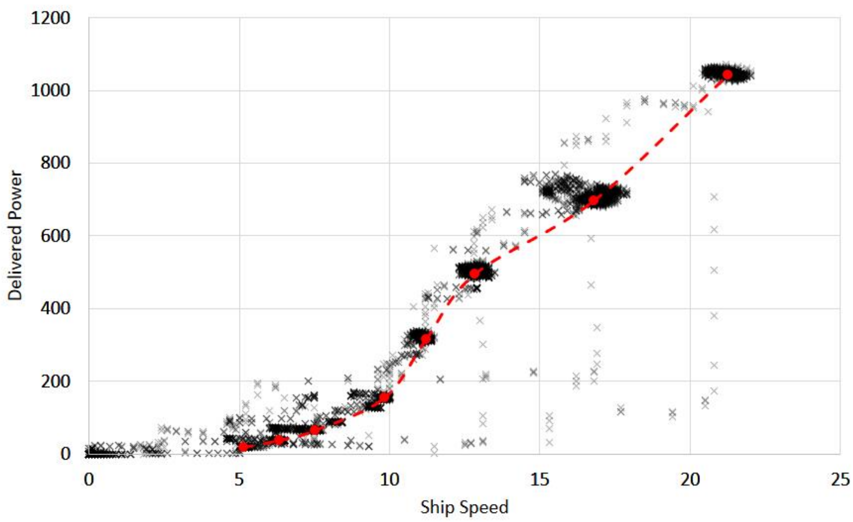

Fig. 23. Raw (blue markers) and corrected (red line and markers) performance measurements on the Princess Royal

The filtered data are corrected to represent the calm weather behavior of the ship according to a modified Taniguchi-Tamura method, (Taniguchi and Tamura, 1966), which makes use of propeller characteristics and vessel geometry. Corrections are applied for wind, head waves and water density using benchmarked data obtained from model tests or numerical simulations following relevant established methods (e.g. ITTC, 2014). The change in loading is negligible on this vessel, but a suitable correction can be applied in general. Figure 24 below shows the consistency of UNEW's SPMS in different trials with similar hull and propeller roughness.

(iv) <u>Analysis</u>

The long-term analysis of the corrected data obtained in *(iii)* allows thus to assess the change in calm water power due to alterations in the wetted surface roughness. From it, the propeller only feels a change in the loading condition, or in other words a change in the water inflow at a same rotational speed. Its usual definition as:

$$V_a = V_S(1-w) \tag{5}$$

implies that the propeller perceives a change in ship speed V_S (increased ship resistance) and in effective wake fraction w (increased hull surface boundary layer). Moreover, if the propeller blades are also fouled, for the same condition earlier defined the propeller will also register a higher torque due to its own fouling. Long term monitoring of the effective wake obtained from the propeller torque is thus a powerful measure of the change in roughness of jointly hull and propeller, in that it shows the real increase of boundary layer on the hull surface and the effect of propeller fouling on the propeller performance. When the propeller thrust is measured and propeller open water curves are available, the comparison of the wake fraction as derived from torque and thrust allows to evaluate the change in frictional drag of the hull alone, as thrust is affected but negligibly by blade fouling. In addition, considering that, in nondimensional form, the corrected total ship resistance can be written:

$$C_T = C_F(1+k) + C_W \tag{6}$$

and knowing the viscous form factor $(1+k)$, the wave making coefficient C_W can be calculated for a clean hull condition. The later changes in the viscous coefficient $C_F(1+k)$ can be estimated due to change in fouling control system and biofouling growth. This would eventually allow direct validation of the earlier explained procedures.

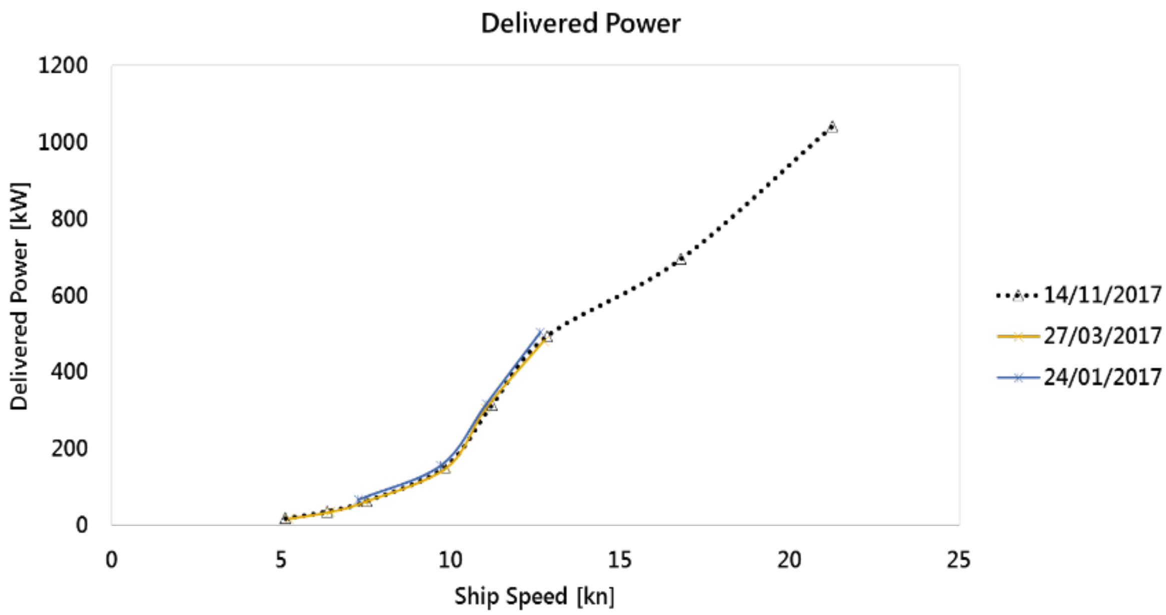

Fig. 24. In service Speed-Power curves of UNEW's research vessel "The Princess Royal"

Uncertainty analysis of the whole process presented above showed that the uncertainty caused by the monitoring and analysis system alone accounts for a maximum of about ±3% in shaft power at the 95% Confidence Interval, (Carchen et al., 2017b). This uncertainty level can be only reduced improving the quality of the sensors, the filtering techniques, and the analysis method. The variability of the weather, even when applying corrections, brings further uncertainty in the system, with total values being about ±4% to ±9% in shaft power at the 95% confidence interval (depending on ship speed). These results are supported also by previous findings in the literature. The contribution of weather to the uncertainty can be reduced by applying stricter filtering for the "non-extreme" weather conditions used for the analysis and by improving the corrections methods. As bigger vessels are less affected by weather the uncertainty contribution due to weather will be smaller in relation to the same filtering criteria.

7. Concluding Remarks

Based on two decades of bridging the gap between laboratory measurements and predicting the performance of commercial maritime vessels, in this paper, a rational approach to predicting the effects of modern-day fouling control systems on "in-service" ship performance is presented. This is further supported by a validation approach that involves the development of a dedicated performance monitoring and analysis systems on-board a full-scale research vessel which is currently underway

1. The proposed approach is generic and can be applied to any ship type and hull coating system in the presence of biofouling and it may even be combined with passive drag reduction systems.

2. The approach involves both the combination of experimental data from flat test panels treated with representative surface finishes and extrapolation of this data to full-scale. However, for more accurate and direct estimation of performance prediction at full-scale, the extrapolation

procedure needs to be replaced with Computational Fluid Dynamics (CFD) methods, especially for deteriorated hull surfaces due to fouling; at present, such experimental data are still required.

3. The rational nature and hence strength of the proposed approach is to represent the effect of the actual hull surfaces “in-service” by using state-of-the art experimental methods and data. This provides the option of an extrapolation procedure for practical performance estimations and also enables the use of CFD methods by avoiding the most difficult barrier of describing the actual hull surface numerically in CFD.

4. Validation of the proposed approach requires full-scale data to be collected using a bespoke ship performance monitoring and analysis system which is dedicated to assessing the effect of coating systems in the presence of fouling. Such a system is under development as reported in the paper.

5. Currently a new FTFC has been designed and is to be commissioned at the Kelvin Hydrodynamics Laboratory of the University of Strathclyde in September 2018. The new channel will have a special testing section, which will allow to test surfaces not only with coating and light biofouling (i.e. slime) but also with macro-scale (e.g. calcareous) fouling and passive drag reduction systems to support the ongoing research on biofouling hydrodynamics and drag reduction systems.

Acknowledgements

Three PhD researches referred in this paper due to Candries (2001), Hasselaar (2011) and Yeginbayeva (2017) were sponsored by Akzo-Nobel as well as the development of the UNEW multi-purpose flume facility and part of the performance monitoring system on-board the UNEW RV, The Princess Royal. This is gratefully acknowledged by the Authors. In addition, the financial supports obtained from the EU-FP6 AMBIO project, FP7 TARGETS project, FP7 FOUL-X-SPEL project and FP7-SEAFRONT project in various parts of the research presented in this paper are also gratefully acknowledged. Furthermore, the Authors are indebted to the technical personnel of the Emerson Cavitation Tunnel, RV The Princess Royal and Kelvin Hydrodynamics Laboratory for their invaluable efforts during the conduct of the experimental works presented in the paper.

8. References

Almeida, E., Diamantino, T.C. and de Sousa, O. (2007) Marine Paints: The Particular Case of Antifouling Paints, Progress in Organic Coatings, 59 (1), pp. 2-20.

Anderson, C., Atlar, M., Callow, M., Candries, M. and Townsin, R.L. (2003) The Development of Foul-Release Coatings for Seagoing Vessels, Journal of Marine Design and Operations, No. B4, pp. 11-23.

Atlar, M. (2011) Recent Upgrading of Marine Testing Facilities at Newcastle University, Proceedings of the 2nd International Conference on Advanced Model Measurement Technology for EU Maritime Industry (AMT'11). Newcastle Upon Tyne

Atlar, M., Ünal, B., Ünal, U. O., Politis, G., Martinelli, E., Galli, G., Davies, C. & Williams, D. (2013a) An experimental investigation of the frictional drag characteristics of nanostructured and fluorinated fouling-release coatings using an axisymmetric body. Biofouling, 29, 39-52.

Atlar, M., Aktas, B., Sampson, R., Seo, K.C., Viola, M.I., Fitzsimmons P., Fetherstonehaug, C. (2013b) A multi-purpose marine science and technology research vessel for full-scale observations and measurements. 3rd International conference on advanced model measurement technology for the maritime industry (AMT'13), September, Gdansk.

Atlar, M., Bashir, M., Turkmen, S., Yeginbayeva, I., Carchen, A. and Politis, G. (2015) Design, Manufacture and Operation of a Strut System Deployed on a Research Catamaran to Collect Samples of Dynamically Grown Biofilms In-Service, Proceedings of the 4th International Conference on Advanced Model Measurement Technology for Maritime Industry (AMT'15). Istanbul, Turkey.

Atlar, M., Glover, E.J., Candries, M., Mutton, R., Anderson, C.D. (2002) The effect of a Foul Release coating on propeller performance, Conference Proceedings Environmental Sustainability (ENSUS). University of Newcastle.

BMT Smart (2017) Smarter operations. http://www.bmtsmart.com/

Callow, M.E. and Callow, J.A. (2002) Marine Biofouling: A Sticky Problem, *Biologist*, 49(1), pp. 1-5.
Candries, M. (2001) Drag and Boundary Layer On Antifouling Paint. PhD thesis. University of Newcastle-Upon Tyne.

Candries, M., Atlar, M., (2003) On the Drag and Roughness Characteristics of Antifoulings, International Journal of Maritime Engineering, RINA, Vol. 145 A2.

Candries, M., Atlar, M., Mesbahi, E. and Pazouki, K. (2003) The Measurement of the Drag Characteristics of Tin-Free Self-polishing Co-polymers and Fouling Release Coatings Using a Rotor Apparatus, Biofouling, 19 (Supplement), pp. 27-36.

Carchen, A., Pazouki, K., and Atlar, M., (2017a) Development of an Online Ship Performance Monitoring System Dedicated for Biofouling and Anti-Fouling Coating Analysis". Hull Performance and Insight Conference, HullPIC, Ulrichshusen, De.
Carchen, A., Turkmen, S. Pazouki, K., Murphy, A., Aktas, B. and Atlar, M., (2017b) Uncertainty analysis of full-scale ship performance monitoring onboard the Princess Royal. Proceedings of the 5th International Conference on Advanced Model Measurement Technology for Maritime Industry (AMT'15) Glasgow, UK.

CASPER (2017) CASPER, the power for your sip-mile, http://www.propulsiondynamics.net/index.html
Chambers, L.D., Stokes, K.R., Walsh, F.C. and Wood, R.J.K. (2006) Modern approaches to marine antifouling coatings, Surface and Coatings Technology, 201(6), pp. 3642-3652.

Demirel, Y.K. (2015) Modelling the roughness effects of marine coatings and biofouling on ship frictional resistance, PhD Thesis, Department of Naval Architecture, Ocean and Marine Engineering. University of Strathclyde.

Demirel, Y.K., Turan, O., Incecik, A., (2016) Predicting the effect of biofouling on ship resistance using CFD. Applied Ocean Research 62, 100-118.
Dürr, S. and Thomason, J.C. (2010) Biofouling. 1st edn. Blackwell Publishing Ltd.
ENIRAM (2007) "Maximizing the efficiency of the marine industry", https://www.eniram.fi/

Granville P. S. (1958) The frictional resistance and turbulent boundary layer of rough surfaces. Journal of Ship Research. 2:52-74.

Granville, P.S. (1987) Three Indirect Methods for the Drag Characterization of Arbitrarily Rough Surfaces on Flat Plates, Journal of Ship Research, 31, pp. 70-77.

Hasselaar, T. W.F. (2011) An investigation into the development of an advanced ship performance monitoring and analysis system, PhD Thesis, Newcastle University.

Hellio, C. and Yebra, D. (2009) Advances in Marine Antifouling Coatings and Technologies. Abington Hall, Granta Park, Great Abington, Cambridge CB21 6AH, UK: Woodhead Publishing Ltd.

IMO (2009) Second IMO (International Maritime Organization) GHG Study. London. [Online]. Available at:
http://www.imo.org/en/OurWork/environment/pollutionprevention/airpollution/pages/greenhouse-gas-study-2009.aspx.

ISO (2016) ISO 19030-1:2016 Ships and marine technology -- Measurement of changes in hull and propeller performance -- Part 1: General principles, https://www.iso.org/standard/63774.html

Intertrac (2017) https://www.international-marine.com/in-focus/digital-solutions

ITTC (2014) Analysis of Speed/Power Trial Data, Recommended Procedures and Guidelines: Full Scale Measurements.

Munk, T. (2006) Evaluating Hull coatings for precise impact on vessel performance, Paint and Coatings, Expo Tampa PACE2006 , Florida USA.

Naval Ships' Technical Manual (2002) Waterborne underwater hull cleaning of navy ships. S9086-CQ-STM-010/CH-081R5. Naval Sea Systems Command. 2002.

Patel, V. C. (1998) Perspective: Flow at high Reynolds number and over rough surfaces—Achilles heel of CFD. Journal of Fluids Engineering, 120, 434-444.

Politis, G., Atlar, M., Kidd, B. and Stenson, P. (2013) A Multipurpose Flume for the Evauation of Hull Coatings', Proceedings of the 3rd International Conference on Advanced Model Measurement Technology for the Maritime Industry (AMT'13). Gdansk, Poland.

Schultz, M.P. (, 2007) Effects of coating roughness and biofouling on ship resistance and powering. Biofouling 23 (5), 331-341.

Schultz, M.P. and Flack, K.A. (2013) Reynolds-Number Scaling of Turbulent Channel Flow', Physics of Fluids, 25(025104), pp. 1-13.

Schultz, M.P., Flack, K., (2007) The rough-wall turbulent boundary layer from the hydraulically smooth to the fully rough regime. Journal of Fluid Mechanics 580, 381-405.

SEAFRONT (2014-2017) Synergistic Fouling Control Technologies. Available at: http://seafront-project.eu/.

Seo, K-C, Atlar, M. and Goo B. (2016) A study on the hydrodynamic effect of biofouling on marine propeller", Journal of the Korean Society of Marine Environment & Safety, V 22, No1, 123-128.

Taniguchi, K. and Tamura, K. (1966) On a new method of correction for wind resistance relating to the analysis of speed trial results, 11th ITTC.

TARGETS, (2011) Targeted Advanced Research for Global Efficiency of Transportation Shipping- TARGETS, EU-FP7 Collaborative Project, SST.2010-RTD-1-266008.

Yeginbayeva, I. (2017) An investigation into hydrodynamic performance of marine coatings "in-service" conditions, PhD Thesis, Newcastle University.

Yeginbayeva, I., Atlar, M., Turkmen, S., Kidd, B. and Finnie, A.A. (2016) Investigating The Impact Of Surface Condition On The Frictional Resistance Of Fouling Control Coating Technologies, The 31st Symposium On Naval Hydrodynamics (SNH). Monterey, USA, 11-16 September.

Zhou, F. (2015) Antifouling Surfaces and Materials: from land to marine environment. Berlin: Springer.

Gemi Boyalarında Yeni Ufuklar

Yigit Kemal Demirel

yigit.demirel@strath.ac.uk

University of Strathclyde, Glasgow, United Kingdom

Özet

Gemiler üzerindeki biyolojik yüzey kirliliği direnç artışı, yakıt tüketimi artışı, GHG emisyonlarının artışı ve zararlı canlı türlerinin taşınımı gibi hem ekonomik hem de çevresel açılardan önemi artmakta olan bir problemdir. Gemi boyaları, gemi yüzeyindeki biyolojik kirlenmeyi azaltmak ve gemi yüzeyini pürüzsüzleştirmek için yaygın olarak kullanılmaktadır. Bu çalışma, gemilerde kullanılan antifouling boyalar ile ilgili yeni bakış açıları ve yaklaşımları tanıtmayı amaçlamaktadır. Çalışmada ilk olarak gemiler üzerinde oluşan yüzey kirliliği ve bu kirlenmeyi önleme yöntemleri kısaca anlatılmaktadır. Devamında boya / yüzey kirliligi hidrodinamiği ile ilgili son araştırmalar sunulmaktadır. Sonrasında ise antifouling boya teknolojisinde biyo-benzetim (biomimetic) yaklaşımı, bio-ilham (bio-inspired) antifouling boya stratejileri ve bio-ilham antifouling boyaların dizaynında karşılaşılan zorluklar detaylı olarak tartışılmaktadır. Gemi boyaları konusunda sürdürülen araştırmaların, insan yapımı deniz yapıları ve deniz yaşamı arasındaki uyumu korurken, gemi yüzey kirliliğinin etkili bir şekilde azaltılmasına olanak sağlayacağına inanılmaktadır.

Anahtar kelimeler: Gemi boyaları, boya/yüzey kirliliği hidrodinamiği, biyo-benzetim.

New Horizons in Marine Coatings

Yigit Kemal Demirel

yigit.demirel@strath.ac.uk

University of Strathclyde, Glasgow, United Kingdom

Abstract

Marine biofouling is an increasing problem from both economic and environmental points of view in terms of increased resistance, increased fuel consumption, increased GHG emissions and transportation of harmful non-indigenous species. Marine coatings are prevalently used to mitigate biofouling and smooth the surfaces of hulls. This paper aims at introducing new horizons and novel approaches in marine antifouling coatings. Firstly, marine biofouling and fouling prevention methods are briefly introduced. Afterwards, latest research in coating/fouling hydrodynamics is presented. Biomimetic approach to antifouling technology, bio-inspired antifouling strategies and the challenges in designing bio-inspired antifouling coatings are then discussed in detail. It is believed that, the on-going research in marine coatings will lead to an effective mitigation of marine biofouling while maintaining the harmony between man-made structures and marine life.

Keywords: Marine coatings, coating/fouling hydrodynamics, biomimetics.

1. Introduction

Fouling is an unwanted phenomenon for marine transportation because ships consume less fuel when their hulls are smooth and clean, viz. free from fouling. This is the reason why people have been trying to avoid or to mitigate fouling using various antifouling technologies since the very first days of shipping history.

It is predicted that approximately 300 million tonnes of fuel are consumed per year by waterborne transportation thereby there is an increasing focus on environmental footprint of shipping (IMO, 2009). The air emissions, due to the increasing fuel consumption by shipping, is expected to increase between 38% and 72% by 2020, unless corrective measures is taken or new technologies are introduced (IMO, 2009). Therefore environmental issues lead universities, research organisations and shipping companies to focus on energy saving, greenhouse gas (GHG) emission reduction and other measures to achieve more environmentally friendly transportation.

Antifouling coatings are the primary protective measure to mitigate marine biofouling and surface roughness on ship's hulls. It is estimated that $60 billion of fuel saving, 384 million tonnes of reduction in carbon dioxide and 3.6 million tonnes of reduction in sulphur dioxide emissions can be achieved by using of antifouling coatings (IMO, 2009).

There have been many types of antifouling coatings which mitigate the settlement and growth of the marine species on hulls by means of either releasing biocides or its own surface properties. The antifouling paints containing TBT had been highly preferred for years since they had low initial roughness and perfect antifouling properties. Nevertheless, the research demonstrated that TBT has many negative effects on marine environment, such as toxicity to marine lives, persistence in the aquatic environment. For these reasons, IMO banned the applications of TBT containing coatings. Therefore, the research on environmentally friendly antifouling coating has been accelerated since 2000's. Nonetheless, the desired antifouling coating has not been developed yet.

This paper presents new horizons in marine coatings and is organised as follows: Marine biofouling and the effects of fouling were briefly presented in Section 2, while the current fouling prevention methods were discussed in Section 3. In Section 4, the latest research of the author in coating/fouling hydrodynamics was presented together with research carried out within the EU funded FOUL-X-SPEL Project. In Section 5, new methods in marine coatings addressing biomimetics and bio-inspired antifouling technology were presented. Finally, the results of the study are discussed in Section 6, along with recommendations for future avenues of research.

2. Marine Biofouling

The bio-accumulation of marine organisms on the surfaces of submerged, or semi-submerged, natural or artificial objects is termed marine biofouling (Lewis, 1998). This infestation is inevitable because the marine environment has a unique bio-diversity. It is estimated that the number of types of marine organisms that cause biofouling may exceed 2500 (Anderson et al., 2003). Some species have a tendency to attach on surfaces, settle and then grow on them. These marine organisms are termed marine foulers and may be mainly classified into micro and macro foulers as shown in Figure 1 (Taylan, 2010).

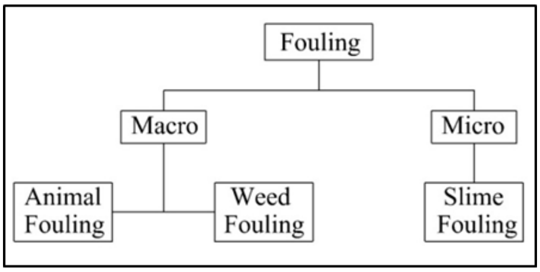

Fig. 1. Fouling organisms, adapted from Taylan (2010)

A detailed classification of marine foulers is demonstrated in Figure 2 (Atlar, 2008)

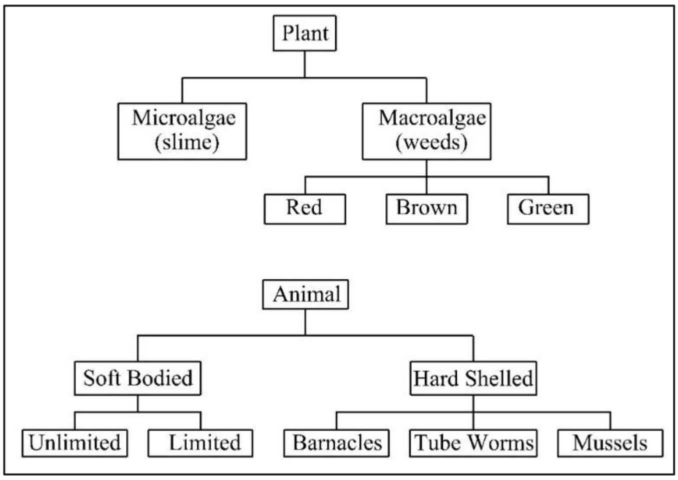

Fig. 2. Classification of marine foulers, adapted from Atlar (2008)

Fouling begins to occur immediately after a ship is immersed in water, and will continue to occur throughout a ship's life at sea until a cleaning process is performed. Fouling is particularly likely to occur when a ship is stationary, such as when it is in a port. Fouling builds up more quickly in tropical waters and it also varies depending on a ship's operational geographical area (Candries et al., 2003). The level of fouling depends on several factors, including the length of time spent at sea, the water temperature, the geographical location of the ship, surface conditions and the salinity of the sea. The longer the ship's immersion time, the greater the level of fouling. Such fouling is responsible for a dramatic increase in a ship's frictional resistance (Demirel et al. 2014).

Fouling causes surface roughness, resulting in an increase in a ship's frictional resistance and fuel consumption (Kempf, 1937). Milne (1990) stated that the fuel consumption may increase by up to 40%, unless any precautions are taken to prevent fouling. According to Taylan (2010), the increase in resistance due to microorganism fouling is around 1-2%, whereas an accumulation of hard shelled organisms may cause an increase in resistance of up to 40%. Schultz (2007) investigated the effect of fouling on the required shaft power for a frigate at a speed of 15 knots. He found that the presence of slime alone caused a 21% increase in shaft power, compared to an otherwise identical slime-free frigate, whereas heavy calcareous fouling led to an 86% increase in shaft power requirements. Demirel et al. (2017) recently carried out experimental and numerical studies and predicted a 66% increase in total resistance of a containership for a 20% coverage of barnacles each 5 mm in height.

3. Fouling Prevention Methods

Fouling mitigation is very desirable from a practical point of view. Fouling has been a challenging problem to solve for many years and efforts to find an effective protection method began long ago. The conventional antifouling method involves the application of antifouling paints, which contain toxic chemicals, on ships' hulls. These toxic chemicals, which are termed biocides, are gradually released into seawater due to exposure to water, and consequently a toxic layer is formed around the hull. This layer prevents fouling species from attaching to the hull. Several different methods have been trialled; it even seems that the toxic antifouling principle was in use as early as the 5th century BC. An Aramaic papyrus details the antifouling strategy of those days (ABS, 2011):

> *"…the arsenic and sulfur have been well mixed with the Chian oil that you brought back on your last voyage, and the mixture evenly applied to the vessel's sides, that she may speed through the blue waters freely and without impediment.''*

Christopher Columbus also suffered from fouling problems, with his fouling prevention method as follows (ABS, 2011):

> *"All ships' bottoms were covered with a mixture of tallow and pitch in the hope of discouraging barnacles and teredos, and every few months a vessel had to be hove-down and graved on some convenient beach. This was done by careening her alternately on each side, cleaning off the marine growth, re-pitching the bottom and paying the seams."*

Antifouling strategies have changed over time due to new technologies and legislations. The historical development of antifouling strategies is detailed in Table 1 (Dafforn et al., 2011).

The most remarkable success against marine biofouling can be attributed to tributyltin (TBT) based antifouling paints. Self-polishing copolymer (SPC) TBT systems had been widely used from the 1960's until the 2000's due to their unbeatable antifouling ability. Unfortunately, research demonstrated that TBT exposure causes the malformation of oyster shells (Alzieu et al., 1986) and imposex of gastropod molluscs (Gibbs and Bryan, 1986). Moreover, TBT compounds persist in water, show toxic effects to marine organisms even with a low concentration, and they may accumulate in marine organisms and hence enter the food chain (Okay, 2004). As a consequence, IMO banned the application of antifouling coatings which contain TBT in 2003, and banned the operation of ships coated with TBT paints in 2008 (IMO (2001), Champ (2003)). Due to this ban, TBT has been replaced with other toxic biocides. These chemical systems release toxic compounds to the marine environment just like TBT, whereas they are not as effective as TBT.

Table 1. Historical development of antifouling strategies, adapted from Dafforn et al. (2011)

Timeline	Major events
1500-300 BC	Use of lead and copper sheets on wooden vessels
1800-1900s	Heavy metals (copper, arsenic, mercury) incorporated into coatings
1800s-present	Continued use of copper in AF coatings
1960s	Development of TBT conventional coatings
1974	Oyster farmers report abnormal shell growth
1977	First foul release AF patent
1980s	Development of TBT SPC coatings allowed control of biocide release rates
1980s	TBT linked to shell abnormalities in oysters (Crassostrea gigas) and imposex in dogwhelks (Nucella lapillus)
1987-90	TBT coatings prohibited on vessels <25 m in France, UK, USA, Canada, Australia, EU, NZ and Japan
1990s–present	Copper release rate restrictions introduced in Denmark and considered elsewhere e.g. California, USA
2000s	Research into environmentally friendly AF alternatives increases
2001	International Maritime Organization (IMO) adopts "AFS Convention" to eliminate TBT from AF coatings from vessels through: 2003 – prohibition of further application of TBT 2008 – prohibition of active TBT presence
2008	IMO "AFS Convention" comes into force

Today, several types of coatings are used to mitigate fouling. They can be classified into two main categories based on their compositions; namely, biocidal and non-biocidal coatings. Biocidal coatings can be listed as Controlled Depletion Polymer (CDP), Self-Polishing Copolymer (SPC) and Hybrid SPC. Non-biocidal coatings are foul-release coatings (FR), which are also called non-stick coatings.

CDPs use a hydration process and release biocides into the marine environment. They are used for vessels which have short drydock intervals and are preferred for ships operating in low fouling regions (Atlar, 2008). Their effectiveness is said to be up to 3 years (Van Rompay, 2012). Self-Polishing Copolymers (SPC) have good initial hydrodynamic performance owing to their smooth surfaces and have better antifouling abilities due to controlled release of the biocide via hydrolysis. They are preferred for vessels which have longer drydock intervals (Taylan, 2010). SPCs can remain effective for up to 5 years (Van Rompay, 2012). Hybrid SPCs' biocide release method may be regarded as a hybrid of hydrolysis and hydration. The life span of Hybrid SPCs is between 3 and 5 years (Taylan, 2010).

However, all biocidal antifouling coatings are under scrutiny regarding their toxic effects; hence, they all are affected by legislative issues and may still be banned in the near future.

Foul release (FR) coatings, on the other hand, prevent the attachment of marine species on hulls owing to their physical surface properties (Wahl, 1989), which act like a non-stick coating and prevent the build-up of fouling organisms. The term foul release is in fact misleading because FR coatings cannot release all of the slime on a hull. Additionally, they are only effective above a certain speed, since the release mechanism works by the creation of a shear force to detach the marine organisms. Because of this, FR coatings are not appropriate for slow ships and for ships spending a long time in ports (Candries et al., 2003). Also, they are very expensive compared to other types of coatings and may be damaged easily by hard shelled fouling organisms or any mechanical effects such as cleaning. Due to these limitations, a great deal of effort is being devoted towards developing a novel and environmentally friendly antifouling solution that can eliminate all of the drawbacks of the current antifouling coatings.

4. Latest Research in Coating/Fouling Hydrodynamics

Several different aspects need to be considered when designing a new antifouling system. These aspects concern the environment, the coating and the substrate. Details of the main aspects are given in Figure 3 (Chambers et al., 2006). The main difficulty during the development of a novel antifouling system is to find a compromise among different and conflicting parameters. The requirements for an optimal antifouling coating are described in detail by Chambers et al. (2006) in Table 2.

One of the recent antifouling projects is the EU funded FP7 Project FOUL-X-SPEL (Environmentally Friendly Antifouling Technology to Optimise the Energy Efficiency of Ships, Project number 285552, FP7-SST-2011-RTD-1). *"The basic idea concerns the modification of usual hulls by providing a new antifouling coating, by fixing bioactive molecules, which can provide biocide activity, in order to avoid leaching and to promote a long-term effect of surface protection"* (FOUL-X-SPEL, 2011).

Besides the direct impacts and product(s) of this FOUL-X-SPEL project, it has led to extensive research and has developed an increased understanding on the subject of fouling, antifouling technologies and fouling effects on ship resistance, fuel consumption and GHG emissions. It is believed that it will be a leap forward towards environmentally friendly antifouling systems. It is of note that the research presented in this paper was partially generated as part of this FOUL-X-SPEL project. Examples of other recent EU funded research projects are AMBIO (2005), LEAF (2012), BYEFOULING (2013) and SEAFRONT (2014).

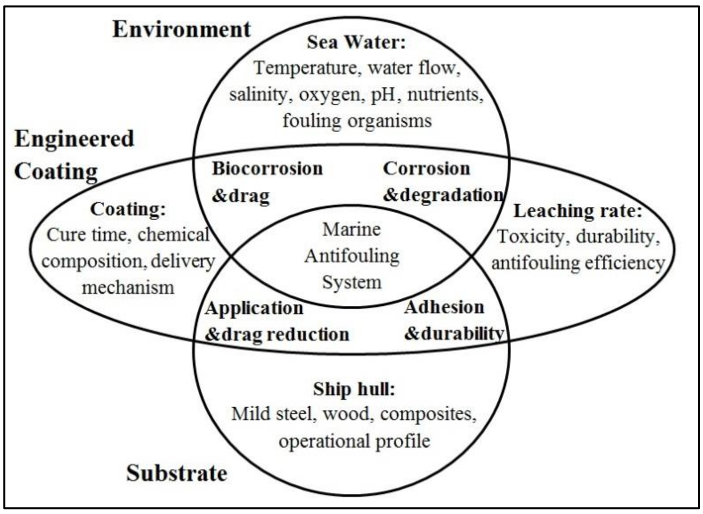

Fig. 3. Key parameters for antifouling systems, adapted from Chambers et al. (2006)

Table 2. Requirements for an optimal antifouling coating, adapted from Chambers et al. (2006)

Must be	Must not be
Anticorrosive	Toxic to the environment
Antifouling	Persistent in the environment
Environmentally acceptable	Expensive
Long life	Chemically unstable
Compatible with underlying system	A target for non-specific species
Resistant to abrasion/ biodegradation/erosion	
Capable of protecting regardless of operational profile	
Smooth	

4.1 Experimental studies

Demirel et al. (2015, 2017b) carried out a series of towing tests using flat plates coated with different marine coatings and covered with artificial barnacles. The tests were designed to allow the examination of the as applied drag performances of several paints and the effects of the barnacle height and percentage coverage on the resistance and effective power of ships. The drag coefficients and roughness function values were evaluated for the flat plates. Roughness effects of the fouling conditions on the ship frictional resistances were predicted. Added resistance diagrams were then plotted using these predictions, and powering penalties for these ships were calculated using the generated diagrams. The results indicate that the effect of barnacle size is significant, since a 10% coverage of barnacles each 5mm in height causes a similar level of added power requirements to a 50% coverage of barnacles each 1.25 mm in height.

Figure 4 illustrates the frictional resistance coefficients, C_F, of all of the test surfaces coated with different paints together with their added resistance coefficient, C_R, values. It is clearly seen that the newly developed F0034 showed the best frictional resistance performance among all of the antifouling coatings, with an average decrease of 0.79% with respect to the Reference Plate (Demirel et al., 2015).

Figure 5 shows the added resistance diagram for 230 m containership with different fouling conditions whereas Figure 6 demonstrates the increases in the frictional and total resistance and hence in the effective power of the containership at a design speed of 24 knots.

The increase in the C_F and P_E values of the containership due to S-type barnacle accumulation at a ship speed of 24 knots was predicted to be 27%, 17.5% for 10% coverage, 42%, 27% for 20% coverage, 66%, 42% for 40% coverage and 69.5%, 44.6% for 50% coverage. These values changed to 49%, 31% for 10% coverage, 67%, 43% for 20% coverage, 97%, 63% for 40% coverage and 103%, 66% for 50% coverage when it comes to M-type barnacle accumulation. The increases in C_F and P_E were predicted to be 72%, 46% for 10% coverage and 103%, 66% for 20% coverage for B-type surface condition. The effect of size of barnacle on added resistance is significant as 10% coverage of B-type surface causes same level of added power requirements as 50% coverage of S-type surface (Demirel et al., 2017b).

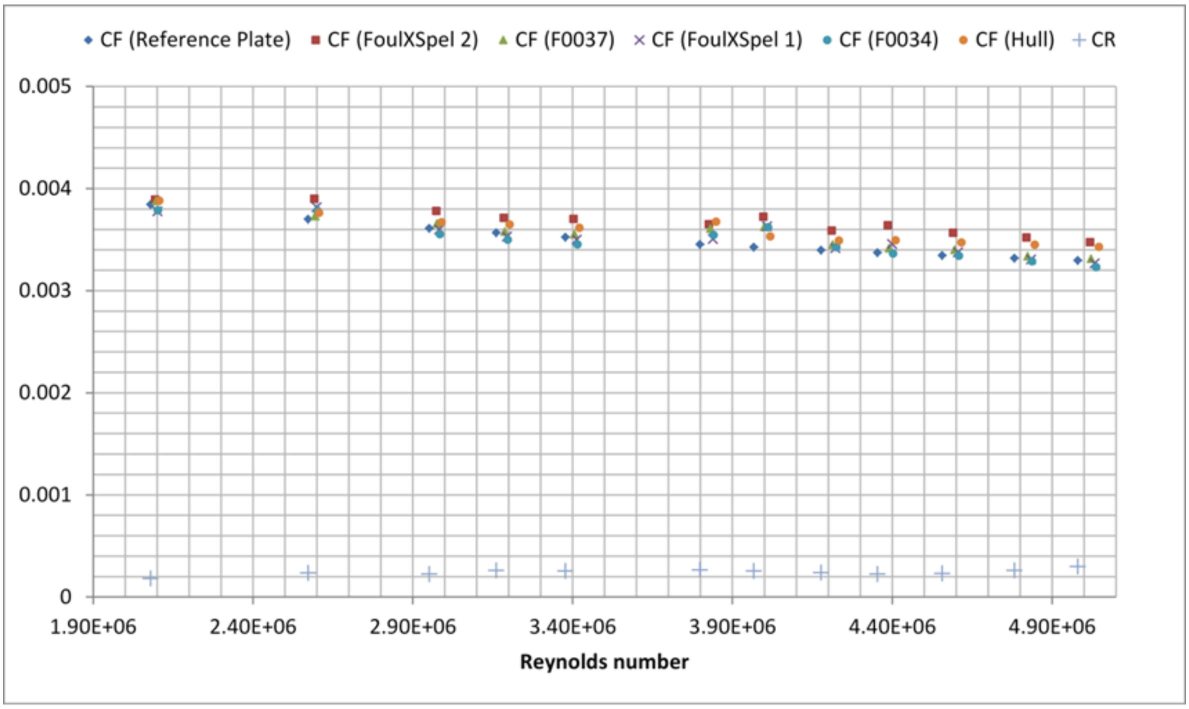

Fig. 4. Frictional resistance coefficients of all test surfaces together with CR values (Demirel et al., 2015)

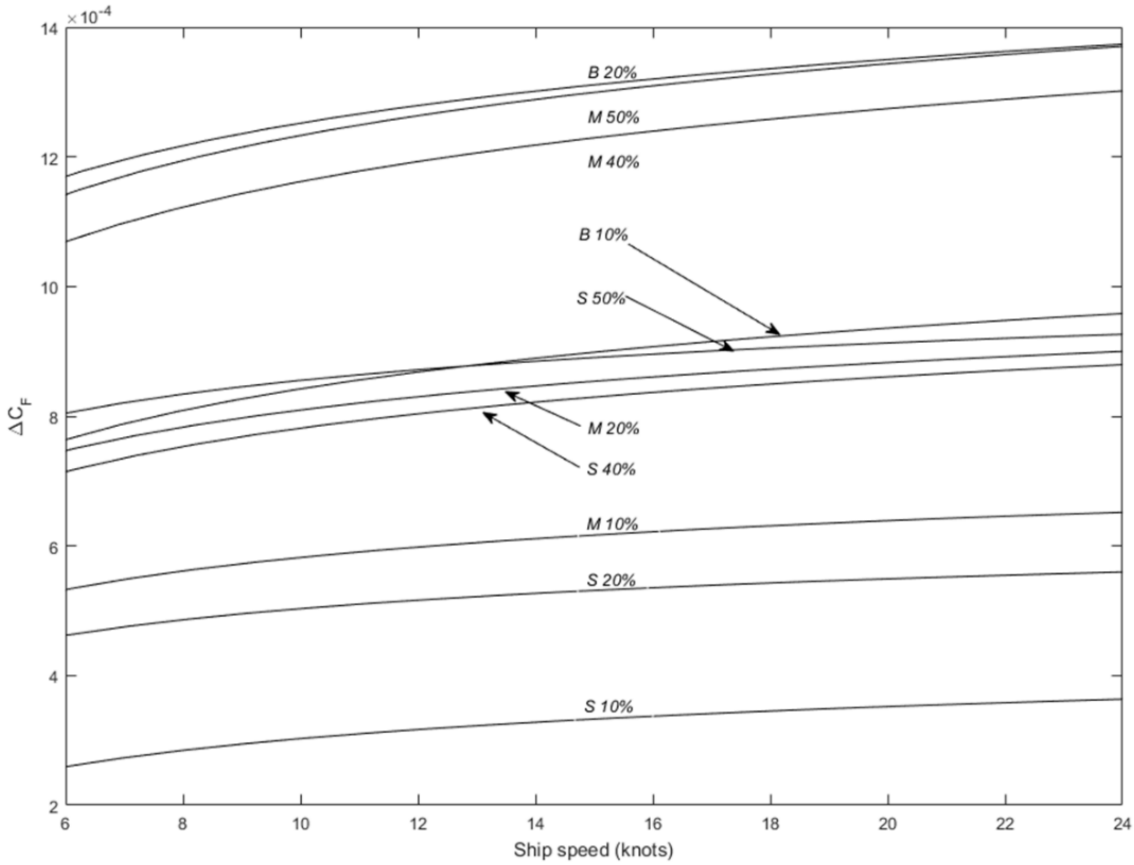

Fig. 5. Added resistance diagram for a 230 m container ship with different barnacle fouling conditions (Demirel et al., 2017b)

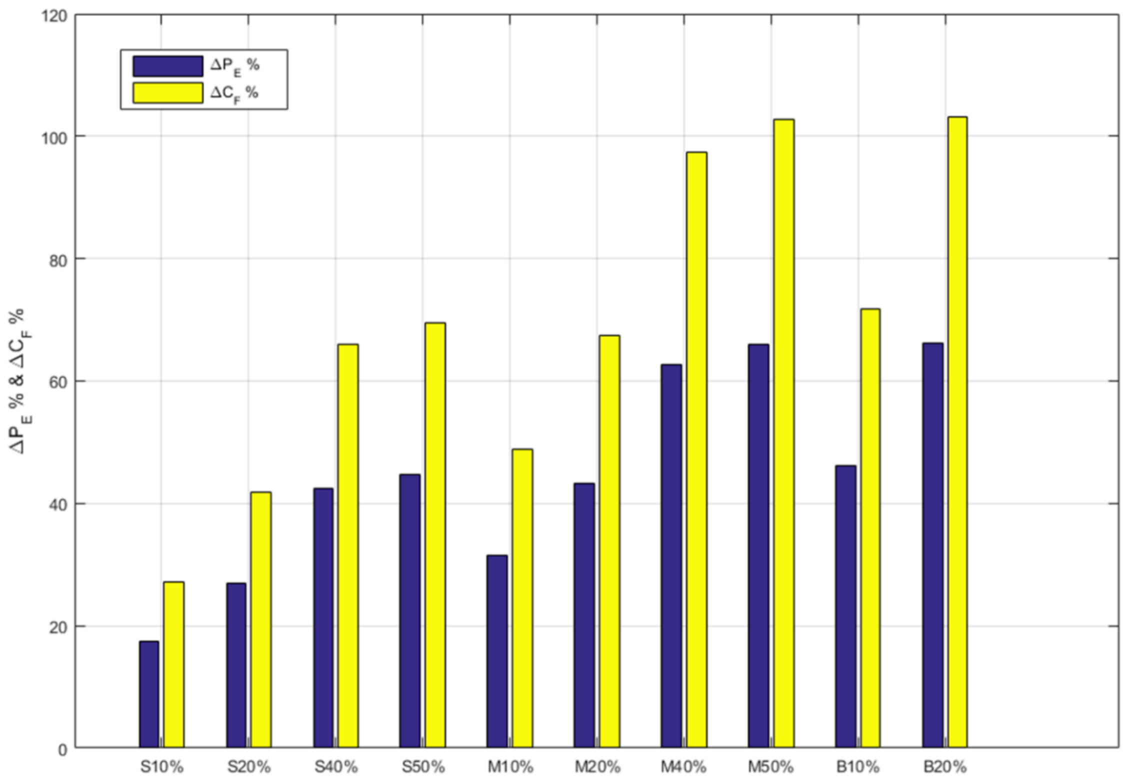

Fig. 6. Percentage increases in CF and PE values of a 230 m container ship with respect to the smooth hull condition (Demirel et al., 2017b)

4.2 Numerical studies

Demirel et al. (2014, 2017a) proposed Computational Fluid Dynamics (CFD) based unsteady RANS models which enable the prediction of the effect of marine coatings and biofouling on ship resistance. Demirel et al. (2017a) presented CFD simulations of the roughness effects on the resistance and effective power of the full-scale 3D KRISO Container Ship (KCS) hull. This can be considered as an alternative method to traditional similarity law scaling procedure, which uses the flat plate approach. Initially, a roughness function model representing a typical coating and different fouling conditions was developed by using the roughness functions given in the literature. This model then was employed in the wall-function of the CFD software and the effects of a typical as applied coating and different fouling conditions on the frictional resistance of flat plates representing the KCS were predicted for a design speed of 24 knots and a slow steaming speed of 19 knots using the proposed CFD model. The roughness effects of such conditions on the resistance components and effective power of the full-scale 3D KCS model were then predicted at the same speeds. The resulting frictional resistance values of the present study were then compared with each other and with results obtained using the similarity law analysis. The increase in the effective power of the full-scale KCS hull was predicted to be 18.1% for a deteriorated coating or light slime whereas that due to heavy slime was predicted to be 38% at a ship speed of 24 knots. In addition, it was observed that the wave resistance and wave systems are significantly affected by the hull roughness and hence viscosity.

The increase in the frictional resistance of the KCS due to different surface conditions with respect to those of a hydraulically smooth, predicted using the different techniques, are demonstrated in Figure 7.

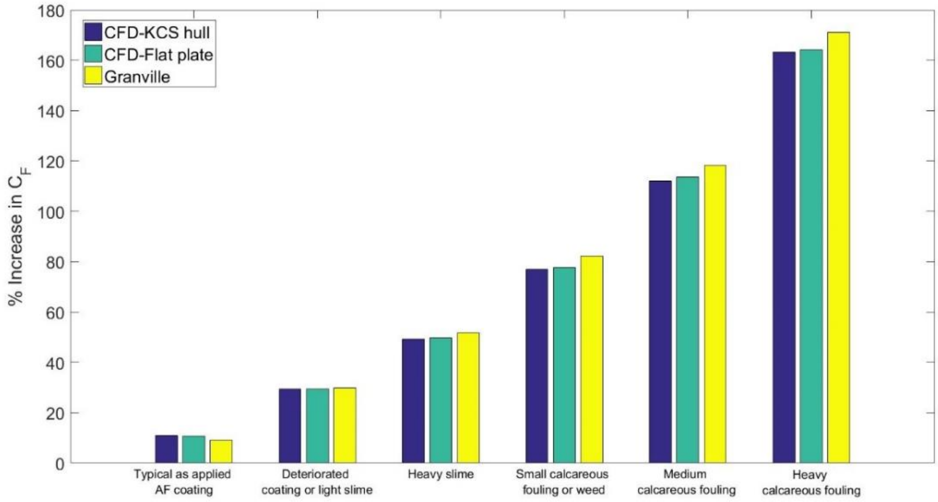

Fig. 7. Estimation of the percentage increase in the frictional resistance of the KCS due to different surface conditions at 24 knots (Re=2.89 x 109) (Demirel et al., 2017a)

The results obtained using "CFD-KCS hull" method presented in Figure 7 indicate that the increase in C_F due to the hull roughness of a typical antifouling (AF) coating is 10.9% at 24 knots and 7.4% at 19 knots, whereas the increase in C_F due to biofouling is predicted to be dramatic, which would lead to a drastic increase in the fuel consumption and hence CO2 emissions. The increase in the frictional resistance of the KCS due to a deteriorated coating or light slime surface condition was predicted to be 29.4% at a ship speed of 24 knots and to be 26.3% at a ship speed of 19 knots. These values became 49.2% and 45.6% when calculating the increase in C_F due to a heavy slime condition. Calcareous fouling causes significant increase in C_F values, ranging from ~77% to ~163% at 24 knots and ~73% to ~157% at 19 knots, depending on the type of calcareous fouling and ship speed.

Figure 8 compares the global wave patterns around the hull surface of the KCS in smooth and heavy calcareous fouling conditions at 24 knots, while Figure 9 shows the wave profile along a line with constant y = 0.1509.

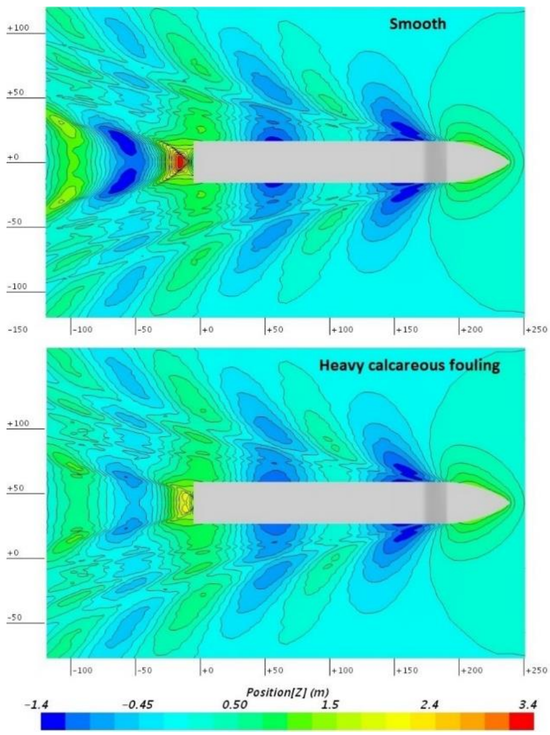

Fig. 8. Wave pattern around the KCS for smooth and heavy calcareous fouling conditions (V=24 knots) (Demirel et al., 2017a)

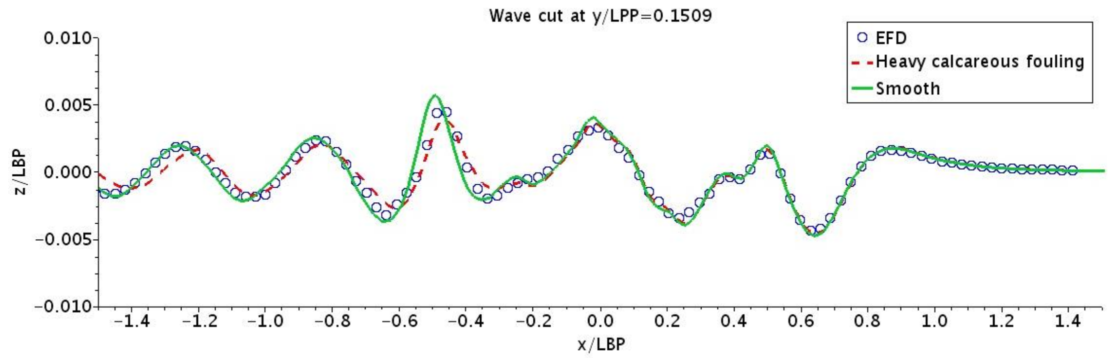

Fig. 9. Wave profiles at y = 0.1509 (V=24 knots) (Demirel et al., 2017a)

It is seen from the comparison in Figure 8 and Figure 9 that wave amplitudes appear to be reduced by roughness effects. This is an indication of the effect of viscosity on the wave systems. The resulting free surface elevation around the KCS hull was recorded to range from -1.406m to 3.357m for smooth condition, and -1.345m to 2.266 for heavy calcareous fouling condition (Figure 9).

Figure 10 demonstrates the increase in the total resistance and hence in the effective power of the KCS due to different surface conditions with respect to the smooth condition at a design speed of 24 knots and at a slow steaming speed of 19 knots, respectively.

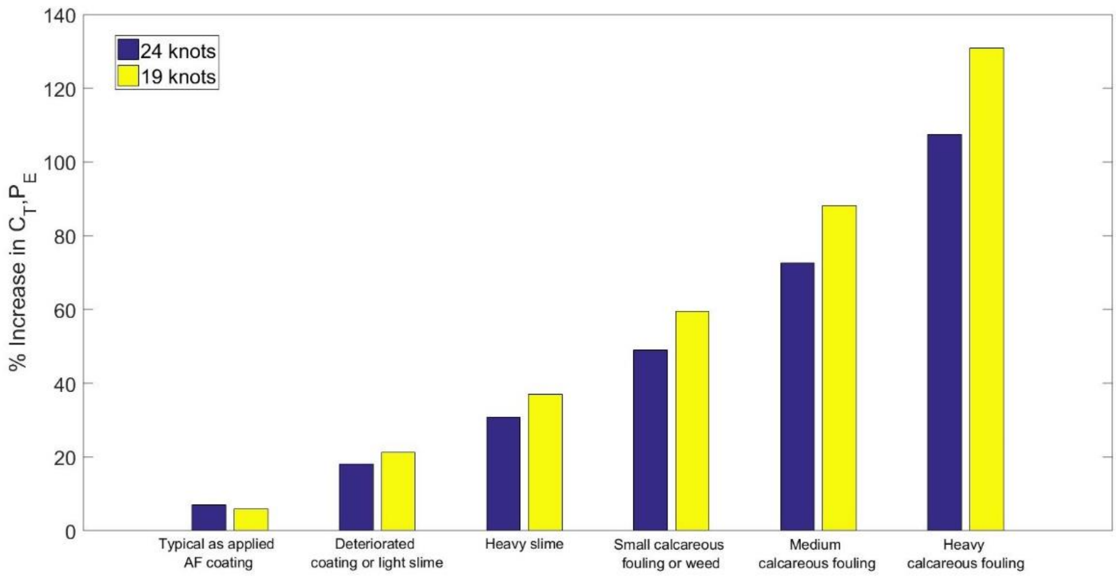

Fig. 10. Estimation of the percentage increase in the resistance and effective power of the KCS due to different surface conditions (Demirel et al., 2017a)

The results presented in Figure 10 indicate that the increase in the C_T and P_E of the KCS due to a typical, as applied antifouling (AF) coating were predicted to be 7.1% and 5.9% whereas those due to a deteriorated coating or light slime may increase to 18.1% and 21.2% at ship speeds of 24 knots and 19 knots, respectively. The effect of heavy slime on the KCS hull was calculated to cause an increase in the C_T and P_E of 30.8% at 24 knots and 37% at 19 knots. The calcareous fouling would increase P_E by up to 107.5% at 24 knots and 130.9% at 19 knots.

An interesting point to note is that the effect of a particular fouling condition on the effective power of the KCS is more dominant at lower speeds. This can be attributed to the fact that the contribution of the frictional resistance becomes more important than residuary resistance at lower speeds. In other words, at higher speeds, the wave-making resistance becomes dominant due to wave generation. Therefore, the effect of a given fouling condition on the total resistance of a ship is greater at low to moderate speeds than at higher speeds (Schultz, 2007).

Recently, Owen et al. (2018) investigated the effect of biofouling on propeller characteristics of Potsdam Propeller Test Case (PPTC) propeller using CFD. The effect proved to be drastic with the most severe fouling condition resulting in a 11.94% efficiency loss at J=0.6 ranging to an alarming 30.33% loss at J=1.2 compared to the smooth condition. Figure 11 is useful in showcasing all three open water characteristics in one plot allowing the variation in each to be demonstrated. J = 1.2 was chosen as the clearest difference between fouling conditions occurs here.

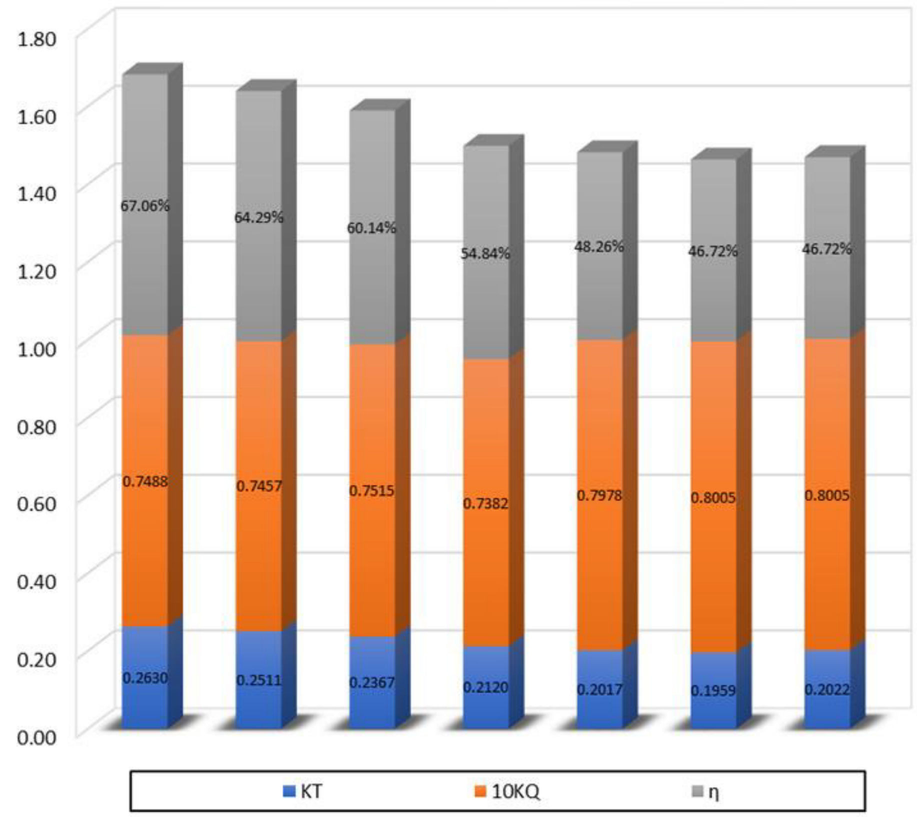

Fig. 11. Open water characteristics for different surface conditions at J=1.2 (Owen et al., 2018)

Results showed that with increasing propeller surface fouling, the magnitude of the propeller thrust coefficient decreases while the magnitude of the torque coefficient increases. This results in a net decrease in open water efficiency of up to 30% at the highest simulated fouling level.

The decreases in the efficiency of the propeller were predicted to be 1.40% at J=0.6 and 4.12% at J=1.2 for a typical as applied antifouling (AF) coating, 3.88% at J=0.6 and 10.31% at J=1.2 for a light slime condition and 11.94% at J=0.6 and 30.33% at J=1.2 for a heavy calcareous fouling condition. These values altered to 6.38%, 11.11% and 11.94% at J=0.6 and 18.22%, 28.03% and 30.33% at J=1.2 for heavy slime, small calcareous fouling or weed and medium calcareous fouling, respectively.

5. Biomimetics

The study of natural systems and copying their functions by means of reverse engineering is called biomimetics. Antifouling strategies are one of the most remarkable features of marine creatures to mimick. Many antifouling strategies have been evolved by marine creatures to keep their surface clean and free from other marine organisms. Ironically, the most nuisance foulers generally have a good antifouling surface topography to avoid the other foulers to attach on themselves (Salta et al., 2012).

5.1 Natural Antifouling Strategies

Many organisms in the nature use various types of antifouling strategies and also combination of them. Some examples of the organisms that use antifouling methods can be expanded from human red blood cell to shark, lotus and birds. This study is focused on the antifouling strategies of marine creatures since the scope of the study covers marine antifouling coatings. In general 3 types of antifouling strategies are used by marine creatures:

- Chemical
- Physical
- Stimuli-Responsive

Many types of chemical secretions are produced by marine creatures to avoid fouling. Some examples of the producers of natural chemical antifouling secretions can be listed as parazoa, algae, bryozoans, cnidarian and mollusca (Chambers et al., 2006). Some tunicate species have acidic pH body fluids at body surface (Ralston and Swain, 2009).

The surface topography and texture are widely used and may be called physical strategies. Physical strategies consist of low drag, low adhesion, wettability and microtexture (Bixler and Bhushan, 2012). Shark skin has inspirational antifouling surface strategies and it also generates low drag and fast swimming properties due to its riblet microtexture and flexion of scales (Bixler and Bhushan, 2012). These scales are longitudinal along the body and they affect the flow properties, such as shear stress, which is the source of frictional resistance (Bixler and Bhushan (2012), Bechert et al. (2000)). Moreover, micro-organisms cannot attach and accumulate on shark skin due to these mechanisms (Kesel and Liedert, 2007). The shark skin demonstration is given in Figure 12 (Bixler and Bhushan, 2012).

Generally, marine creatures combine these strategies to prevent fouling. For example pilot whale skin uses the combination of chemical and physical strategies (Baum et al., 2002).

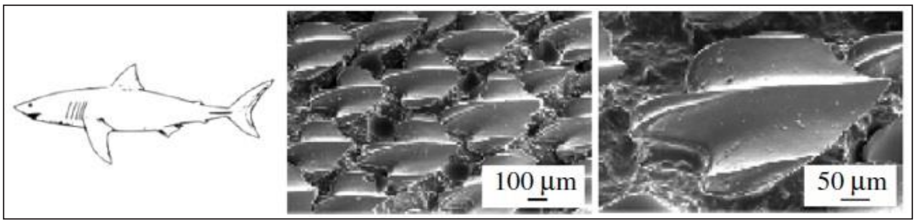

Fig. 12. Shark skin (Bixler and Bhushan, 2012)

The skins of marine mammals and fishes have responsive properties to stimulus such as temperature or pH in the marine environment. The skin of pilot whale, which demonstrates a self-cleaning mechanism by enzymatic digestion (Baum et al., 2002), the denticles of shark skin, which can be bristled actively or passively for drag reduction (Lang et al., 2008) are some examples of surfaces using stimuli responsive strategies.

It is strongly expected that bio-inspired antifouling materials will mimic the physical and chemical activities of the nature to generate the natural defence mechanism against fouling and this principle will play significant role on the development of environmentally friendly antifouling materials/coatings to control and prevent the marine fouling while maintaining an advanced ship performance and hence reduced air emissions.

The use of the antifouling strategies should be associated with operational profile of the vessel and the environmental properties of the region which the vessel in question operates. In other words, the bio-inspired antifouling coating should be a tailored solution, since there are several natural antifouling mechanisms, developed regarding the specific demands of the transportation. The factors affecting the development of bio-inspired antifouling coating are shown in Figure 13. It is clearly seen that biomimetics offers a promising solution and researchers should take the advantage of the natural antifouling strategies to tie them to the marine antifouling coatings.

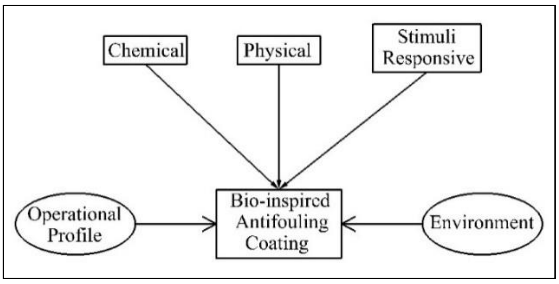

Fig. 13. Development of bio-inspired antifouling coatings

5.2 Challenges

Although, bio-inspired antifouling technology rises up as one of the best possible solution, there are many challenges and questions far from answered.

One remarkable drawback of the idea of using natural chemicals for antifouling purposes would be their lifespan which last only a few months (de Nys and Steinberg, 2002). It should be taken into consideration that there are many unknowns about these chemicals and the effects of excessive use of these chemicals on marine environment.

Solely physical antifouling methods are effective for a few months and against only specific foulers (Bers and Wahl, 2004). On the other hand, physical strategies are compatible with the existing antifouling coatings and also promising for future studies (Ralston and Swain, 2009).

Because of the fact that natural surfaces and properties are totally distinct from man-made marine structures' surfaces, it is not easy to achieve a harmony. For instance, producibility in large quantities is one of the most important issues. Hitherto, it is not commercially feasible to do.

Marine creatures are generally moving at very low Reynolds number compared to ships. Another challenge is to adapt these antifouling properties to man-made marine vehicles that move in relatively higher Reynolds numbers. The different Reynolds numbers of marine creatures and ships are demonstrated in Figure 14 (Salta et al., 2012). A major problem with biomimicry is to maintain the physical and chemical properties for long time since these properties normally remain on the living things.

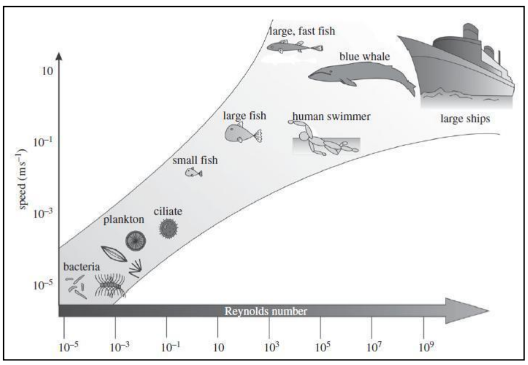

Fig. 14. Reynolds number range of different marine creatures and ships (Salta et al., 2012)

6. Conclusions

New horizons in marine coatings were covered in this study. Marine biofouling problem and the current antifouling methods, the latest research in coating/fouling hydrodynamics and also novel approaches to the solution were presented from a naval architecture point of view. The recent research project FOUL-X-SPEL developed a novel, non-leaching antifouling polymer systems, in which the biocide is fixed in and hence the surface has active antifouling principle in order to avoid fouling while avoiding biocide releasing.

Another novel and pioneering approach is bio-inspired antifouloing technology utilizing biomimetics. Nature has diverse antifouling strategies and nature often uses the combination of them. The tailored combination of these strategies could be used to achieve an effective fouling prevention for both ships and stationary marine structures.

Novel antifouling technologies should be developed concerning the possible direct harmful effects of existing antifouling methods to marine environment and also indirect effects such as increasing emissions. For these reasons, more research effort should be devoted to enhance the marine antifouling coatings/technologies as well as to achieve more environmentally friendly shipping.

All in all, it is believed that, the research activities on antifouling coatings will lead to very effective prevention of marine biofouling while maintaining the harmony between man-made structures and marine life.

7. References

ABS. (2011). Surveyor [Online]. Available:
http://www.eagle.org/eagleExternalPortalWEB/ShowProperty/BEA%20Repository/News%20&%20Events/Publications/Quarterly/Surveyor/2011/Surveyor_2011Fall 14/07/2013].

Alzieu, C. L., Sanjuan, J., Deltreil, J. P. and Borel, M. (1986). Tin contamination in Arcachon Bay: Effects on oyster shell anomalies. Marine Pollution Bulletin, 17, 494-498.

AMBIO. (2005). AMBIO: Advanced nanostructured surfaces for the control of biofouling [Online]. http://www.birmingham.ac.uk/generic/ambio/index.aspx.

Atlar, M. (2008) An update on marine antifoulings. 25th ITTC Group Discussions 3 – Global Warming and Impact on ITTC Activities, Fukuoka, 2008.

Baum, C., Meyer, W., Stelzer, R., Fleischer, L. G. and Siebers, D. (2002). Average nanorough skin surface of the pilot whale (Glibicephala melas, Delphinidae): considerations on the self-cleaning abilities based on nanoroughness, Mar. Biol. 140, 653–657.

Bechert, D.W., Bruse, M. and Hage, W. (2000). Experiments with three-dimensional riblets as an idealizedmodel of shark skin', Exp. Fluids 28:403–12.

Bers, A. and Wahl, M. (2004). The influence of natural surface microtopographies on fouling', Biofouling 20 43–51.

Bixler, G.D. and Bhushan, B. (2012). Biofouling: lessons from nature. Phil. Trans. R. Soc. A 2012 370, 2381-2417.

BYEFOULING. (2013). BYEFOULING: Low-toxic cost-efficient environment-friendly antifouling materials [Online]. http://cordis.europa.eu/project/rcn/110983_en.html.
Candries, M., Atlar, M. and Anderson, C. (2003). Estimating the impact of new-generation antifoulings on ship performance: the presence of slime. Journal of Marine Engineering & Technology, 2, 13-22.

Chambers L.D., Stokes K.R., Walsh F.C. and Wood R.J.K. (2006). Modern approaches to marine antifouling coatings. Surface & Coatings Technology 201: 3642–3652.

Champ, M. A. (2003). Economic and environmental impacts on ports and harbors from the convention to ban harmful marine anti-fouling systems. Marine Pollution Bulletin, 46, 935-940.

Dafforn, K. A., Lewis, J. A. and Johnston, E. L. (2011). Antifouling strategies: History and regulation, ecological impacts and mitigation. Marine Pollution Bulletin, 62, 453-465.

de Nys, R. and Steinberg, P.D. (2002). Linking marine biology and biotechnology. Current Opinion in Biotechnology 13 (3), 244-248.

Demirel YK, Khorasanchi M, Turan O, Incecik A and Schultz MP. (2014). A CFD model for the frictional resistance prediction of antifouling coatings. Ocean Engineering.89:21-31.

Demirel, Y.K., Turan, O., Incecik, A. (2017a). Predicting the effect of biofouling on ship resistance using CFD. Applied Ocean Research 62, 100-118. http://dx.doi.org/10.1016/j.apor.2016.12.003

Demirel, Y.K., Turan, O., Incecik, A., Day, S., Fang, H.I., Downie, S., Olsen, S.M. (2015). Experimental determination of the roughness functions of marine coatings. In: Proceedings of International Conference on Shipping in Changing Climates (SCC 2015), 24 – 26 November 2015. Glasgow, UK.

Demirel, Y.K., Uzun, D., Zhang, Y., Fang, H.-C., Day, A.H., Turan, O. (2017b). Effect of barnacle fouling on ship resistance and powering. Biofouling 33 (10), 819-834. https://doi.org/10.1080/08927014.2017.1373279

FOUL-X-SPEL. (2011). FOUL-X-SPEL : Environmentally friendly antifouling technology to optimise the energy efficiency of ships [Online]. http://www.foulxspel-antifouling.com/.

Gibbs, P. and Bryan, G. (1986). Reproductive failure in populations of the dog-whelk, Nucella lapillus, caused by imposex induced by tributyltin from antifouling paints. Journal of the Marine Biological Association of the United Kingdom, 66, 767-777.

IMO (2009). International Shipping and World Trade Facts and Figures, Maritime Knowledge Centre. London.

IMO. (2001). International convention on control of harmful anti-fouling systems on ships.
Kempf, G. (1937). On the effect of roughness on the resistance of ships. Trans INA, 79, 109-119.

Kesel, A. and Liedert, R. (2007). Learning from nature: non-toxic biofouling control by shark skin effect. Comp. Biochem. Physiol. A. 146, S130.

Lang A.W., Motta P., Hidalgo P. and Westcott M. (2008). Bristled shark skin: a microgeometry for boundary layer control?', Bioinsp. Biomim. 3:046005.

LEAF. (2012). LEAF: Low emission antifouling coatings based on the novel discovered post settlement penetration triggered antifouling [Online]. http://leaf-antifouling.eu/.

Milne, A. (1990). Roughness and drag from the marine paint chemist's viewpoint. Marine Roughness and Drag Workshop, 1990 London.

Okay, O. S. (2004). Antifouling içeren gemi boyalarının uluslararası kurallar çerçevesinde kirletici etkilerinin incelenmesi. TMMOB, Gemi Mühendisliği Odası, Gemi Mühendisliği ve Sanayimiz Sempozyumu, 24-25 December 2004 Istanbul, Turkey.

Owen, D., Demirel, Y.K., Oguz, E., Tezdogan, T., Incecik, A. (2018). Investigating the effect of biofouling on propeller characteristics using CFD. Ocean Engineering. https://doi.org/10.1016/j.oceaneng.2018.01.087

Ralston, E. and Swain, G. (2009). Bioinspiration—the solution for biofouling control?. Bioinspir. Biomim. 4, 015007.

Salta, M., Wharton, J.A., Stoodley, P., Dennington, S.P., Goodes, L.R., Werwinski, S., Mart, U., Wood, R.J.K., and Stokes, K.R. (2012). Designing biomimetic antifouling surfaces', Phil. Trans. R. Soc. A 2010 368, 4729-4754.

Schultz, M. P. (2007). Effects of coating roughness and biofouling on ship resistance and powering. Biofouling, 23, 331-341.

SEAFRONT. (2014). SEAFRONT: Synergistic fouling control technologies [Online]. http://cordis.europa.eu/project/rcn/111293_en.html.

Taylan, M. (2010). An overview: effect of roughness and coatings on ship resistance. International Conference on Ship Drag Reduction SMOOTH-SHIPS, 2010 Istanbul, Turkey.

Van Rompay, B. (2012). Surface Treated Composites White Book, Tahoka Press.

Wahl, M. (1989). Marine epibiosis. I. Fouling and antifouling: some basic aspects. Marine Ecology Progress Series, 58, 175-189.

Hidrodinamik Sürtünme Direncinin Araştırılmasında Kullanılacak Deneysel Bir Yöntemin Geliştirilmesi

Serkan Turkmen[1], Mehmet Atlar[2], Irma Yeginbayeva[3], Simon Benson[4]

serkan.turkmen@ncl.ac.uk[1], mehmet.atlar@strath.ac.uk[2], irmay@chalmers.se[3]

[1] Newcastle University, Newcastle upon Tyne, UK,

[2] University of Strathclyde, Glasgow, UK,

[3] Chalmers University of Technology, Gothenburg, SE

[4] Newcastle University, Newcastle upon Tyne, UK

Özet

Newcastle Üniversitesi (UNEW) hali hazırda çalışan kapalı çevrim su kanalını geliştirdi. Yeni ölçüm bölümü kaplanmış standart bir test panel yüzeyi (boy x en x kalınlık ölçüler 0.6m x 0.22m x 0.015m) boyunca basınç azalışını (dolayısıyla sürtünme direncini) ölçmeye yarar. Panel hem temiz hem de hafif yosunlanmış olarak test edilebilir. Basınç değişimine bağlı olarak, test edilen yüzeyin sürtünme direnç katsayıları hesaplandı ve sonuçlar kabul edilmiş yöntemlerle karşılaştırılarak basınç azalım yöntemi değerlendirilmiştir.

Bu çalışmada, su kanalının tasarımı ve kalibrasyonu sunulmuş ve kaplamış üç farklı yüzeyin sürtünme dirençleri tam gelişmiş türbülanslı akımda incelenmiştir.

Anahtar Kelimeler: Sürtünme direnci, su kanalı, biyolojik kirlilik pürüzlülüğü

Development an Experimental Method to Investigate Hydrodynamic Drag

Serkan Turkmen[1], Mehmet Atlar[2], Irma Yeginbayeva[3], Simon Benson[4]

serkan.turkmen@ncl.ac.uk[1], mehmet.atlar@strath.ac.uk[2], irmay@chalmers.se[3]

[1] Newcastle University, Newcastle upon Tyne, UK,

[2]University of Strathclyde, Glasgow, UK,

[3]Chalmers University of Technology, Gothenburg, SE

[4] Newcastle University, Newcastle upon Tyne, UK

Abstract

Newcastle University's (UNEW's) enhanced the test section of their existing flow-cell facility. New measurement section is to measure the pressure drop (and hence frictional drag) across coated surface of a standard flat test panel (of Length x Width x Thickness: 0.6m x 0.22m x 0.015m in size). The panel can be tested as cleanly coated as well as exposed to light biofilm growth. Based on pressure gradients the calculated skin friction coefficients of these surfaces were compared with the results of the measurements obtained by other well-established methods to predict the skin friction, i.e. measuring boundary layer of the same surfaces using a Laser Doppler Velocimetry (LDV) system in the UNEW's Emerson Cavitation Tunnel (ECT), to evaluate the pressure drop methodology.

This paper presents design and calibration of the flowcell to investigate skin-friction of three different surfaces coatings in a fully developed turbulent flow.

Keywords: Drag, flowcell, biofouling, roughness

1. Introduction

When a sailing ship's submerged part of the hull is concerned, one of the main parameters affects the total resistant is frictional resistance, beside wave-making resistance. Frictional resistance is caused by normal and tangential components of the viscous flow. The normal component of the viscous resistance is affected by the hull shape and it is called form factor in the literature. The tangential component of the viscous resistance (shear stress) is parallel to ship's hull and causes a net force opposing the motion. This phenomenon is also called skin friction (Harvald Sv 1983).

Ships are paying the big economic penalty due to marine biological fouling on their hull. For instance, skin friction can increase 30-40%, depends on the light or hard fouling that lead to consume more fuel or reduce the operation speed (Woods Hole Oceanographic Institution (WHOI) 1952, Townsin 2003, Banerjee, Pangule et al. 2011, Schultz et al. 2011). In fact, increasing fuel consumption causes further trouble as the vessel is not able to satisfy the mandatory regulations for carbon emission of ships e.g. Energy Efficiency Design Index (EEDI) and the Ship Energy Efficiency Management Plan (SEEMP).

Marine coatings are essential to prevent biofouling development on ships. Self-Polishing Co-Polymer (SPC) and Foul Release (also called non-stick, low surface energy) silicone elastomer are the most common antifouling coatings since Tributyltin (TBT) was completely banned from application in 2003. The effectiveness of the coated hull surface can be differed due to being hydraulically rough and aging as well as fouling. The development of test methodologies for the evaluation of the hydrodynamic performance of fouling control coating is particularly complex. There are several established methods to assess the hydrodynamic performance of a rough and biofilmed surface (Candries 2001, Politis, Atlar et al. 2013). This development has to be designed in such a way to replicate/mimic the physical and environmental conditions that the coating will experience when applied on the surface of the hull of a ship. The most common techniques are flume, circulating water tunnel, towing tank, axy-symmetrical slender body, rotating disk and drum Taylor-Couette flow facility. Among of them rectangular flow channels, generally known as flume (or flowcell), a fast and economical method to test such coatings is a turbulent sea water flow channel.

Newcastle University enhanced the pressure drop flume by replacing its measuring section with a sophisticated pressure drop facility to assess skin friction characteristic of a standard test panel (of Length x Width x Thickness: 0.6m x 0.22m x 0.015m in size) allows easy transportation. The dimension of the panels was chosen to be compatible with different facilities of Newcastle University, i.e. the Cavitation Tunnel, Flowcell, coating aging flume, slime farm and strut arrangement of the RV Princess Royal (Politis, Atlar et al. 2013).

The test panels containing the biofilm samples can be transferred to the UNEW testing facilities in the shortest time in wet containers for hydrodynamic testing when the required amount of biofilms are collected. Therefore, clean and biofouled flat panels can be tested to measure their skin friction in fully turbulent flows by modern experimental facilities is more robust and attractive.

The main purpose of this state of the art device is to investigate skin friction characteristics of flat test panels which can be non-coated or coated as well as they can be in clean or subjected to biofilm in seawater condition. Design and calibration process of the Flowcell were presented in the paper. Further tests were conducted to investigate skin friction of three surfaces coatings, with different roughness profile. Results were given to correlate roughness and hydrodynamic drag performance evaluated by the Flowcell.

2. The flowcell and experimental apparatus

2.1. The UNEW's flowcell

Figure 1 shows the layout of the new pressure drop measurement section of this facility and test panels arrangement. As shown in Figure 1 the measurement section is made of stainless steel with a 2.7 m length and installed between a contraction section with a contraction (cross-sectional area) ratio of 34.7:1 and the settling tank. Two identical test panels can be placed at the top and bottom of the pressured drop section. The rectangular measurement section has 10mm channel height (H) and 180mm width

(W) shows a ratio W/H=18:1. This high aspect ratio ensures the channel flow is two-dimensional (Dean 1978, Zanoun, Nagib et al. 2009). Length to height ratio is 270 that is much higher than recommended channel length for fully developed turbulent flow (Monty 2005). The panel surfaces are flush with the inner walls of the testing section to ensure the channel height remains the same.

Figure 2 shows a picture of this new stainless steel test section installed on the existing flowcell circuit with the new contraction section. A very rigid frame (in blue colors) supports the heavy stainless steel section which provides much rigid, level, steady and quite water channel as opposed to the old, uneven and cracking acrylic measuring section that was at the end of its working life.

The new pressure drop section has a 150 mm long glass window at one side that can be used to measure the flow velocity profiles between the test panels using LDV or other optical devices (e.g. PIV). There are four pressure taps on the bottom wall and nine pressure taps on one of the side walls of the test section that enable to collect a wide range of pressure drop data using differential pressure transducers. An inspection hatch, which is the replica of the hatch for housing the test panels, is also installed in upstream of the latter hatch, for cleaning and maintaining purposes

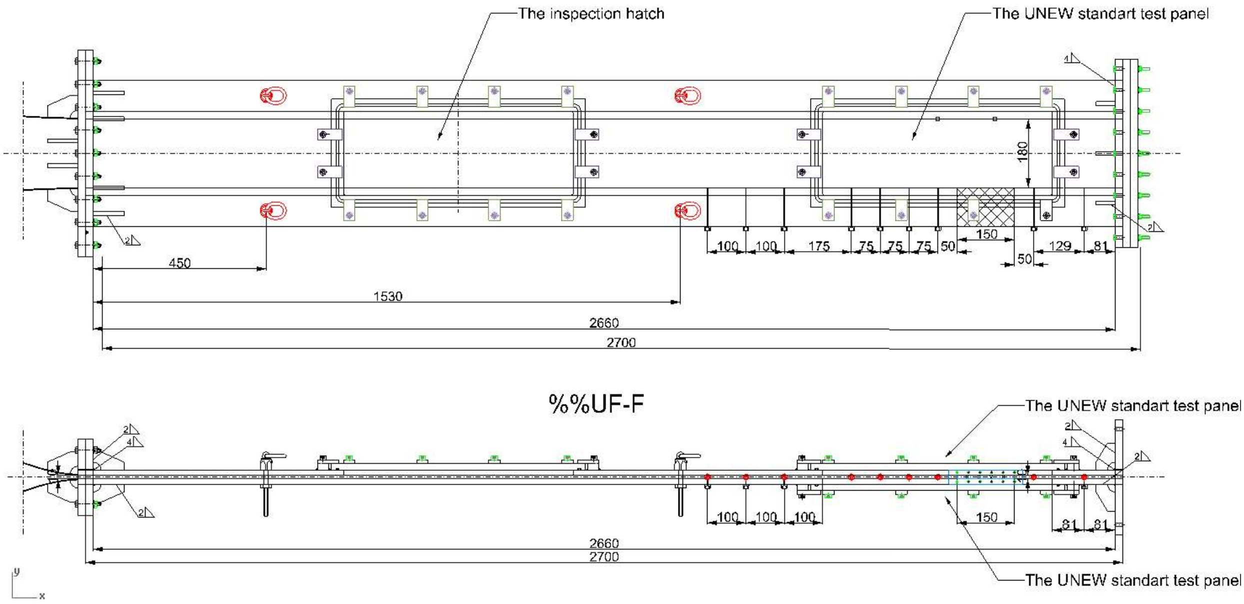

Fig. 1. Pressure drop section with contraction (inlet) and discharge (outlet)

Fig. 2. A view of new test section of the UNEW Flow Cell

2.2. Measuring equipment

Pressure drop measurements are taken by using differential pressure transmitters (transducers) with different pressure ranges. The water temperature is monitored during the tests to avoid extreme temperature rise. The inflow speed measured in the test section is presented as a function of the pump speed. In fact, the calibration curves mentioned in Section 3.1 were represented in this manner. A data acquisition system (DAQ) is used to log both pump speed and the pressure drop values.

Flowcell has a 15kW pump which can provide flow rate up to 300l/s. In practice, the user relates the channel inflow speed to the pump speed as stated inthe calibration curve.

Differential type pressure sensors are used to measure the pressure differences (pressure drop) between interchangeable two pressure taps. The range of the pressure drop was defined by computational fluid dynamic calculation. Two XMD differential pressure transmitters were installed for the range 0-75mbar and 0-500mbar with the accuracy of 0.1%. The pressure drop data was also recorded with a sampling rate of 10Hz. An overview of the data logging system and measurement equipment for the pump speed and pressure drop is given in Figure 3.

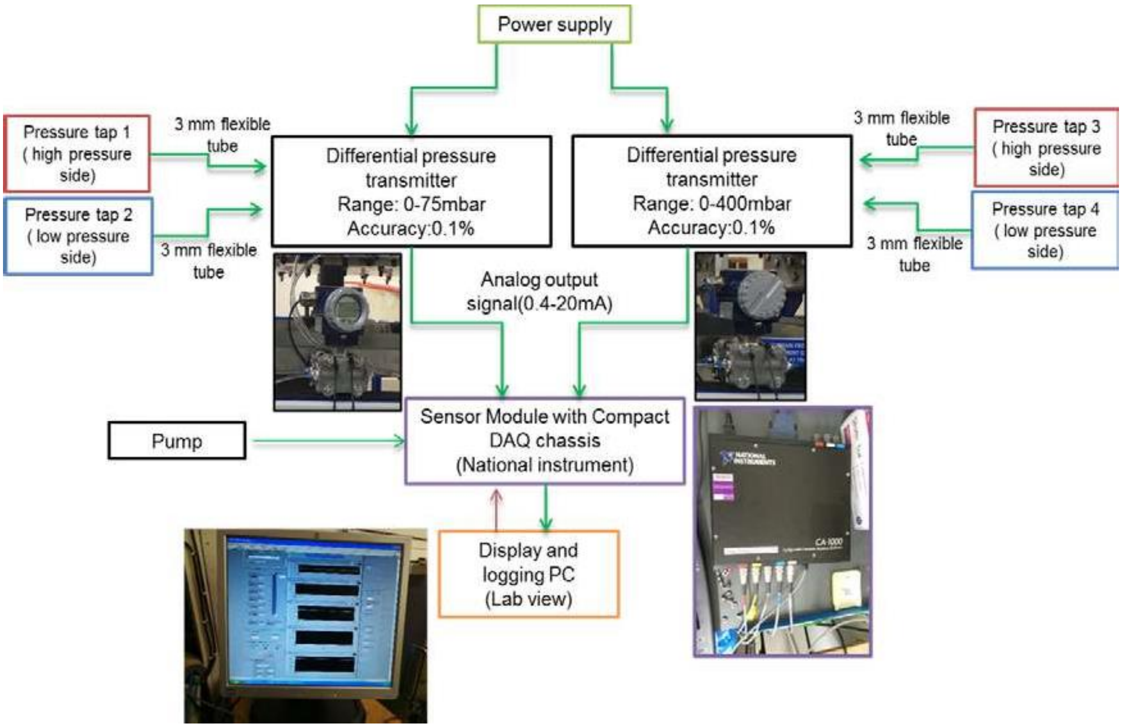

Fig. 3. Experimental apparatus layout for main pump speed drive and pressure data logging.

2.3. Calibration

There are two main objectives of the calibrations. The first is to relate the flow details (i.e. flow velocity and turbulence components as well as the pressure drop) over the reference smooth surface at the measuring section to the entire range of the main pump speeds since the pump speed is the most practical driver for the flowcell user.

It is expected from a flume that can generate fully develop turbulence flow over the panels. This is possible when the measurement section is long enough. Although dimension of the standard panel is significantly bigger than former test panels (75mm x 25 mm, microscopic slides) flow field was measured at different cross section along the measurement section. Therefore, the second objective of the calibration is to prove fully developed turbulence flow is generated in the measurement section.

Hydrodynamic characteristics of the flow in the measurement section were captured by using 2D Dantec Laser Doppler Velocimetry (LDV) system. Although there are other flow measurement devices (e.g. pitot tubes, hot wire anemometry, ultrasonic devices) the LDV system has the biggest advantage of being a non-intrusive device as well as taking time-dependent point measurements at any specific point. The flowcell was filled with fresh water for the calibration and the water was seeded for the LDV with silver coated glass particles of 2-micron size.

LDV measurements were taken at three longitudinally selected frames with 150 mm intervals and at nine transverse positions with 22.5mm intervals. Figure 5 shows the LDV probe (500 mm focus length) and traverse that drives the LDV probe at any desired point(s) using a computer control with a great accuracy and efficiency. During the calibrations, the traverse was located next to the measurement section for easy reach. The flow velocity components, streamwise (U) and transverse (V), as well as their respective turbulence intensities were measured at these points. The location of the measurement points is demonstrated in Figure 4.

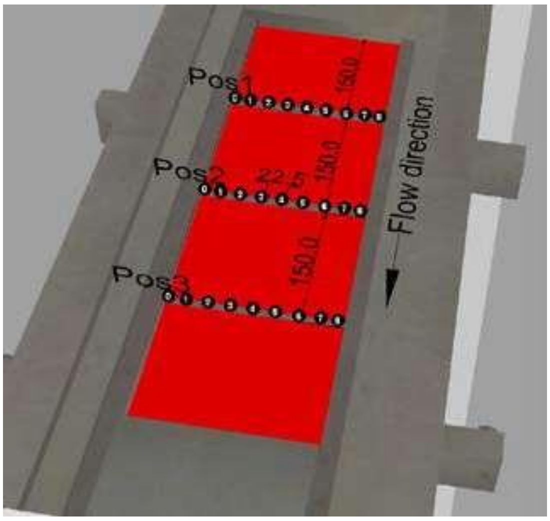

Fig. 4. Locations of flow measurement points along the pressure drop section

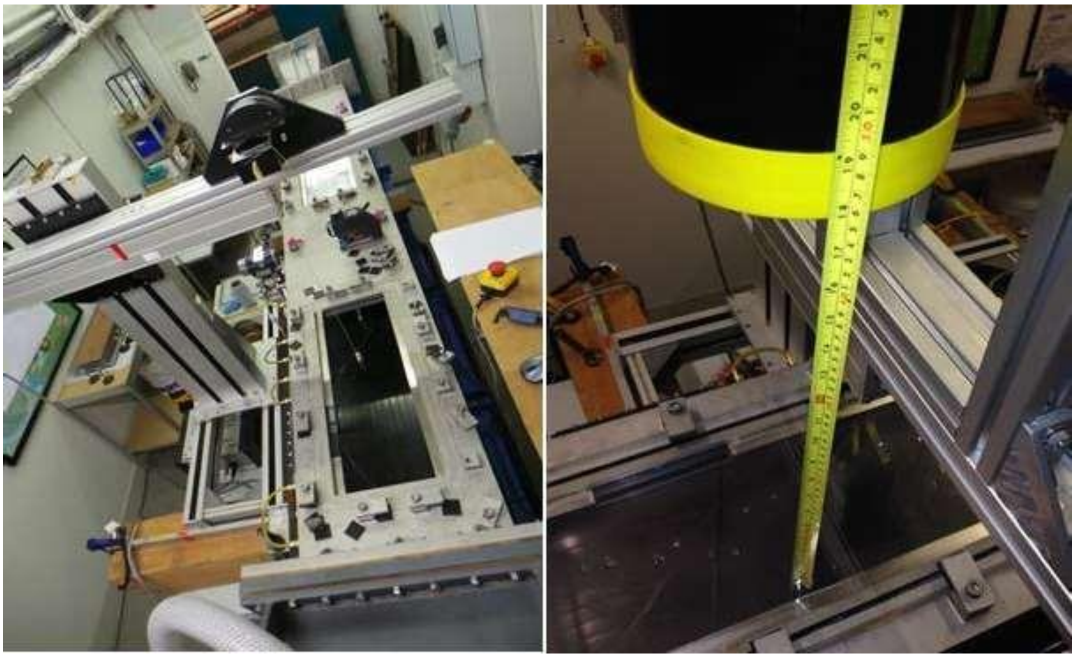

Fig. 5. Traverse arrangement of LDV during calibrations

Monty (2005) stated that a study comparing turbulence statistics at a number of streamwise stations is necessary to determine the point of full development. Figure 6 presents the flow speed in streamwise (U) and transverse (V) direction, respectively, for the pump speed of 600rpm. Whereas Figure 7 shows the streamwise (U) velocity vector distribution in a vertical and transverse direction at the three different longitudinal positions (Pos1, Pos2 and Pos3) overlapping with the mean U velocities at these positions. Calibration tests showed that the new test section can effectively develop fully turbulent flow at the pressure drop measurement section.

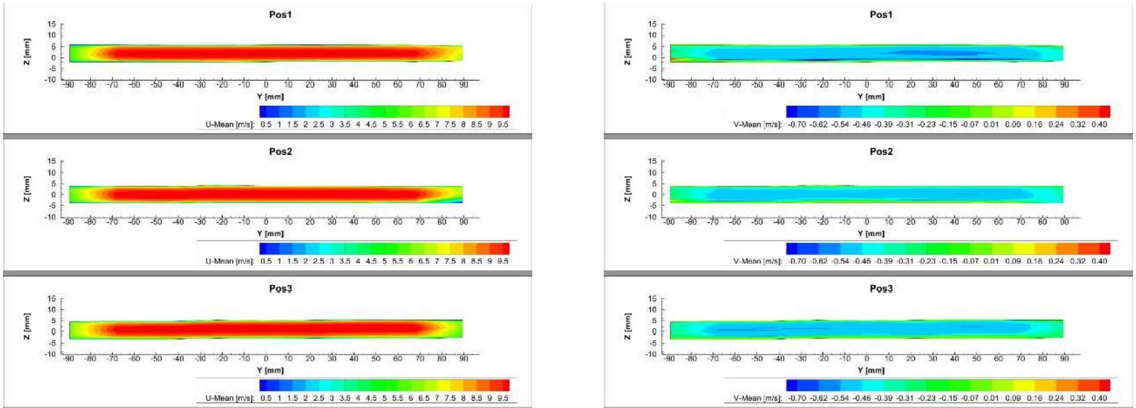

Fig. 6. The flow speed in U (right) and V (left) axis at pump speed of 1600rpm

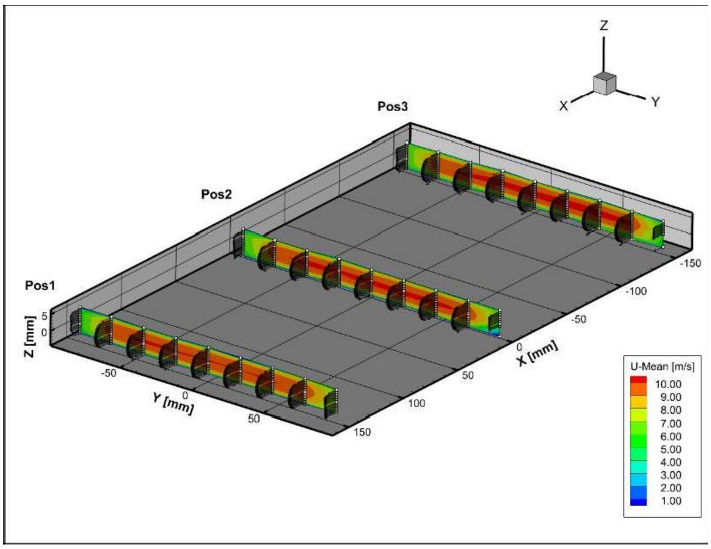

Fig. 7. The development of the velocity boundary layer between target plates at pump speed of 1600rpm

3. The pressure drop methodology

In order to obtain the static pressure gradient $\frac{dp}{dx}$ (ratio of the pressure drop per unit of length), the pressure drop (i.e. p1-p2) is divided by observation length l (distance between the taps in the side of the channel). The relationship between the wall shear stress (τ_w) and the static pressure gradient may be obtained by Equation 1 (Nikuradse 1933).

$$\tau_w = -\frac{H}{2}\frac{dp}{dx} \tag{1}$$

where H is the channel height, dp is the pressure difference between two pressure taps and dx is the distance between the two pressure taps used to measure the pressure differences. The friction velocity u is introduced as a function of the wall shear stress and density.

$$u_\tau = \left(\frac{\tau_w}{\rho}\right)^{0.5} \tag{2}$$

where, the water density ρ is taken as 998 kg/m3 (at the temperature 20°C). The friction coefficient Cf for a rectangular duct is defined as a function of the wall shear stress, bulk (mean) velocity $\bar{U}$ and the density of the fluid:

$$C_f = \left(\frac{\tau_w}{0.5\rho\bar{U}^2}\right) \tag{3}$$

The skin friction coefficient Cf can be rewritten from Equation 2 and Equation 3 as:

$$C_f = 2\left(\frac{u_\tau}{\bar{U}}\right)^2 \tag{4}$$

The Reynold's number can be also described based on the full height (H) of the measurement section and bulk mean velocity $\bar{u}$ (or mean velocity):

$$Re_m = \frac{H\bar{u}}{\nu} \tag{5}$$

where ν is the kinematic viscosity of the water (1.004x10^{-6} m^2/s).

3.1. Description of test surfaces

For the evaluation of the pressure drop methodology the pressure drop data were measured over three different surfaces described as follows:

1. Hydrodynamically smooth, clean acrylic panel, which is referred as "Reference" surface (indicated as "Surface A" in presentations)

2. Clean, newly applied Foul Release (FR) coated panel to represent low to medium range rough surface (Indicated as "Surface B" in presentations);

3. Clean, newly applied Self Polishing Copolymer (SPC) coated panel with introduced extra roughness to represent a rough surface (indicated as "Surface C" in presentations).

The three surfaces each in two replicates of the UNEW test panels were placed onto the flowcell pressure drop section for the calibration as shown Figure 8: top panel on the left (replicate 1 of Surface A); bottom panel on the right (replicate 2 of Surface A).

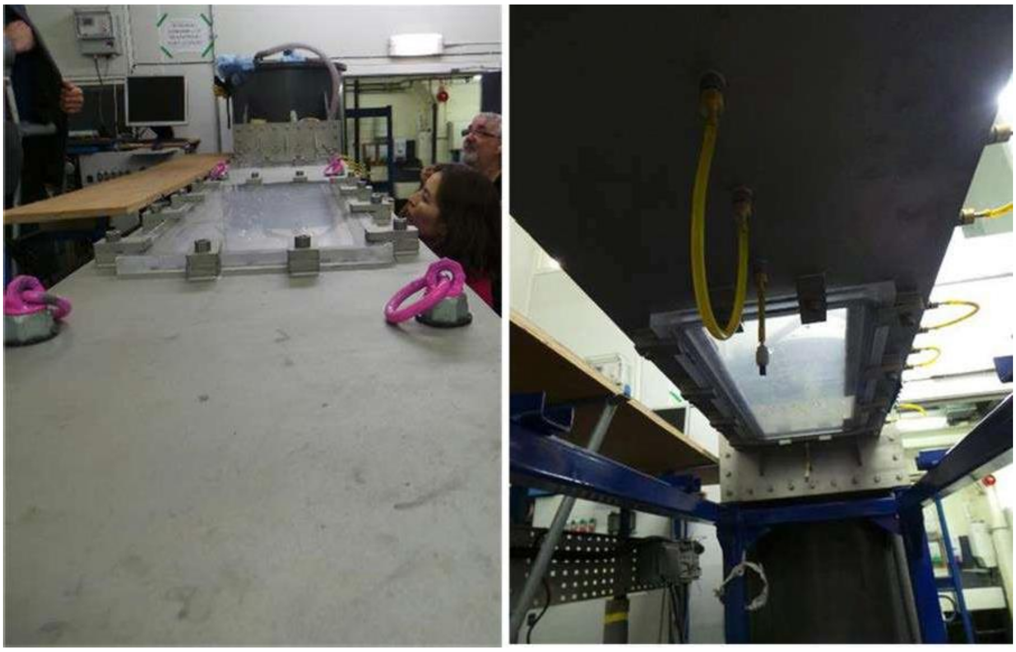

Fig. 8. Two parallel smooth test panels (Surface A and its replicate) in place, top panel (left); bottom panel (right)

3.2. Roughness measurements

The roughness measurements of the three surfaces were carried out using Uniscan's OSP100 device. This instrument is a non-contact, laser-based, high accuracy surface profiling system, used to measure and analyse the roughness. The arithmetic mean of the roughness (Ra) is the general way to describe general surface roughness. From the measured surface profiles the mean Ra values are calculated by comparing all the peaks and valleys to the mean line and then averaged over the entire cut off length of 5 mm. Table 1 shows the results of the mean Ra values as well as other roughness parameters of the three surfaces measured. Surface A, the clean acrylic surface, gives to the smallest Ra of 0.72 µm as being the hydraulically smooth "Reference" surface. The Ra value of Surface B (low to medium rough surface) is 1.94 µm representing a newly coated foul release surface. The third surface, Surface C, is the roughest one with an average Ra value of around 29 µm and representing a coated surface "in-service" conditions.

Table 1. Intervals of design variables

	Ra(µm)	Rq(µm)	Rt(µm)	Sk	Ku
Surface A	0.72	1.09	6.99	0.8	5.98
Surface B	1.94	2.35	12.77	0.17	3.59
Surface C	28.83	33.93	125.83	0.29	2.82

4. Measurements, analyses and presentation of results

The pressure drop measurements were carried out for a range of pump speeds. Equation 5 was used to calculate the Reynolds number (Re_m) varying from 24000 to 113000. The skin friction coefficient (C_f) of the tested panels were plotted against to Reynold's number in Figure 9. The hierarchy amongst the tested surfaces as a function of the surface roughness is clearly apparent as expected by considering the roughness characteristics of these test surfaces.

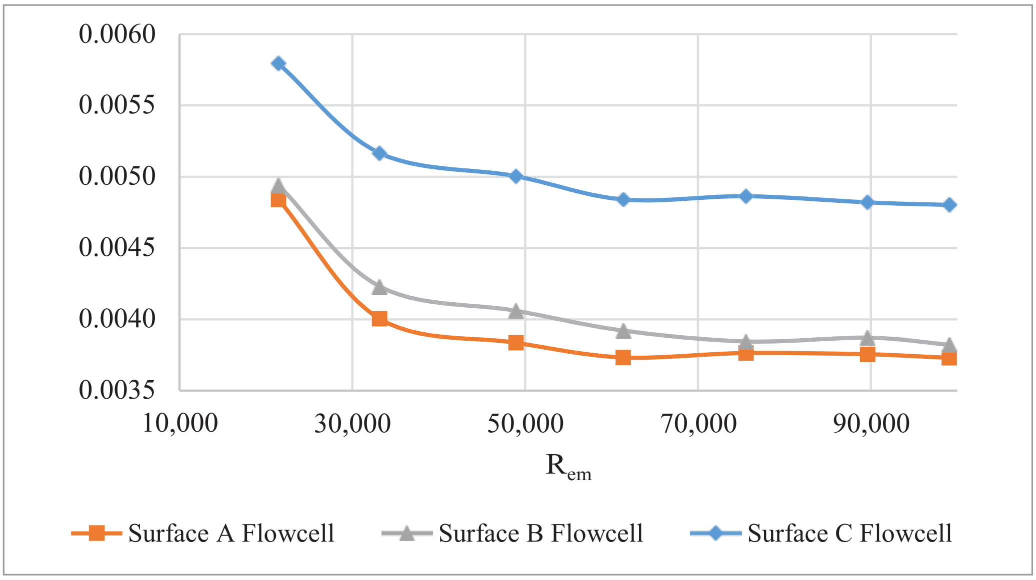

Fig. 9. The comparative friction coefficient of test panels as a function of flow speed.

4.1. The error

Precision uncertainty estimates for the pressure drop measurements were made using repeatability test. Seven replicate measurements were taken on the acrylic and the SPC coated panels. Error in the pressure drop repeatability was estimated based on the measured data by Equation 6. Very small error

(maximum 1.01%) was found and included in Table 3.

$$Error = \frac{Test1 - Test2}{Test1} x100 \quad (6)$$

Table 3. Error of the pressure drop repeatability test

Flow speed (m/s)	1.62	2.87	4.01	5.17	6.29	7.45	8.3
Error (%)	0.92	1.01%	0.08%	0.44%	0.10%	0.01%	0.16%

5. Concluding Remarks

An extensive experimental programme was carried out for the evaluation of the pressure drop methodology by using UNEW's enhanced Flowcell, which was recently modified to accommodate a new pressure drop section, and the Emerson Cavitation Tunnel's boundary layer measurement set-up using LDV. The methodology can be used to calculate the hydrodynamic performance (i.e. skin friction characteristics) of any type of flat surface with different roughness profiles. The skin friction data of these surfaces can be provided in a short time which can substitute the skin friction analysis based on the traditional boundary layer measurement method.

In order to evaluate the new methodology three flat test panels with different surface finishes. The analysed results indicated the following conclusions:

• Calibration tests with the flowcell showed that the enhanced facility with the new stainless still test section can generate the fully tubulent flow at the pressure drop measurement section. The calibration curves for the enhanced flow cell are represented by two reference velocities at the pressure drop measurement section which are the maximum inflow velocity measured at the centre of the pressure drop section and averaged velocity (or bulk velocity) determined from the spatially measured inflow velocities in the same section.

• It was clear that pressure drop methodology displayed the direct relationship between the roughness and the drag characteristics of the tested surfaces: the rougher the surface the higher the measured friction velocities.

• The relative merits of the measured surfaces (i.e. hierarchy of C_f for Surface A, B, C) from the ECT and Flowcell are almost the same. This is extremely encouraging for the new measurement methodology (i.e. Flowcell/Pressure Drop) as it will enable us to evaluate the relative merits of the surfaces with different coatings and biofilms effectively in a very short measurement time.

The future plans is to correlate the roughness characteristics of surfaces with drag performances. The correlation will be able to use the roughness functions for extrapolation of results to full scale.

Acknowledgements

The research leading to these results has receieved funding from the European Union Seventh Framework Programme (FP7-OCEAN-2013) project Seafront under grand agreement No: 614034.

6. References

Banerjee, I., Pangule, R., C. and Kane, R., S. (2011). Antifouling Coatings: Recent Developments in the Design of Surfaces That Prevent Fouling by Proteins, Bacteria, and Marine Organisms, Advanced Materials, Vol. 23, no. 6, pp 690-718.

Candries, M. (2001). Drag, boundary layer and roughness characteristics of marine surfaces coated with antifoulings, . Ph.D., Newcastle University.

Dean, R. B. (1978). Reynolds Number Dependence of Skin Friction and Other Bulk Flow Variables in Two- Dimensional Rectangular Duct Flow, Journal of Fluids Engineering, Vol. 100, no. 2, pp. 215-223.
Harvald Sv, A. (1983). Resistance and Propulsion of Ships, John Wiley & Sons, New York.

Monty, J., P. (2005). Developments in smooth wall turbulent duct flows, University of Melbourne, Ph.D., Department of Mechanical and Manufacturing Engineering.

Nikuradse, J. (1933). Laws of flow in rough pipes, VDI Forschungsheft, Citeseer.

Politis, G., Atlar, M., Kidd, B. and Stenson, P. (2013). A Multipurpose Flume for The Evaluation of Hull Coatings, 3rd International Conference on Advanced Model Measurement Technology for the Maritime Industry (AMT'13), Gdansk, Poland

Schultz, M., P., Bendick, J., A., Holm, E., R. and Hertel, W., M. (2011). Economic impact of biofouling on a naval surface ship, Biofouling, Vol. 27, no. 1, pp. 87-98.

Townsin, R. L. (2003). The Ship Hull Fouling Penalty, Biofouling, Vol. 19, no.1, pp. 9-15.

Woods Hole Oceanographic Institution (WHOI). (1952). Marine fouling and its prevention; prepared for Bureau of Ships, George Banta Publishing Company, Annapolis, Maryland.

Zanoun, E., Nagib, S., H. and Durst, F. (2009). "Refined cf relation for turbulent channels and consequences for high-Re experiments." Fluid dynamics research 41(2): 021405.

Zaman Çarteri Esnasında Meydana Gelen Karina Kirlenmesi: Geminin Düşük Performansından Doğan Sorumluluk

Ceren Cerit Dindar

cerencerit.6@gmail.com

Institute of International Shipping and Trade Law, Swansea University, UK

Özet

Zaman çarteri sözleşmesinde, teslimle birlikte donatılmış bir geminin ticari yönetimi belli bir ücret karşılığında çarterere tahsis edilmektedir. Çarterer anlaşılan çarter süresi boyunca gemiyi çarter sözleşmesinde belirtilen coğrafi sınırlar içerisindeki her yere gönderebilir. Bu yüzden, çarter sözleşmesinde bu konuda bir sınır olmadıkça, prensipte çartererin gemiyi tropikal sularda kullanmaya yönelik talimat vermesini engelleyen hiçbir şey yoktur. Çartererin bu tarz bir talimatı meşru bir talimat olarak kabul edilmektedir ve gemi sahibinin bu talimata uyması gerekmektedir. Eğer ki gemi sahibi çartererin bu talimatını haklı bir sebebi olmadan reddedecek olursa, kendisinin bu davranışı fesih hakkı veren (repudiatory) sözleşme ihlali oluşturabilecek ve böylece çarterere sözleşmeyi sonlandırma hakkı verebilecektir. Bu noktada problem şu ki gemi tropikal sularda, uzun süre kaldığı zaman, gemi karinasında kirlenme (hull fouling) çoğunlukla gündeme gelmektedir. Bu doğa olayı deniz organizmalarının geminin karinasında toplanması kümelenmesi olarak tanımlanabilir. Bu durum, geminin performansını etkileyebilecek ve de geminin çarter sözleşmesinde belirtilen hızdan daha düşük bir hızla ve de belirtilen yakıt tüketiminden daha fazla bir tüketimle ilerlemesine sebep olabilecektir. Böyle bir durum söz konusu olduğunda, eğer ki çarter sözleşmesi geminin belli bir hızla ve yakıt tüketimiyle anlaşılan çarter süresi boyunca ilerleyeceğine dair gemi sahibi tarafından verilmiş bir taahhüt içeriyorsa, gemi sahibi, çartererin geminin performasının düşük olduğuna ilişkin olan iddiası ile karşılaşması muhtemeldir.

Bu açıklamalar akabinde, şurası net ki çartererin geminin tropikal sularda uzun süre kullanımına ilişkin talimatı gemi sahibinin çekinmeden uyabileceği türde bir talimat değildir. Çartererin bu talimatı üzerine, gemi sahibi genellikle bir çelişkinin içerisine düşmektedir. Bir tarafta, hukukun kendisine uymayı hükmettiği çartererin talimatı söz konusu iken diğer tarafta kendisinin geminin sözleşmede belirtilen hıza ve yakıt tüketimine sözleşme boyunca uyacağına dair vermiş olduğu bir taahhüt söz konusudur. Bu makalenin amacı; gemi sahibinin, çartererin geminin kullanımına ilişkin olan talimatına uyması sonucunda ortaya çıkan karina kirlenmesinden kaynaklanan geminin düşük performansından dolayı doğacak sorumluluğunun sınırlarını araştırmaktır. Makale ayrıca ‘’BIMCO Hull Fouling for Time Charterparties’’ klozunun sözleşmeye dahil edilmesi durumunda karina kirlenmesinden kaynaklanan geminin düşük performansıyla ilgili anlaşmazlıkların ne ölçüde azalacağını analiz etmeyi amaçlamaktadır.

Anahtar kelimeler: Karina kirlenmesi, geminin düşük performans göstermesi, BIMCO Hull Fouling Klozu.

Hull Fouling During Time Charter Service: Liability for Deficient Performance of the Ship

Ceren Cerit Dindar

cerencerit.6@gmail.com

Institute of International Shipping and Trade Law, Swansea University, UK

Abstract

Under a time charter, upon delivery commercial exploitation of a ship is placed in the hands of the charterer in exchange for payment of hire. During the agreed charter period, the charterer can send the ship to anywhere within the geographical limits of the charter. There is, therefore, nothing in principle that prevents the charterer from ordering the ship to proceed to tropical waters unless the charter contains a restriction in this regard. Such an order of the charterer is accepted as legitimate employment order and the shipowner is required to comply with it. If the shipowner refuses this order without any good reason, his conduct may constitute a repudiatory breach, so that entitles the charterer to terminate the charter. The problem is that where the ship remains in tropical waters for a long period, hull fouling mostly arises. This natural event can be defined as an accumulation of marine organism such as barnacles and weeds on the ship's hull. It may affect performance of the ship and cause that the ship proceeds at less speed and consumes more fuel than the specified in the charter. In such a case, if the charter contains an undertaking by the shipowner that the ship proceeds at particular speed and consumes particular amount of bunker on that speed during the period of charter, it is likely the shipowner exposes the charterer's claim for underperformance of the ship.

Following these explanations, it is clear that the charterer's order concerning the employment of the ship in tropical waters for a prolonged period is not a kind of order which the shipowner can follow without any concern. Upon the charterer's this order, the shipowner usually confront a dilemma. On the one hand, there is an order which the law requires him to comply with it, but on the other hand his continuous undertaking as to the ship's speed and bunker consumption under the charter. The purpose of this paper is to evaluate the limits of the shipowner's liability for underperformance caused by hull fouling that arises as a result of complying with the charterer's employment order. The paper also aims to analyse to what extent incorporation of BIMCO Hull Fouling Clause for Time Charterparties into the charter reduces underperformance disputes arising from hull fouling.

Keywords: Hull fouling, underperformance of the ship, the BIMCO hull fouling clause.

1. General Considerations as to Time Charter and the Shipowner's Obligation to Provide a Ship that Complies with Charter Description

A time charter is a contract for use of a ship for a particular period of time within agreed trading limits by a charterer in consideration of payment of hire. Under this type of charter, it is common to see a clause that describes the particular features of a ship, such as nationality, cargo capacity, speed and bunker consumption. All these contractual descriptions as to the ship are significant for the charterer since most of the time these are the only considerations which the charterer can rely on while entering a charter and agreeing to pay a fixed hire for an unknown ship during an agreed charter period. Depending on the layout of charter forms, the details as to the ship's features can be set out either under a separate clause[1] or in the preamble of the charter.[2] In both cases, existence of descriptions as to the ship's features imposes an obligation on the shipowner to provide a ship that complies with the charter description. Where there is a misdescription as to the features of the ship, the shipowner will be found liable for breach of contract and the charterer will be entitled to damages for the loss he suffered. The answer to the question of whether the charterer can also terminate the charter in such a case depends on the nature of the term which is breached.

Under English law, contractual terms are classified into three groups. These are conditions, warranties and intermediate terms. The word 'condition' is used to classify a term of the contract of major importance for the parties and any breach of it regardless of how minor entitles the party not in default to terminate the charter and sue for damages.[3] Definition as to the ship's class can likely be shown by the example of this kind of contractual term.[4] On the other hand, the 'warranty' emphasises a term which has minor importance for the parties and is not at the heart of the existing contract so it is accepted that breach of it gives rise only to the right to damages.[5] The third group of contractual terms, intermediate terms, was added to these two later with the Court of Appeal judgment in The Hongkong Fir.[6] In contrast to the other two classes, where an intermediate term is breached, its legal consequence – whether it only gives rise to the right to damages or entitles the party not in default to terminate the contract – is not certain at the beginning. This is determined by considering the factual consequences arising from the breach. In case of breach of an intermediate term, termination of the contract can be an issue only if the breach 'deprive(s) the party not in default of substantially the whole benefit which it was intended that he should obtain from the contract'.[7] The breach should be so serious to go to the root of the contract. These explanations show that to determine the charterer's remedies where there is a misdescription by the shipowner as to particular features of the ship, it is first necessary to determine the nature of the term.

2. The Shipowner's Description as to Speed and Bunker Consumption of the Ship

When it is compared with other items of the ship's description, it can be said that accuracy of description as to speed and bunker consumption of the ship, in other words, performance warranties, has a particular significance for the charterer since these parameters are in relation to two main costs which the charterer is responsible for under the charter. One of these costs is the payment of fixed hire for the ship during the agreed period of charter. When there is a misdescription by the shipowner as to the ship's speed and the ship proceeds with less speed than promised in the charter, this results in the completion of a particular voyage taking longer than expected. Due to this, fewer voyages will

[1] See Shelltime 3 cl. 1 and Shelltime 4 cl. 1.

[2] See preamble of NYPE 46, NYPE 93, NYPE 2015 and Baltime 1939 (as revised 2001).

[3] Poussard v Spiers and Pond (1876) 1 QBD 410.

[4] Routh v MacMillan (1863) 9 LT 541; Cosmos Bulk Transport Inc. v China National Foreign Trade Transportation Corporation (The Apollonius) [1978] 1 Lloyd's Rep. 53, p. 61.

[5] Bettini v Gye (1876) QBD 183.

[6] Hongkong Fir Shipping Company Ltd v Kawasaki Kisen Kaisha Ltd (The Hongkong Fir) [1962] 2 Lloyd's Rep. 478.

[7] Hongkong Fir Shipping Company Ltd v Kawasaki Kisen Kaisha Ltd (The Hongkong Fir) [1962] 2 Lloyd's Rep. 478, p. 494.

be performed within the agreed charter period than expected by the charterer. In such a case, since the charterer is still required to pay an agreed fixed hire regardless of how many voyages are completed during the agreed period, it could be said that failure of the ship to comply with the described speed will mean a reduction in the profitability of the charter, which is an undesirable result for any charterer. The other cost which the charterer is responsible for is bunker expenses of the ship during the charter period. When parameters given by the shipowner as to consumption of the ship are not accurate and the ship consumes more bunker than promised in the charter, the charterer will find himself in a position of allocating more money for bunker expenses than he is ready to pay under the charter and this adversely affects his expectations as to charter expenditures.

Where the ship fails to perform in accordance with warranted speed and consumption, one of the remedies available to the charterer is damages. Since the general belief is that the description as to performance of the ship has an intermediate term status,[8] misdescription on the part of the shipowner in this regard may also entitle the charterer to terminate the charter if the charterer can establish that the shipowner's breach goes to the root of the contract.[9] Imagine that the ship is chartered by a respected logistics company to carry cargo between two designated ports for a period of 10 months. However, due to the ship's continual failure to perform the warranted speed, the company is always delayed in the delivery of the goods to the cargo owners. After a time, this situation may come to affect the standing of the company in a negative way and cargo owners may not want to transport their cargoes via this company. In such a case, the company's assertion that noncompliance of the ship to warranted speed goes to the root of the contract could be considered reasonable which may entitle it to terminate the charter.

In determining when the ship must comply with the described speed and consumption in the charter, the wording of the charter is crucial. The shipowner and the charterer may state the relevant time in this regard to be at the time the charter is made or at the time of delivery of the ship in the charter.[10] Unfortunately, no clear answer has yet been provided as to which point of time will be considered if the charter is silent on this issue.[11] If the parties want to avoid uncertainty, it is advised that they make the applicable time of performance warranties clear in the charter. Some charters may go one step further and contain a continuous warranty as to performance of the ship.[12] Under this type of warranty, it is accepted that the shipowner promises that the ship will achieve the warranted performance during the whole period of charter. There is no doubt that this kind of performance warranty by the shipowner is the most advantageous one from the charterer's perspective since all risks which arise during the period of charter and cause failure of the ship to comply with promised speed and consumption, such as hull fouling, fall on the shoulders of the shipowner.

[8] Such a view is submitted in Coghlin T. and others (2014). Time Charters, Informa, Abingdon, p. 75, para. [3.77]; Bennett, H. (ed.) (2017). Carver on Charterparties, Sweet & Maxwell, London, p. 784, para. [7-755].

[9] Dolphin Hellas Shipping SA v Itemslot Ltd (The Aegean Dolphin) [1992] 2 Lloyd's Rep. 178.

[10] See Shelltime 3 cl. 24 and Boxtime 2004 cl. 2.

[11] It was suggested in Lorentzen v White Shipping Co Ltd (1942) 74 Ll.L. Rep. 161 that the ship needs to comply with warranted performance at the time when the charter is made. However, Cosmos Bulk Transport Incorporated v China National Foreign Trade Transportation Co (The Apollonius) [1978] 1 Lloyd's Rep. 53 made the point that the relevant time in this regard should be at the time of delivery.

[12] See Shelltime 4 cl. 24.

3. Hull Fouling that Occurs as a Result of the Charterer's Order and its Impact on Performance of the Ship

There is no doubt that one of the common reasons for underperformance of the ship during the charter service is hull fouling. This natural event can be described as an accumulation of a variety of marine organisms on the ship's bottom and sides. It commonly occurs as a result of the ship being at standstill in tropical waters for more than three consecutive weeks. Since hull fouling increases resistance against the ship's propulsion and causes a blockage in the ship's engine cooling intakes, by its nature, this results in a reduction in the ship's speed and increases bunker consumption.[13] When this occurs, hull fouling becomes a significant problem from the charterer's perspective. It should not be forgotten that under a time charter, the shipowner transfers the earning capacity of the ship to the charterer at the time of delivery in return for payment of hire. As a result of this transfer, the charterer is entitled to give orders to the shipowner as to economic utilisation of the ship, in other words, as to the employment of the ship. The extent of the charterer's power to employ the ship is delimited through trading limits in the charter. For example, most charters contain a limitation as to the kind of cargo that can be carried on board.[14] Similarly, they usually contain trading limits as to geographical employment area of the ship. Such a limitation might have been included to keep the ship away from ice-bound[15] and piracy areas.[16] The risk of war or existence of war may also cause the charterer to be prohibited to send the ship into particular areas.[17] However, except for these indicated geographical limitations, under most time charters the charterer is entitled to use the ship worldwide. This means that the charterer has the freedom to send the ship wherever he wants during the charter. In principle, this also means that the charterer is allowed to employ the ship in tropical waters for a long period of time. Therefore, such an order of the charterer should be treated as a legitimate order unless the charter contains an express restriction in this regard and the shipowner is required to comply with it. Refusal of this order of the charterer by the shipowner without any good reason may result in the shipowner being found guilty of a repudiatory breach of the charter and the charterer will be entitled to terminate the charter.[18]

4. The Shipowner's Concern for Employment of the Chartered Ship in Tropical Waters

Most charters require the shipowner to comply with the charterer's order to employ the ship in tropical waters for a prolonged period. However, this is not a kind of order which the shipowner can easily follow without any concern, especially if the charter contains a continuous performance warranty under which the shipowner promises that the ship will achieve the described speed and consumption throughout the period of charter.[19] The shipowner's hesitation is understandable because when he complies with the charterer's order there is a possibility that the ship's hull is fouled and this subsequently causes the ship to proceed at less speed and to consume more bunker than warranted in the charter.

[13] Grainger, S. (Jun. 2003). Getting to the bottom of it, Maritime Risk International. For more details on how the ship's propulsion components are affected from the hull fouling see Dere, Ç., Kandemir, Ç., Zincir B. and Deniz C. (2016). Hull Fouling Effect on Propulsion System Components, Proceedings of the 2nd Global Conference on Innovation in Marine Technology and the Future of Maritime Transportation, Muğla, Turkey, pp. 142-148.

[14] Both previous NYPE forms and new NYPE form require that cargo on the board must be lawful merchandise. See NYPE 2015 cl. 16, NYPE 93 cl. 4 and NYPE 46 lines 24-25.

[15] See NYPE 93 cl. 33, NYPE 2015 cl. 35 and BPTime 3 cl. 27.

[16] See NYPE 2015 cl. 39.

[17] See clause NYPE 2015 cl. 34(b) and BPTime 3 cl. 30.2.

[18] Abu Dhabi National Tanker Co v Product Star Shipping Ltd (The Product Star) (No 2) [1993] 1 Lloyd's Rep. 397.

In such a case, the charterer may be tempted to bring a claim against the shipowner for breach of continuous performance warranty even though failure of the ship to comply with warranted speed and consumption during the charter service had resulted from his own employment order. He may even try to terminate the charter by stating that the shipowner's breach as to performance warranty goes to the root of the contract. The question that arises here is whether or not in such a case the shipowner will be found liable for deficient performance of the ship.

It was suggested in *The Pamphilos* that in this situation the shipowner can rely on the fact that underperformance of the ship derives from the charterer's employment order as a defence and he can escapes from liability.[20] Such an approach clearly sets aside the shipowner's concern about complying with the charterer's order to employ the ship in tropical waters because the shipowner will know from very beginning that he will not be held liable for breach of continuous performance warranty when hull fouling arises upon the performance of the charterer's order and this causes deficient performance of the ship. From the author's point of view, the suggestion made in *The Pamphilos* also seems logical as it employs the principles of factual causation. Since the charterer is the one who provides the order and his order causes deficient performance of the ship, he should be the one held responsible for his own misfortune. However, this approach has very recently been rejected under English law.

In *The Coral Sea* it was held that the fact that hull fouling occurs upon the charterer's legitimate employment order and this causes deficient performance of the ship during the period of charter does not constitute an automatic defence for the shipowner against the charterer's underperformance claims.[21] It was submitted that to determine whether the shipowner is found liable for underperformance of the ship in such a case, the relevant test is whether or not underperformance was caused by a risk which the shipowner agreed to bear under the charter.[22] This test in one sense requires that the attention is given to the issue of whether the hull fouling is a risk which the shipowner contractually accepts. If the answer to this question is in the affirmative, the shipowner will still be found liable for breach of his obligation to provide a vessel that complies with the parameters of continuous performance warranty and is required to compensate the charterer for the loss suffered regardless of the fact that underperformance of the ship derives from an event which occurs as a result of the charterer's employment order.

The problem regarding the suggestion made in *The Coral Sea* is the difficulty to determine when hull fouling is accepted as a risk which the shipowner agrees to bear under the charter in a particular case. No objective criteria have been introduced which the court can consider while evaluating the acceptance of the risk issue. Therefore, during such an evaluation each case will turn on its own facts and the wording of the charter in question will be the primary concern. One of the consequences of this is that, most of the time, the shipowner is not so sure whether he will be held liable for breach of continuous performance warranty when he complies with the charterer's order as to usage of the ship in tropical waters and this causes hull fouling and subsequently underperformance of the ship. Due to this uncertainty, from his perspective the dilemma that he confronts when he receives the charterer's

[19] See Shelltime 4 cl. 24.

[20] Bulfracht (Cyprus) Ltd v Boneset Shipping Co Ltd (The Pamphilos) [2002] 2 Lloyd's Rep. 681, p. 690. For a similar suggestion also see Coghlin T. and others (2014). Time Charters, Informa, Abingdon, p. 75, para. [3.75].

[21] Bunge SA v C Transport Panamax Ltd (The Coral Seas) [2016] 2 Lloyd's Rep. 293, p. 299, para. [31].

[22] Ibid.

order to employ the ship in tropical waters continues. If there is a desire to reduce the uncertainties that may derive from this common law rule, the BIMCO hull fouling clause might be a good option.

5. The BIMCO Hull Fouling Clause for Time Charterparties as a Solution to Set Aside the Shipowner's Concern

The BIMCO hull fouling clause stipulates that:

" (a) If, in accordance with Charterers' orders, the Vessel remains at or shifts within a place, anchorage and/or berth *for an aggregated period exceeding*:

(i) a period as the parties may agree in writing in a Tropical Zone or Seasonal Tropical Zone*; or

(ii) a period as the parties may agree in writing outside such Zones*

any warranties concerning speed and consumption shall be suspended pending inspection of the Vessel's underwater parts...

*If no such periods are agreed the default periods shall be 15 days.

(b) In accordance with sub-clause (a), either party may call for inspection which shall be arranged jointly by Owners and Charterers and undertaken at Charterers' risk, cost, expense and time.

(c) If, as a result of the inspection either party calls for cleaning of any of the underwater parts, such cleaning shall be undertaken by the Charterers at their risk, cost, expense and time in consultation with the Owners.

(i) ...

(ii) If, at the port or place of inspection, cleaning as required under this Sub-clause (c) is not

permitted or possible, or if Charterers choose to postpone cleaning, *speed and consumption*

warranties shall remain suspended until such cleaning has been completed.

(iii) If, despite the availability of suitable facilities and equipment, Owners nevertheless

refuse to permit cleaning, *the speed and consumption warranties shall be reinstated from the*

time of such refusal. " [23] [emphases added].

It is not the intention of the author to evaluate every aspect of the BIMCO hull fouling clause here. Its relevant parts as to the ship's performance will be in consideration, which is why only those parts are quoted above.[24] It appears that the clause ends the uncertainty that derives from the test introduced in *The Coral Sea* and serves the purpose of reducing the shipowner's concern about complying with the charterer's order to employ the vessel in tropical waters. Where the clause is incorporated into the charter, the focus needs to be on whether or not the ship remains in tropical zones more than the duration agreed by the parties.[25] It is a straightforward exercise. The duration expressed by the parties in one sense is used as a cut-off point in determining whether the shipowner agrees to bear the risk of hull fouling in a particular case. For example, where the duration during which the ship remains in

[23] The clause was issued through Special Circular, No. 3, 24 June 2013 and is available in the BIMCO's website.

[24] Whole clause with a short explanatory note is available in Special Circular, No. 3, 24 June 2013 in the BIMCO's website.

[25] See section (a) of the BIMCO hull fouling clause.

tropical zones is determined by the parties as 20 days, if hull fouling arises before the expiry of this duration, it will be treated as a risk accepted by the shipowner. Therefore, even if the hull fouling which arises upon the charterer's order to trade in tropical waters causes the ship's performance to be affected negatively, continuous warranties as to speed and consumption of the ship have not been suspended and the shipowner will be found liable for breach of his obligation to provide a ship that complies with the parameters stated in the warranty. On the other hand, if the hull fouling arises after the ship spends more than 20 days in tropical waters, this risk is treated as one which the shipowner does not agree to bear. Therefore, after the expiry of 20 days, according to section (a) of the clause it is accepted that the shipowner's warranties as to performance of the ship are suspended and the shipowner will not be found liable for underperformance of the ship arising from hull fouling. Such an approach definitively brings about certainty for the parties because they know when the risk of hull fouling and underperformance of the ship upon the charterer's order to proceed in tropical waters is transferred from the shipowner to the charterer taking into account the agreed duration. The clause gives freedom to the parties to choose the length of the duration. However, considering the possibility that this can be disregarded by the parties, 15 days are determined as a default period.

Apart from the stipulation in section (a), section (c) (ii) and (iii) of the BIMCO hull fouling clause also contains a stipulation relevant to the performance of the ship. Section (c) (ii) of the clause makes the point that if the cleaning of the hull is prevented by the charterer, then the shipowner's continuous warranties as to performance of the ship continue to be suspended. This is sensible because in such a case if the charterer was allowed to sue the shipowner for breach of performance warranty, in one sense the charterer would be allowed to get the benefit of his own wrong (this is not allowing the cleaning operation here) and this is not acceptable. In contrast to this, section (c) (iii) of the clause stipulates that where the cleaning is prevented by the shipowner, the performance warranty becomes applicable upon the refusal so that it will be possible for the charterer to bring a claim for underperformance of the ship after that point.

6. Conclusion

Trading of a vessel in tropical waters regularly leads to the problem of hull fouling and this may have a significant effect on the performance of the chartered ship. At this point, if the charter contains a continuous performance warranty, disputes as to performance of the ship will be inevitable. Despite the popularity of the subject, it is indeed surprising that the law has only just been settled through the judgment in *The Coral Sea*. The case sets a clear criterion by stating that while determining the liability of the shipowner for deficient performance of the ship, the attention should be given to the issue of whether the shipowner bears the risk of hull fouling that occurs following the charterer's order to trade the ship in tropical waters. However, as stated above, application of this criterion is not easy and requires further consideration by a court in every case. This brings about uncertainty from the shipowner's perspective. Since he can never be sure under this test whether he will be found liable for deficient performance of the ship when he complies with the charterer's order to proceed in tropical waters and hull fouling subsequently arises, his concern as to complying with the charterer's employment order continues to exist. The BIMCO hull fouling clause is a significant step to set aside the shipowner's concern in this regard because it considers the agreed duration by the parties for the vessel remaining in tropical waters, and so the shipowner knows whether he will be found liable for breach of continuous performance warranty. Therefore, it is believed it will be in the shipowner's best interests to incorporate the clause into the charter. Due to the certainty that comes with the clause, the clause has commonly begun to be preferred in practice.

7. References

Bennett, H. (ed.) (2017). Carver on Charterparties, Sweet & Maxwell, London.

Coghlin, T. and others (2014). Time Charters, Informa, Abingdon.

Dere, Ç., Kandemir, Ç., Zincir B. and Deniz C. (2016). Hull Fouling Effect on Propulsion System Components, Proceedings of the 2nd Global Conference on Innovation in Marine Technology and the Future of Maritime Transportation, Muğla, Turkey, pp. 142-148.

Grainger, S. (Jun. 2003). Getting to the bottom of it, Maritime Risk International.

List of Cases

Abu Dhabi National Tanker Co v Product Star Shipping Ltd (The Product Star) (No 2) [1993] 1 Lloyd's Rep. 397.

Bettini v Gye (1876) QBD 183.

Bulfracht (Cyprus) Ltd v Boneset Shipping Co Ltd (The Pamphilos) [2002] 2 Lloyd's Rep. 681.

Bunge SA v C Transport Panamax Ltd (The Coral Seas) [2016] 2 Lloyd's Rep. 293.

Cosmos Bulk Transport Inc. v China National Foreign Trade Transportation Corporation (The Apollonius) [1978] 1 Lloyd's Rep. 53.

Dolphin Hellas Shipping SA v Itemslot Ltd (The Aegean Dolphin) [1992] 2 Lloyd's Rep. 178.

Hongkong Fir Shipping Company Ltd v Kawasaki Kisen Kaisha Ltd (The Hongkong Fir) [1962] 2 Lloyd's Rep. 478.

Lorentzen v White Shipping Co Ltd (1942) 74 Ll.L. Rep. 161.

Poussard v Spiers and Pond (1876) 1 QBD 410.

Routh v MacMillan (1863) 9 LT 541.


GMO
TMMOB Gemi Mühendisleri Odası
Endaze Bülteni
ŞUBAT 2018
Odamız,
ISO 10002 Müşteri Memnuniyeti Belgesi
Almak için Harekete Geçti...
ISO
ISO 10002
ÜYELERİMİZE DAHA İYİ HİZMET
Cevap Verebilirlik
Şeffaflık
Objektiflik
Erişebilirlik
%100 ÜYE MEMNUNİYETİ
Endaze Bülteni, Gemi Mühendisleri Odası üyelerine e-posta yolu ile iletilir.
Ulaşmasını istediğiniz e-posta detaylarını lütfen Gemi Mühendisleri Odası'na bildiriniz.
Adres: Postane Mahallesi Nil Sokak No:10 Tuzla-İstanbul
Telefon: (216) 447 40 30-31-32 - Faks: (216) 447 40 33
www.gmo.org.tr www.facebook.com/tmmobgmomerkez twitter.com/Gemimuhendis
instagram/gemimuhendisleriodasi Link edin/tmmobgemimühendisleriodası


GMO
TMMOB Gemi Mühendisleri Odası
Endaze Bülteni
OCAK 2018
BİR AJANDA BİR FİDAN
TEMA
Aidatını ödeyerek hem çevreye hem odaya katkıda bulunan
siz değerli üyelerimize teşekkür ederiz !
Endaze Bülteni, Gemi Mühendisleri Odası üyelerine e-posta yolu ile iletilir.
Ulaşmasını istediğiniz e-posta detaylarını lütfen Gemi Mühendisleri Odası'na bildiriniz.
Adres: Postane Mahallesi Nil Sokak No:10 Tuzla-İstanbul
Telefon: (216) 447 40 30-31-32 - Faks: (216) 447 40 33
www.gmo.org.tr www.facebook.com/tmmobgmomerkez twitter.com/Gemimuhendis
instagram/gemimuhendisleriodasi Link edin/tmmobgemimühendisleriodası


GMO
TMMOB
Gemi Mühendisleri Odası
Endaze Bülteni
Mart 2018
46. DÖNEM
Endaze Bülteni, Gemi Mühendisleri Odası üyelerine e-posta yolu ile iletilir.
Ulaşmasını istediğiniz e-posta detaylarını lütfen Gemi Mühendisleri Odası'na bildiriniz.
Adres: Postane Mahallesi Nil Sokak No:10 Tuzla-İstanbul
Telefon: (216) 447 40 30-31-32 - Faks: (216) 447 40 33
www.gmo.org.tr www.facebook.com/tmmobgmomerkez twitter.com/Gemimuhendis
instagram/gemimuhendisleriodasi Link edin/tmmobgemimühendisleriodası


GMO
TMMOB
Gemi Mühendisleri Odası
Endaze Bülteni
NİSAN 2018
"Sizler hepiniz geleceğin bir gülü,
yıldızı, bir mutluluk parıltısısınız!
Memleketi asıl aydınlığa boğacak sizsiniz"
23 Nisan Ulusal Egemenlik ve
Çocuk Bayramı Kutlu Olsun!
Endaze Bülteni, Gemi Mühendisleri Odası üyelerine e-posta yolu ile iletilir.
Ulaşmasını istediğiniz e-posta detaylarını lütfen Gemi Mühendisleri Odası'na bildiriniz.
Adres: Postane Mahallesi Nil Sokak No:10 Tuzla-İstanbul
Telefon: (216) 447 40 30-31-32 - Faks: (216) 447 40 33
www.gmo.org.tr www.facebook.com/tmmobgmomerkez twitter.com/Gemimuhendis
instagram/gemimuhendisleriodasi Link edin/tmmobgemimühendisleriodası


GMO
TMMOB
Gemi Mühendisleri Odası
Endaze Bülteni
MAYIS 2018
19 MAYIS
ATATÜRK'Ü ANMA,
GENÇLİK VE SPOR
BAYRAMIMIZ KUTLU OLSUN
Endaze Bülteni, Gemi Mühendisleri Odası üyelerine e-posta yolu ile iletilir.
Ulaşmasını istediğiniz e-posta detaylarını lütfen Gemi Mühendisleri Odası'na bildiriniz.
Adres: Postane Mahallesi Nil Sokak No:10 Tuzla-İstanbul
Telefon: (216) 447 40 30-31-32 - Faks: (216) 447 40 33
www.gmo.org.tr www.facebook.com/tmmobgmomerkez twitter.com/Gemimuhendis
instagram/gemimuhendisleriodasi Link edin/tmmobgemimühendisleriodası


GMO
TMMOB
Gemi Mühendisleri Odası
Endaze Bülteni
HAZİRAN 2018
GEMİ MÜHENDİSLERİ ODASI
MEZUNİYET HATIRASI
Mesleğine Hoşgeldin
Endaze Bülteni, Gemi Mühendisleri Odası üyelerine e-posta yolu ile iletilir.
Ulaşmasını istediğiniz e-posta detaylarını lütfen Gemi Mühendisleri Odası'na bildiriniz.
Adres: Postane Mahallesi Nil Sokak No:10 Tuzla-İstanbul
Telefon: (216) 447 40 30-31-32 - Faks: (216) 447 40 33
www.gmo.org.tr www.facebook.com/tmmobgmomerkez
twitter.com/Gemimuhendis
instagram/gemimuhendisleriodasi Link edin/tmmobgemimühendisleriodası


GMO
TMMOB
Gemi Mühendisleri Odası
Endaze Bülteni
TEMMUZ 2018
GMO
1 TEMMUZ
DENİZCİLİK VE KABOTAJ
BAYRAMIMIZ KUTLU OLSUN
Denizciliği Türkün büyük milli ülküsü olarak düşünmeli ve onu az zamanda başarmalıyız.
Endaze Bülteni, Gemi Mühendisleri Odası üyelerine e-posta yolu ile iletilir.
Ulaşmasını istediğiniz e-posta detaylarını lütfen Gemi Mühendisleri Odası'na bildiriniz.
Adres: Postane Mahallesi Nil Sokak No:10 Tuzla-İstanbul
Telefon: (216) 447 40 30-31-32 - Faks: (216) 447 40 33
www.gmo.org.tr www.facebook.com/tmmobgmomerkez twitter.com/Gemimuhendis
instagram/gemimuhendisleriodasi Link edin/tmmobgemimühendisleriodası


GMO
TMMOB
Gemi Mühendisleri Odası
Endaze Bülteni
AĞUSTOS 2018
Biz Türkler tarih boyunca
Hürriyet ve istiklale timsal olmuş bir milletiz.
MUSTAFA KEMAL ATATÜRK
Endaze Bülteni, Gemi Mühendisleri Odası üyelerine e-posta yolu ile iletilir.
Ulaşmasını istediğiniz e-posta detaylarını lütfen Gemi Mühendisleri Odası'na bildiriniz.
Adres: Postane Mahallesi Nil Sokak No:10 Tuzla-İstanbul
Telefon: (216) 447 40 30-31-32 - Faks: (216) 447 40 33
www.gmo.org.tr www.facebook.com/tmmobgmomerkez twitter.com/Gemimuhendis
instagram/gemimuhendisleriodasi Link edin/tmmobgemimühendisleriodası


GMO
TMMOB
Gemi Mühendisleri Odası
Endaze Bülteni
EYLÜL 2018
27 Eylül 1538
Preveze Deniz Zaferi ve Deniz
Kuvvetleri Günü Kutlu Olsun !
Endaze Bülteni, Gemi Mühendisleri Odası üyelerine e-posta yolu ile iletilir.
Ulaşmasını istediğiniz e-posta detaylarını lütfen Gemi Mühendisleri Odası'na bildiriniz.
Adres: Postane Mahallesi Nil Sokak No:10 Tuzla-İstanbul
Telefon: (216) 447 40 30-31-32 - Faks: (216) 447 40 33
www.gmo.org.tr www.facebook.com/tmmobgmomerkez twitter.com/Gemimuhendis
instagram/gemimuhendisleriodasi Link edin/tmmobgemimühendisleriodası